AD-A254 411

WL-TR-92-3049

Large-Amplitude Plate Vibration in an Elevated Thermal Environment

Jon Lee

Structural Dynamics Branch
Structures Division

June 1992

Final Report for period May 1991- December 1991

Approved for public release; distribution is unlimited.

FLIGHT DYNAMICS DIRECTORATE
WRIGHT LABORATORY
AIR FORCE SYSTEMS COMMAND
WRIGHT-PATTERSON AFB, OH 45433-6553

92   10 114

92-22632

NOTICE

When Government drawings, specifications, or other data are used for any purpose other than in connection with a definitely Government-related procurement, the United States Government incurs no responsibility or any obligation whatsoever. The fact that the government may have formulated or in any way supplied the said drawings, specifications, or other data, is not to be regarded by implication, or otherwise in any manner construed, as licensing the holder, or any other person or corporation; or as conveying any rights or permission to manufacture, use, or sell any patented invention that may in any way be related thereto.

This report is releasable to the National Technical Information Services (NTIS). At NTIS, it will be available to the general public, including foreign nations.

This technical report has been reviewed and is approved for publication.

JON, LEE, Mathematician
Acoustics and Sonic Fatigue Group

RALPH M. SHIMOVETZ, Group Leader
Acoustics and Sonic Fatigue Group

FOR THE COMMANDER

JEROME PEARSON, Chief
Structural Dynamics Branch

If your address has changed, if you wish to be removed from our mailing list, or it the addressee is no longer employed by your organization please notify WL/FIBGD, WPAFB, OH 45433-6553 to help us maintain a current mailing list.

Copies of this report should not be returned unless return is required by security considerations, contractual obligations, or notice on a specific document.

REPORT DOCUMENTATION PAGE

Public reporting burden for this collection of information is estimated to average 1 hour per response, including the time for reviewing instructions, searching existing data sources, gathering and maintaining the data needed, and completing and reviewing the collection of information. Send comments regarding this burden estimate or any other aspect of this collection of information, including suggestions for reducing this burden, to Washington Headquarters Services, Directorate for Information Operations and Reports, 1215 Jefferson Davis Highway, Suite 1204, Arlington, VA 22202-4302, and to the Office of Management and Budget, Paperwork Reduction Project (0704-0188), Washington, DC 20503.

1. AGENCY USE ONLY (Leave blank)	2. REPORT DATE	3. REPORT TYPE AND DATES COVERED
	Jun 1992	Final, May 1991- Dec 1991

4. TITLE AND SUBTITLE

Large-Amplitude Plate Vibration in an Elevated Thermal Environment

6. AUTHOR(S)

Jon Lee (513-255-5229)

5. FUNDING NUMBERS

PE:61102F
PR:2304
TA-N1
WU-13

7. PERFORMING ORGANIZATION NAME(S) AND ADDRESS(ES)

Flight Dynamics Directorate, Wright Laboratory
(WL/FIBG) Wright-Patterson AFB, OH 45433

8. PERFORMING ORGANIZATION REPORT NUMBER

WL-TR-92-3049

9. SPONSORING/MONITORING AGENCY NAME(S) AND ADDRESS(ES)

AFOSR/NM, Bolling AFB, Washington, DC 20332

10. SPONSORING/MONITORING AGENCY REPORT NUMBER

11. SUPPLEMENTARY NOTES

12a. DISTRIBUTION/AVAILABILITY STATEMENT

Approved for public release;
distribution is unlimited

12b. DISTRIBUTION CODE

13. ABSTRACT (Maximum 200 words)

At elevated temperatures the dynamics of vibrating plate (or shell) must include the three thermal effects: (i) the global expansion that is due to uniform plate temperature, (ii) the local expansion by temperature variation over the plate, and (iii) the thermal moment induced by temperature gradient across the plate thickness. Using the single-mode model of Galerkin representation, we have shown that (i) and (ii) give rise to the combined stiffness responsible for thermal buckling, whereas (iii) contributes to the combined forcing of thermal and mechanical excitations. Anticipating the high-temperature sonic fatigue test facility being fabricated at the structural dynamics Branch (WL/FIBG) in support of NASP program, the present study attempts to estimate the mean square displacement and root-mean-square stress and strain components by using the equivalent linearization technique of stochastic dynamics.

14. SUBJECT TERMS

Plate/shell at elevated temperatures, Large-amplitude vibration, Thermal buckling, Equivalent linearization

15. NUMBER OF PAGES
91

16. PRICE CODE

17. SECURITY CLASSIFICATION OF REPORT	18. SECURITY CLASSIFICATION OF THIS PAGE	19. SECURITY CLASSIFICATION OF ABSTRACT	20. LIMITATION OF ABSTRACT
UNCLASSIFIED	UNCLASSIFIED	UNCLASSIFIED	UL

FOREWORD

This report was prepared in the Structural Dynamics Branch (WL/FIBG), Structures Division, Flight Dynamics Directorate, Wright Laboratory, Wright-Patterson AFB, OH 45433. The work reported herein was performed under the workunit 2304N113, Nonlinear Dynamics, during the period of May to December 1991. The present investigation was prompted by the need to understand the basic mechanics of isotropic metal and multi-layered composite plate specimens to be tested in the high-temperature sonic fatigue facility of WL/FIBG, which can simulate the combined thermal-acoustic environment typical of proposed National Aerospace Plane flights.

The author wishes to thank Howard Wolfe, Steve Whitehouse, and Jay Levraea for their valuable comments and suggestions on the first draft of the report. Also, Ken Wentz's help in providing him with much of the technical literature on sonic fatigue should be acknowledged.

DTIC QUALITY INSPECTED 5

Accesion For	
NTIS CRA&I	☑
DTIC TAB	☐
Unannounced	☐
Justification	
By	
Distribution /	
Availability Codes	
Dist	Avail and / or Special
A-1	

-iii-

TABLE OF CONTENTS

NOMENCLATURE

a, b	Sides of the plate in x and y coordinates.
D	Flexural rigidity
E	Modulus of elasticity
F	Airy's stress function
f	frequency
$f(t)$, f_0	Mechanical, thermal loading
H	Hamiltonian
h	Plate thickness
I_1, I_2, I_3, I_4	Terms defined by Eq. (3.13)
J_1, J_2, J_3, J_4	Terms defined by Eq. (3.23)
N_x, N_y, N_{xy}	Averaged stress components across the plate thickness
P_x, P_y, P_{xy}	Integration constants representing averaged edge loading
P_{mn}, p_{mn}	Modal external forces
Q_2	Buckled plate amplitude
q	Single-mode displacement
R_1, R_2, R_3, R_4	Symbolic form for the four terms in Eq. (3.7)
T, T_0	Plate temperature
$\bar{T}$	Mid-plate temperature
T_b^*, T_c^*	Critical buckling temperature for the simply-supported and clamped plates
u, v, w	Displacements in x, y, and z coordinates
x, y, z	Plate coordinates
W_{mn}, w_{mn}	Modal displacements
α	Coefficient of thermal expansion
β	Aspect ratio, b/a
δ_v, δ_g	Numerical factors for temperature variation and gradient
ε_x, ε_y, ε_{xy}	Stress tensor
$\phi_m(x)$, $\varphi_m(x)$	Basis functions for a clamped plate
γ	Time scale $[\rho h b^4/\pi^4 D]^{1/2}$
$\ell_1 - \ell_8$	Functions of W_{mn} used in Sec. III.
κ	Coefficient for cubic terms
μ	Poisson's ratio
$s_{ff}(\omega)$, $g_{ff}(f)$	Power spectral density of acoustic loading
ρ	Cross-sectional mass density
σ_x, σ_y, σ_{xy}	Strain tensor
$\theta(x,y)$, $\Theta(x,y)$	Temperature gradient and differential across the plate
$\Psi_m(x)$, $\psi_m(x)$	Basis functions for a simply-supported plate
ω	Angular frequency
ξ	Damping coefficient
$<.>$	Statistical average
$<<.>>$	Average over the plate

I. Introduction

Transatmospheric vehicle (National Aero-Space Plane) technology presents a grand challange of the rest of this century and the next for aerospace science and engineering communities [1]. In contrast to ballistic re-entry vehicles (space shuttles) piercing through the atmosphere nearly vertically, the trans-atmospheric vehicle will remain in the dense layer of the atmosphere for a good portion of its flight, and hence the air near the moving vehicle is heat-ed to very high temperatures (aerodynamic heating). According to computational fluid dynamic simulations of hypersonic lifting body, the skin temperature can readily reach 2000^0F and, in particular, the nose cone and external skin panels near the jet efflux are estimated to have temperatures over 3500^0F [1]. At these high-temperature hypersonic flights, acoustic fatigue becomes a severe structural problem because not only are the pressure fluctuations anti-cipated in the range of 160-180 dB, but also the skin panels can vibrate chaotically about the thermally buckled positions whose amplitudes increase as the square root of temperature above the critical buckling temperature (oil-canning effect) [2]. Realizing the importance of elevated temperatures on acoustic fatigue, work has begun as early as in the 70's to establish fatigue failure criteria in a combined thermal-acoustic environment [3].

Strictly speaking, sonic fatigue is a fluid-structure interaction problem which requires simultaneous solution of the Navier-Stokes equations for pressure and temperature together with the structural dynamic equations for ensuing stress/strain distributions. For large-amplitude deflections, the shape of structures representing the fluid-structure interface is not known *a priori*, and hence must be determined from simultaneous solution of the fluid and structural equations. However, much progress has been made in the past by decoupling the structural part of the problem from solving the Navier-Stokes equations for pressure fluctuations. Following in this tradition, we shall in this report investigate dynamics of a piece of hypersonic vehicle structure modelled by the so-called von Karman-Herrmann-Chu plate equations subjected to prescribed pressure fluctuations and temperature variations.

Although Bolotin [4] derived the basic plate/shell equations for large-amplitude deflection subjected to temperature variation in the late 50's (Sec. II), it is fair to say the role of thermal effects has not yet been elucidated in its full generality. This is perhaps due to the complexity of nonlinear equations and, moreover, a wide variety of boundary and edge conditions that one may impose on the plate. To exhibit the essential physics, we expand the transverse displacement, Airy's stress function, and temperature distribution in trigonometric functions, and thus obtain modal equations for both simply-supported and clamped plates (Sec. III). Note that the original plate equations are partial differential equations, whereas the modal equations are ordinary differential equations. However, the price paid for this reduction

-1-

(Galerkin's procedure) is indeterminancy because the system of modal equations is not closed because of nonlinearity. We shall therefore truncate the system to obtain modal equations for the first four even modes in Sec. IV, and thereby permitting comparison with the previous formulations of Levy [5] and Paul [6]. It is important to point out that after a suitable nondimensionalization the modal equations of simply-supported and clamped plate can exhibit a similar form for the three temperature terms. The first is global thermal expansion by uniform temperature, the second corresponds to local thermal expansion by temperature variation over the plate, and the third term represents the thermal moment owing to temperature gradient through the plate thickness.

Even for the low order modal equations, there are too many cubic terms for us to readily ascertain the correctness of Galerkin's procedure carried out in Sec. IV. We therefore demonstrate credibility of the modal equations by way of constructing the Hamiltonian which embodies the kinetic and potential (strain) energies of the plate being conserved in the absence of viscous damping (Sec. V). To proceed further, it is necessary to specify the temperature variation over the plate and temperature gradient across the plate. We have adopted in Sec. VI very simple, but nontrivial profiles for the temperature variation and gradient to expedite the subsequent analysis.

Much insight into thermal terms can be gained by the prototype single-mode equation shared by both the simply-supported and clamped plates (Sec. VII). First of all, the uniform temperature and temperature variation represent a kind of thermal stiffness, but they add negatively to the structural stiffness. Hence, the combined thermal-structural stiffness remains positive when the sum of uniform and local temperatures is less than the critical buckling temperature (pre-buckling), whereas it becomes negative when the sum exceeds the critical buckling temperature (post-buckling). In contrast, the temperature gradient across the plate gives rise to thermal moment, hence representing an additional loading, as already observed by Boley and Weiner [7]. Therefore, this together with external pressure forces constitute the combined thermal-applied forcing.

For the acoustic loading it is necessary to consider stochastic dynamic formulation of the single-mode equation and estimate the mean square response amplitude subjected to Gaussian random excitations [8]. Although the equivalent linearization technique [9] has proven useful for nonlinear structural dynamic problems, it cannot be applied directly to the present problem because the thermal moment appears as an additional time-independent forcing. This therefore calls for an extension of the equivalent linearization to nonzero-mean Gaussian excitations. The main thrust of this report (Sec. VIII) is to show the growth of mean square displacement as the plate goes through thermal buckling, the competing mechanical and thermal loading, and the effect of various thermal terms on the extreme-fiber stress and strain tensor components.

Most detailed information has been relegated to the appendices, for the benefit of those readers who demand proofs. In any event, this report contains a complete Galerkin formulation of simply-supported and clamped plates, including the combined stiffness and applied forcing terms.

II. Plate Equations for Large-Amplitude Displacement

Let us begin with the following strain-stress relations for a plate, including the effect of thermal expansion αT

$$\varepsilon_x = \frac{1}{E}(\sigma_x - \mu\sigma_y) + \alpha T,$$

$$\varepsilon_y = \frac{1}{E}(\sigma_y - \mu\sigma_x) + \alpha T,$$

$$\varepsilon_{xy} = \frac{1+\mu}{E}\sigma_{xy}. \tag{1}$$

where E is the modulus of elasticity and μ Poisson's ratio. Besides, T denotes the local temperature of plate with the thermal expansion coefficient α. In the absence of αT, Eq. (1) is the usual linear relationships of the strain tensor components ε_x, ε_y, and ε_{xy} and stress tensor components σ_x, σ_y, and σ_{xy}. For a positive α, raising T would simply result in increased strain, in conformity with the intuitive notion of thermal expansion. By solving Eq. (1) for the stress tensor, the inverse relation is

$$\sigma_x = \frac{E}{(1-\mu^2)}[\varepsilon_x + \mu\varepsilon_y - (1+\mu)\alpha T],$$

$$\sigma_y = \frac{E}{(1-\mu^2)}[\varepsilon_y + \mu\varepsilon_x - (1+\mu)\alpha T],$$

$$\sigma_{xy} = \frac{E}{(1+\mu)}\varepsilon_{xy}. \tag{2}$$

It is important to notice the negative sign for αT terms; hence, the stress may in fact decrease as T is raised.

Following Bolotin [4], we decompose T into

$$T(x,y,z) = \overline{T}(x,y) + z\Theta(x,y), \tag{3}$$

where $\overline{T}(x,y) = h^{-1}\int_{-h/2}^{h/2} T(x,y,z)dz$ is the temperature averaged over the plate thickness h, and $\Theta(x,y)$ is the temperature gradient across h (Fig. 1). Note that only the linear temperature differential in z is included in Eq. (3); any nonlinear temperature variations are ignored according to the thin plate theory. We shall first outline briefly derivation of the compatibility, transverse displacement equation, and plate edge conditions.

<u>Compatibility Equation</u>

For the mean strain tensor $\overline{\varepsilon}_x$, $\overline{\varepsilon}_y$ and $\overline{\varepsilon}_{xy}$ at the mid-plate; i.e.,
$\overline{\varepsilon}_x = h^{-1}\int_{-h/2}^{h/2}\varepsilon_x dz$, $\overline{\varepsilon}_y = h^{-1}\int_{-h/2}^{h/2}\varepsilon_y dz$, and $\overline{\varepsilon}_{xy} = h^{-1}\int_{-h/2}^{h/2}\varepsilon_{xy}dz$, we have the following expressions

$$\bar{\varepsilon}_x = \frac{\partial u}{\partial x} + \frac{1}{2}(\frac{\partial w}{\partial x})^2,$$

$$\bar{\varepsilon}_y = \frac{\partial v}{\partial y} + \frac{1}{2}(\frac{\partial w}{\partial y})^2,$$

$$\bar{\varepsilon}_{xy} = \frac{1}{2}(\frac{\partial u}{\partial y} + \frac{\partial v}{\partial x}) + \frac{1}{2}(\frac{\partial w}{\partial x})(\frac{\partial w}{\partial y}). \tag{4}$$

deduced from geometric considerations. The condition of strain compatibility is obtained by eliminating u and v from Eq. (4) through cross differentiation

$$\frac{\partial^2 \bar{\varepsilon}_x}{\partial y^2} + \frac{\partial^2 \bar{\varepsilon}_y}{\partial x^2} - 2\frac{\partial^2 \bar{\varepsilon}_{xy}}{\partial x \partial y} = (\frac{\partial^2 w}{\partial x \partial y})^2 - (\frac{\partial^2 w}{\partial x^2})(\frac{\partial^2 w}{\partial y^2}). \tag{5}$$

Now, by averaging Eq. (1) over h we obtain the alternate expressions for the mean strain tensor

$$\bar{\varepsilon}_x = \frac{1}{Eh}(N_x - \mu N_y) + \alpha T,$$

$$\bar{\varepsilon}_y = \frac{1}{Eh}(N_y - \mu N_x) + \alpha T,$$

$$\bar{\varepsilon}_{xy} = \frac{1+\mu}{Eh} N_{xy}. \tag{6}$$

Here, $N_x = \int_{-h/2}^{h/2} \sigma_x dz$, $N_y = \int_{-h/2}^{h/2} \sigma_y dz$, and $N_{xy} = \int_{-h/2}^{h/2} \sigma_{xy} dz$ are forces per unit length of plate. They are often expressed by Airy's stress function F

$$N_x = \frac{\partial^2 F}{\partial y^2}, \qquad N_y = \frac{\partial^2 F}{\partial x^2}, \qquad N_{xy} = -\frac{\partial^2 F}{\partial x \partial y}. \tag{7}$$

which automatically satisfy the stress equilibrium at the mid-plate; i.e., $\partial N_x/\partial x + \partial N_{xy}/\partial y = 0$ and $\partial N_{xy}/\partial x + \partial N_y/\partial y = 0$. Substituting Eq. (6-7) into Eq. (5) yields the compatibility condition

$$\nabla^4 F + Eh\alpha\nabla^2 T = Eh\left[(\frac{\partial^2 w}{\partial x \partial y})^2 - (\frac{\partial^2 w}{\partial x^2})(\frac{\partial^2 w}{\partial y^2})\right], \tag{8}$$

where $\nabla^4 = \nabla^2\nabla^2$ is the biharmonic operator.

Transverse Displacement Equation

Next, we consider the balance equation for the shear forces and normal loading q, on one hand, and for the shear forces and bending moments m_x and m_y, and twisting moments $m_{xy} = m_{yx}$, on the other hand. Upon eliminating the shear forces from such force balance equations, we obtain

$$\frac{\partial^2 m_x}{\partial x^2} + \frac{\partial^2 m_y}{\partial y^2} + 2\frac{\partial^2 m_{xy}}{\partial x \partial y} + N_x\frac{\partial^2 w}{\partial x^2} + N_y\frac{\partial^2 w}{\partial y^2} + 2N_{xy}\frac{\partial^2 w}{\partial x \partial y} + q_n = 0, \tag{9}$$

relating the moments with the normal loading q_n. We first express the moments in terms of w

$$m_x = -D\left[\frac{\partial^2 w}{\partial x^2} + \mu \frac{\partial^2 w}{\partial y^2} + \alpha(1+\mu)\theta \right],$$

$$m_y = -D\left[\frac{\partial^2 w}{\partial y^2} + \mu \frac{\partial^2 w}{\partial x^2} + \alpha(1+\mu)\theta \right],$$

$$m_{xy} = -D(1-\mu)\frac{\partial^2 w}{\partial x \partial y}. \tag{10}$$

where $D = Eh^3/12(1-\mu^2)$ is the flexural rigidity. We then include in q_n the inertial force, viscous damping, and external pressure p; i.e.,

$$q_n = -\rho h \frac{\partial^2 w}{\partial t^2} - \rho h \xi \frac{\partial w}{\partial t} + p. \tag{11}$$

where ρ is the cross-sectional mass density and ξ the damping coefficient. Note that $\rho h \xi (\partial w/\partial t)$ has been introduced as a symbolic representation for viscous damping. Perhaps, a more practical damping model would be $\xi D\nabla^4 (\partial w/\partial t)$ of Maekawa [10]. Upon inserting Eqs. (7), (10) and (11) into Eq. (9), we obtain the equation for transverse displacement consistent with the von Karman type of large-amplitude deflection

$$\rho h \frac{\partial^2 w}{\partial t^2} + \rho h \xi \frac{\partial w}{\partial t} - p + D\nabla^4 w + \alpha(1+\mu)D\nabla^2 \theta = \frac{\partial^2 w}{\partial x^2}\frac{\partial^2 F}{\partial y^2} + \frac{\partial^2 w}{\partial y^2}\frac{\partial^2 F}{\partial x^2} - 2\frac{\partial^2 w}{\partial x \partial y}\frac{\partial^2 F}{\partial x \partial y}. \tag{12}$$

The pair of Eqs. (8) and (12) is that given by Eqs. (4.131) and (4.132) (in which k_x and k_y are set to zero) of Bolotin [4], and also agrees in form with Eqs. (13.7.1) and (13.11.3) of Boley and Weiner [7].

Plate Edge Conditions

It must be pointed out that the compatibility is a statement about force balances at the mid-plate. Hence, it implies certain constraints on u and v, which dictate the movement of plate edges. Let us assume that the solution of Eq. (8) is made up of the particular solution and a homogeneous solution F_h of $\nabla^4 F = 0$ which is given by

$$F_h = \frac{P_x y^2}{2} + \frac{P_y x^2}{2} - P_{xy}xy. \tag{13}$$

where integration contants P_x, P_y, and P_{xy} represent the membrane stresses. As shown in Sec. II of Ref. [11], the immovable edge conditions of zero in-plane displacement are

$$\frac{\partial^2 F}{\partial x \partial y} = 0 \quad \text{and} \quad \int_0^a \int_0^b \left(\frac{\partial u}{\partial x}\right)dxdy = 0 \quad \text{at } x=0, a,$$

$$\frac{\partial^2 F}{\partial x \partial y} = 0 \quad \text{and} \quad \int_0^a \int_0^b \left(\frac{\partial v}{\partial y}\right)dxdy = 0 \quad \text{at } y=0, b, \tag{14}$$

Here, the integrals of displacements along the plate edge are suppressed in an

average sense. By combining Eqs. (4) and (6), we find appropriate expressions for the integrands in terms of F and w

$$\frac{\partial u}{\partial x} = \frac{1}{Eh}\left(\frac{\partial^2 F}{\partial y^2} - \mu \frac{\partial^2 F}{\partial x^2}\right) + \alpha T - \frac{1}{2}\left(\frac{\partial w}{\partial x}\right)^2 ,$$

$$\frac{\partial v}{\partial y} = \frac{1}{Eh}\left(\frac{\partial^2 F}{\partial x^2} - \mu \frac{\partial^2 F}{\partial y^2}\right) + \alpha T - \frac{1}{2}\left(\frac{\partial w}{\partial y}\right)^2 , \tag{15}$$

as given by Bolotin's Eq. (4.140) in Ref [4]. On the other hand, the movable edge conditions

$$\frac{\partial^2 F}{\partial x \partial y} = 0, \quad \int_0^b \left(\frac{\partial^2 F}{\partial y^2}\right) dy = 0, \text{ and } u = \text{constant at } x=0, a,$$

$$\frac{\partial^2 F}{\partial x \partial y} = 0, \quad \int_0^a \left(\frac{\partial^2 F}{\partial x^2}\right) dx = 0, \text{ and } v = \text{constant at } y=0, b, \tag{16}$$

permit free movement of edges with zero inplane stress. Here, again, the vanishing of inplane membrane stress is imposed by the integral constraint. We shall be concerned in this report with the immovable edge conditions, and thereby exhibit thermal buckling under general temperature distributions.

Stress Tensor

Rather than displacements, the stress and strain are the more physically relevant quantifiers in structural analysis. We shall, therefore, present here the stress components expressed in F and w, from which the strain components can be recovered by Eq. (1). Let us begin with the following expressions

$$\varepsilon_x = \frac{\partial u}{\partial x} - z \frac{\partial^2 w}{\partial x^2},$$

$$\varepsilon_y = \frac{\partial v}{\partial y} - z \frac{\partial^2 w}{\partial y^2},$$

$$\varepsilon_{xy} = \frac{1}{2}\left(\frac{\partial u}{\partial y} + \frac{\partial v}{\partial x}\right) - z \frac{\partial^2 w}{\partial x \partial y}. \tag{17}$$

computed by assuming that surfaces which are parallel and normal to the mid-plate remain so after heating. (Eq. (17) is identical to Eq. (12.2.1) of Weiner and Boley [7] with the replacement $\gamma_{xy} = 2\varepsilon_{xy}$.) Let us insert Eq. (17) into Eq. (3) to obtain

$$\sigma_x = \frac{E}{(1-\mu^2)}\left\{\left(\frac{\partial u}{\partial x} + \mu \frac{\partial v}{\partial y}\right) - z\left(\frac{\partial^2 w}{\partial x^2} + \mu \frac{\partial^2 w}{\partial y^2}\right) - (1+\mu)\alpha T\right\},$$

$$\sigma_y = \frac{E}{(1-\mu^2)}\left\{\left(\frac{\partial v}{\partial y} + \mu \frac{\partial u}{\partial x}\right) - z\left(\frac{\partial^2 w}{\partial y^2} + \mu \frac{\partial^2 w}{\partial x^2}\right) - (1+\mu)\alpha T\right\},$$

$$\sigma_{xy} = \frac{E}{(1+\mu)}\left\{\frac{1}{2}\left(\frac{\partial u}{\partial y} + \frac{\partial v}{\partial x}\right) - z \frac{\partial^2 w}{\partial x \partial y}\right\}. \tag{18}$$

When the stress tensor is averaged over h, one finds that only the symmetric terms survive and the odd (unsymmetric) terms drop out. Hence, we obtain from Eq. (18)

$$\frac{\partial u}{\partial x} + \mu \frac{\partial v}{\partial y} = \frac{(1-\mu^2)}{Eh} N_x + (1+\mu)\alpha T,$$

$$\frac{\partial v}{\partial y} + \mu \frac{\partial u}{\partial x} = \frac{(1-\mu^2)}{Eh} N_y + (1+\mu)\alpha T,$$

$$\frac{\partial u}{\partial y} + \frac{\partial v}{\partial x} = \frac{2(1+\mu)}{Eh} N_{xy}. \tag{19}$$

Now, substituting Eq. (19) back into Eq. (18) yields the stress tensor expressed in F and w (with the use of Eq. (7))

$$\sigma_x = \frac{1}{h}\frac{\partial^2 F}{\partial y^2} - \frac{Ez}{(1-\mu^2)}\left(\frac{\partial^2 w}{\partial x^2} + \mu\frac{\partial^2 w}{\partial y^2}\right) - \frac{E\alpha z\theta}{(1-\mu)},$$

$$\sigma_y = \frac{1}{h}\frac{\partial^2 F}{\partial x^2} - \frac{Ez}{(1-\mu^2)}\left(\frac{\partial^2 w}{\partial y^2} + \mu\frac{\partial^2 w}{\partial x^2}\right) - \frac{E\alpha z\theta}{(1-\mu)},$$

$$\sigma_{xy} = -\frac{1}{h}\frac{\partial^2 F}{\partial x \partial y} - \frac{Ez}{(1+\mu)}\frac{\partial^2 w}{\partial x \partial y}. \tag{20}$$

after circuitous substitutions.

In retrospect, the assumption that the derivatives $\partial u/\partial x$, $\partial v/\partial y$, $\partial^2 w/\partial x^2$, ..., are constant across the plate was essential in arriving at Eq. (19). Obviously, this cannot be true in composite plates, as pointed out to me by Steve Whitehouse. Furthermore, it is because of this assumption that the nonlinear strain tensor (i.e., the terms $(1/2)(\partial w/\partial x)^2$, $(1/2)(\partial w/\partial y)^2$, and $(1/2)(\partial w/\partial x)(\partial w/\partial y)$ being incorporated into the right-hand sides of ε_x, ε_y, and ε_{xy}, respectively) also gives rise to the same Eq. (20), as pointed out to me by Jay Lavraea.

Note that Eq. (20) is identical to Eqs. (29-31) of Choi and Vaicaitis [12] when N_x^b and N_y^b are set to zero in their equations. For later reference we point out that in Eq. (20) the first term is the membrane stress, the second term the bending stress, and the third term represents the thermal stress induced by temperature gradient across h.

Normalized Coordinates

It is convenient to scale x and y by the respective sides a and b of the plate (Fig 1). Introducing $\hat{x}=x/a$ and $\hat{y}=y/b$ and subsequently dropping the karats, we have the pair of compatibility and displacement equations ($\beta=b/a$)

$$\left(\beta^2\frac{\partial^4 F}{\partial x^4} + 2\frac{\partial^4 F}{\partial x^2 \partial y^2} + \beta^{-2}\frac{\partial^4 F}{\partial y^4}\right) + Eh\alpha b^2\left(\frac{\partial^2 T}{\partial x^2} + \beta^{-2}\frac{\partial^2 T}{\partial y^2}\right) = Eh\left(\left(\frac{\partial^2 w}{\partial x \partial y}\right)^2 - \left(\frac{\partial^2 w}{\partial x^2}\right)\left(\frac{\partial^2 w}{\partial y^2}\right)\right), \tag{21}$$

$$\rho h \frac{\partial^2 w}{\partial t^2} + \rho h \xi \frac{\partial w}{\partial t} - p + \frac{D}{b^4}\left(\beta^4 \frac{\partial^4 w}{\partial x^4} + 2\beta^2 \frac{\partial^4 w}{\partial x^2 \partial y^2} + \frac{\partial^4 w}{\partial y^4}\right) + \frac{\alpha(1+\mu)D}{b^2}\left(\beta^2 \frac{\partial^2 \theta}{\partial x^2} + \frac{\partial^2 \theta}{\partial y^2}\right)$$

$$= \frac{\beta^2}{b^4}\left(\frac{\partial^2 w}{\partial x^2}\frac{\partial^2 F}{\partial y^2} + \frac{\partial^2 w}{\partial y^2}\frac{\partial^2 F}{\partial x^2} - 2\frac{\partial^2 w}{\partial x \partial y}\frac{\partial^2 F}{\partial x \partial y}\right), \tag{22}$$

together with the immovable edge conditions

$$\int_0^1\int_0^1\left\{\frac{1}{Eh}\left(\frac{\partial^2 F}{\partial y^2} - \mu\beta^2\frac{\partial^2 F}{\partial x^2}\right) + \alpha b^2 T - \frac{\beta^2}{2}\left(\frac{\partial w}{\partial x}\right)^2\right\}dxdy = 0,$$

$$\int_0^1\int_0^1\left\{\frac{1}{Eh}\left(\beta^2\frac{\partial^2 F}{\partial x^2} - \mu\frac{\partial^2 F}{\partial y^2}\right) + \alpha b^2 T - \frac{1}{2}\left(\frac{\partial w}{\partial y}\right)^2\right\}dxdy = 0, \tag{23}$$

to be considered in the present investigation. And, the stress tensor now has the form

$$\sigma_x = \frac{1}{hb^2}\frac{\partial^2 F}{\partial y^2} - \frac{Ez}{b^2(1-\mu^2)}\left(\beta^2\frac{\partial^2 w}{\partial x^2} + \mu\frac{\partial^2 w}{\partial y^2}\right) - \frac{E\alpha z\theta}{(1-\mu)},$$

$$\sigma_y = \frac{\beta^2}{hb^2}\frac{\partial^2 F}{\partial x^2} - \frac{Ez}{b^2(1-\mu^2)}\left(\frac{\partial^2 w}{\partial y^2} + \mu\beta^2\frac{\partial^2 w}{\partial x^2}\right) - \frac{E\alpha z\theta}{(1-\mu)},$$

$$\sigma_{xy} = -\frac{\beta}{hb^2}\frac{\partial^2 F}{\partial x \partial y} - \frac{\beta Ez}{b^2(1+\mu)}\frac{\partial^2 w}{\partial x \partial y}. \tag{24}$$

Because of the coordinate normalization, it should be remembered henceforth that x and y extend over (0,1).

Boundary Conditions

Besides the edge constraints, we further assume that the plate edges undergo no transverse displacement

$$w(0,y) = w(1,y) = w(x,0) = w(x,1) = 0. \tag{25}$$

For a simply-supported plate the tangential components of the bending moment being zero implies (Eq. (12.4.2) of Boley and Weiner [7])

$$\beta^2\frac{\partial^2 w}{\partial x^2} + \alpha b^2(1+\mu)\theta = 0 \text{ at } x=0, 1,$$

$$\frac{\partial^2 w}{\partial y^2} + \alpha b^2(1+\mu)\theta = 0 \text{ at } y=0, 1. \tag{26}$$

Since Eq. (26) is the inhomogeneous boundary conditions, the usual sine expansion

$$w(x,y) = \sum_{m=0}^{\infty}\sum_{n=0}^{\infty} w_{mn} \Psi_m(x)\Psi_n(y), \tag{27}$$

where $\Psi_m(x) = \sin(m\pi x)$, cannot be used unless $\theta = 0$ around the plate edge. Then,

Eq. (26) degenerates to the homogeneous boundary conditions

$$\frac{\partial^2 w}{\partial x^2} = 0 \text{ at } x=0, 1 \quad \text{and} \quad \frac{\partial^2 w}{\partial y^2} = 0 \text{ at } y=0, 1. \tag{28}$$

On the other hand, for a clamped plate we have (Eq. (12.3.1) of Boley and Weiner [7])

$$\frac{\partial w}{\partial x} = 0 \text{ at } x=0, 1 \quad \text{and} \quad \frac{\partial w}{\partial y} = 0 \text{ at } y=0, 1, \tag{29}$$

as given by Eq. (12.3.1) of Boley and Weiner [7], which are independent of the temperature gradient. We may therefore continue to use the trigonometric function expansion

$$w(x,y) = \sum_{m=0}^{\infty} \sum_{n=0}^{\infty} w_{mn} \phi_m(x) \phi_n(y), \tag{30}$$

where $\phi_m(x) = \cos(m+1)\pi x - \cos(m-1)\pi x$, as has already been applied to the thermal buckling [6] and sonic fatigue [10] problems.

III. The Derivation of Modal Equations

Using expansion Eqs. (2.27) and (2.30), one can reduce the set of partial differential Eqs. (2.21-2.22) to ordinary differential equations for w_{mn}. However, owing to the presence of Airy's stress function, this reduction would lead to an infinite set of modal equations. It is, therefore, necessary to truncate the modal equations for practical computation -- an *ad hoc* procedure not dictated by the problem. For a simply-supported plate the introduction of Eq. (2.27) into Eqs. (2.21-2.23) gives rise to the modal equations with diagonal mass, damping, and stiffness matrices. On the other hand, Eq. (2.30) will result in the mass, damping, and stiffness matrices which are nondiagonal in the clamped-plate case. This is because ϕ_m are not orthogonal and the form of ϕ_m changes after the second and fourth-order differentiations. The latter simply restates that $Y=\phi_m(x)\phi_n(y)$ is not an engenfunction of $\nabla^4 Y - \lambda Y = 0$. We shall first present in Sec. IIIa the modal equations for a simply-supported plate, prior to the more complicated deriva- tion for the clamped plate in Sec. IIIb.

A. Simply-Supported Plate

Expanding the particular solution of Eq. (2.8) in cosines, we write in view of Eq. (2.13)

$$P = -\frac{P_x b^2 y^2}{2} - \frac{P_y a^2 x^2}{2} + Eh \sum_{p=0}^{\infty} \sum_{q=0}^{\infty} F_{pq} \cos p\pi x \cos q\pi y, \tag{1}$$

where P_x and P_y are integration constants for the homogeneous biharmonic equation. Here, we have invoked $P_{xy}=0$ in anticipation of $\partial^2 P/\partial x \partial y = 0$, as required by the immovable edge condition. Also, a similar expansion in cosines is assumed for T [13]

$$T = t_0 + \sum_{p=0}^{\infty} \sum_{q=0}^{\infty} t_{pq} \cos p\pi x \cos q\pi y, \tag{2}$$

where t_0 is constant temperature over the plate. Note that in Eqs. (1-2) the term for $p=q=0$ is excluded from the double sum. Instead of Eq. (2.27), let us redefine the expansion by

$$w(x,y) = \sum_{m=0}^{\infty} \sum_{n=0}^{\infty} w_{mn} \psi_m(x) \psi_n(y). \tag{3}$$

where $\psi_m = \sqrt{2} \sin(m\pi x)$ are the orthonormal eigenfunctions.

The compatibility With the use of Eq. (3) the right-hand side of Eq. (2.21) can be expanded in a cosine series

$$\left(\frac{\partial^2 w}{\partial x \partial y}\right)^2 - \left(\frac{\partial^2 w}{\partial x^2}\right)\left(\frac{\partial^2 w}{\partial y^2}\right) = \pi^4 \sum_{p=0}^{\infty} \sum_{q=0}^{\infty} g_{pq} \cos p\pi x \cos q\pi y, \tag{4}$$

where g_{pq} is given by Eq. (A7) of Appendix A. Hence, after substituting Eqs.

(1-2) into Eq. (2.21), we collect the following coefficients with the use of Eq. (4)

$$F_{pq} = \frac{\alpha b^2 t_{pq}}{\pi^2 (p^2 \beta^2 + q^2)} + \frac{\mathcal{E}_{pq}}{(p^2 \beta + q^2/\beta)^2} .$$ (5)

As pointed out in Appendix A, $\mathcal{E}_{pq}$ consists of the nine sums $B_1 - B_9$ of Levy [5].

The displacement In parallel to Eq. (3), the θ and p are also expanded by ψ_m

$$\begin{pmatrix} \theta(x,y) \\ p(x,y) \end{pmatrix} = \sum_{m=0}^{\infty} \sum_{n=0}^{\infty} \begin{pmatrix} \theta_{mn} \\ p_{mn} \end{pmatrix} \psi_m(x) \psi_n(y).$$ (6)

For the derivation of modal equations, it is convenient to put Eq. (2.22) in a symbolic form

$$R_1 + R_2 + R_3 + R_4 = 0,$$ (7)

where

$$R_1 = \rho h \frac{\partial^2 w}{\partial t^2} + \rho h \xi \frac{\partial w}{\partial t} - p,$$

$$R_2 = Db^{-4} \left[\beta^4 \frac{\partial^4 w}{\partial x^4} + 2\beta^2 \frac{\partial^4 w}{\partial x^2 \partial y^2} + \frac{\partial^4 w}{\partial y^4} \right],$$

$$R_3 = \alpha(1+\mu)Db^{-2} \left[\beta^2 \frac{\partial^2 \theta}{\partial x^2} + \frac{\partial^2 \theta}{\partial y^2} \right],$$

$$R_4 = -\beta^2 b^{-4} \left[\frac{\partial^2 w}{\partial x^2} \frac{\partial^2 F}{\partial y^2} + \frac{\partial^2 w}{\partial y^2} \frac{\partial^2 F}{\partial x^2} - 2 \frac{\partial^2 w}{\partial x \partial y} \frac{\partial^2 F}{\partial x \partial y} \right].$$

We then introduce Eqs. (1), (3), and (6) into Eq. (7), and sort out the components for w_{rs}, as in the Galerkin procedure. Because of the orthogonality $\int_0^1 \psi_i \psi_j dx = \delta_j^i$, one can write down at once

$$\int_0^1 \int_0^1 R_1 \psi_r(x) \psi_s(y) dx dy = \rho h \frac{\partial^2 w_{rs}}{\partial t^2} + \rho h \xi \frac{\partial w_{rs}}{\partial t} - p_{rs}.$$ (8)

$$\int_0^1 \int_0^1 R_2 \psi_r(x) \psi_s(y) dx dy = \frac{D\pi^4}{b^4} (\beta^2 r^2 + s^2)^2 w_{rs}.$$ (9)

$$\int_0^1 \int_0^1 R_3 \psi_r(x) \psi_s(y) dx dy = - \frac{\alpha(1+\mu)D\pi^2}{b^2} (\beta^2 r^2 + s^2) \theta_{rs}.$$ (10)

On the other hand, the treatment for R_4 is complicated because of the product terms in F and w. After some algebra, we obtain

$$\int_0^1 \int_0^1 R_4 \psi_r(x) \psi_s(y) dx dy = - \frac{\beta^2 \pi^2}{b^4} (P_x b^2 r^2 + P_y a^2 s^2) w_{rs} - \frac{\beta^2 \pi^4 Eh}{4b^4} \mathcal{F}_{rs}(w_{mn}, F_{pq}),$$ (11)

as shown by Eq. (B5) of Appendix B. Here, we have indicated the explicit dependence of $\mathcal{F}_{rs}$ on w_{mn} and F_{pq}. Note that Eq. (11) is still indeterminate owing to the presence of constants P_x and P_y, which we shall evaluate under

-12-

the immovable edge condition of Eq. (2.23). Remembering that $p=q=0$ is excluded from the sums in Eqs. (1-2), we find that

$$P_x = - \frac{Eh}{(1-\mu^2)} \left\{ \frac{1}{2b^2} \left[\beta^2 <<(\frac{\partial w}{\partial x})^2>> + \mu <<(\frac{\partial w}{\partial y})^2>> \right] - (1+\mu)\alpha t_0 \right\},$$

$$P_y = - \frac{Eh}{(1-\mu^2)} \left\{ \frac{1}{2b^2} \left[\mu\beta^2 <<(\frac{\partial w}{\partial x})^2>> + <<(\frac{\partial w}{\partial y})^2>> \right] - (1+\mu)\alpha t_0 \right\}, \qquad (12)$$

where $<<f>> = \int_0^1 \int_0^1 f dx dy$ is the average of f over the plate. After evaluating $<<(\frac{\partial w}{\partial x})^2>>$ and $<<(\frac{\partial w}{\partial y})^2>>$, and inserting P_x and P_y back into Eq. (11), we write the final expression in the following form

$$\int_0^1 \int_0^1 R_4 \psi_r(x) \psi_s(y) dx dy = I_1 + I_2 + I_3 + I_4, \qquad (13)$$

where

$$I_1 = - \frac{\pi^2 Eh\alpha t_0}{b^2(1-\mu)} (\beta^2 r^2 + s^2) w_{rs},$$

$$I_2 = - \frac{\pi^2 \beta^2 \alpha Eh}{4b^2} \mathcal{F}_{rs}(w_{mn}, \frac{t_{pq}}{(\beta^2 p^2 + q^2)}),$$

$$I_3 = \frac{\beta^2 \pi^4 Eh}{2b^4(1-\mu^2)} \left\{ r^2 (\beta^2 \sum_{m,n=1}^{\infty} m^2 w_{mn}^2 + \mu \sum_{m,n=1}^{\infty} n^2 w_{mn}^2) + s^2 (\mu \sum_{m,n=1}^{\infty} m^2 w_{mn}^2 + \beta^{-2} \sum_{m,n=1}^{\infty} n^2 w_{mn}^2) \right\} w_{rs},$$

$$I_4 = - \frac{\pi^4 \beta^2 Eh}{4b^4} \mathcal{F}_{rs}(w_{mn}, \frac{\varepsilon_{pq}}{(\beta p^2 + q^2/\beta)^2}).$$

According to Eq. (`), by setting the sum of Eqs. (8-10) and (13) to zero we obtain the modal equation for w_{rs} of a simply-supported plate. Although it is possible to consolidate Eq. (13) into a more compact form, we prefer to leave it in the present form involving ε_{pq} and $\mathcal{F}_{rs}$, for readability is more important than compactness when one attempts to enumerate the modal equations.

B. Clamped Plate

Although it is most desired to expand $w(x,y)$ by the orthonormal eigenfunctions of $\nabla^4 Y - \lambda Y = 0$ for the clamped-plate boundaries, the use of such eigenfunctions is indeed intractable for the derivation of modal equations, similar to what we have done in Sec. IIIa. Therefore, we shall be content here with the use of ϕ_m which may be expressed alternately by $\phi_m(x) = 2S_m(x)$, where $S_m(x) = \sin(m\pi x)\sin m\pi x$. Since ϕ_m are independent, we construct the orthonormal functions φ_m from S_m by the Gram-Schmidt procedure [14]. Since $S_1(x)$, $S_3(x)$, ... are even functions of x and $S_2(x)$, $S_4(x)$,... are odd functions, one finds that the orthonormalized $\varphi_m(x)$ also split into the even-shaped components

$$\varphi_1(x) = \sqrt{8/3} S_1(x), \quad \varphi_3(x) = \sqrt{24/5} S_3(x) + \sqrt{6/15} S_1(x), \quad \dots$$

and the odd-shaped components

$$\varphi_2(x)=2S_2(x), \quad \varphi_4(x)=\sqrt{16/3}S_4(x)+\sqrt{4/3}S_2(x), \quad \ldots$$

As an illustration, we have compared in Fig. 2 the primitive ϕ_1 and ϕ_3 with the orthonormalized φ_1 and φ_3. Summing up the even and odd components, we have the following orthonormal bases

$$\varphi_m(x) = \Sigma_1^m a_{mi} S_i(x), \tag{14}$$

where

$$a_{mi} = \begin{bmatrix} \sqrt{8/3} & 0 & 0 & 0 & 0 & 0 & . & . \\ 0 & 2 & 0 & 0 & 0 & 0 & . & . \\ \sqrt{8/15} & 0 & \sqrt{24/5} & 0 & 0 & 0 & . & . \\ 0 & \sqrt{4/3} & 0 & \sqrt{16/3} & 0 & 0 & . & . \\ \sqrt{8/35} & 0 & 3\sqrt{8/35} & 0 & \sqrt{40/7} & 0 & . & . \\ 0 & \sqrt{2/3} & 0 & \sqrt{8/3} & 0 & \sqrt{6} & . & . \\ . & . & . & . & . & . & . & . \\ . & . & . & . & . & . & . & . \end{bmatrix}$$

is the lower triangular matrix. Hence, in contrast to Eq. (2.30), the orthonormal expansion for a clamped plate is given by

$$w(x,y) = \Sigma_{m=0}^{\infty}\Sigma_{n=0}^{\infty} w_{mn}\varphi_m(x)\varphi_n(y)$$

$$= \Sigma_{m=0}^{\infty}\Sigma_{n=0}^{\infty}\Sigma_1^m\Sigma_j^n w_{mn}a_{mi}a_{nj}S_i(x)S_j(y). \tag{15}$$

Note that the second equality gives the working definition for modal expansion.

The compatibility Substituting Eqs. (1-2) and (15) into Eq. (2.21), we obtain by collecting the coefficients for p and q

$$P_{pq} = \frac{ab^2 t_{pq}}{\pi^2(p^2\beta^2+q^2)} + \frac{P_{pq}}{(p^2\beta + q^2/\beta)^2}, \tag{16}$$

where P_{pq} is given by Eq. (C12) of Appendix C. Note that P_{pq} is considerably more complicated than $\mathcal{E}_{pq}$ (Appendix A) due to, in part, the use of orthonormal bases. However, it presents no serious handicap in that both $\mathcal{E}_{pq}$ and P_{pq} are too unwieldy for hand enumeration and hence, in any event, will have to be enumerated by symbolic manipulations on a computer (see, Appendix D).

To establish a contact with Paul's tabulated results (Appendix B of Ref. [6]), we must remember that his analysis was based on the nonorthogonal expansion of Eq. (2.30). However, note that Eq. (15) does reduce to Eq. (2.30) under $a_{ij}=\delta_j^i$. For instance, of the 30 quadratic terms listed in Eq. (D1) of Appendix D, there are 10 terms which involve only the diagonal a_{ii}. Hence, with $a(1,1)=a(3,3)=1$ the 10 terms simplify to give

$$\mathcal{L}_{02} - \mathcal{G}_{02} = 32w_{11}^2 - 48w_{11}w_{12} - 64w_{11}w_{31} + 48w_{11}w_{33} + 16w_{13}^2$$
$$+48w_{13}w_{31} - 32w_{13}w_{33} + 160w_{31}^2 - 240w_{31}w_{33} - 80w_{33}^2. \tag{17}$$

On the other hand, Paul presented the following matrix (the tabulation for
P=0 and Q=2 in Appendix B of Ref. [6])

$$Q_{02} = \begin{bmatrix} 32 & 16 & -32 & -16 \\ -64 & 16 & 64 & -16 \\ -32 & -16 & 180 & 80 \\ 84 & -16 & -320 & 80 \end{bmatrix}.$$

to form P_{02} by $W^T Q_{02} W$, where W is the column vector $(w_{11},w_{13},w_{31},w_{03})$ and T is
the transpose. It is easily checked that $W^T Q_{02} W$ is identical to Eq. (17).
Furthermore, other components of P_{pq} can also be checked against Paul's tabu-
lated results in a completely analogous manner.

<u>The displacement</u> In analogy to Eq. (6), we let

$$\begin{Bmatrix} \theta(x,y) \\ p(x,y) \end{Bmatrix} = \sum_{m=0}^{\infty} \sum_{n=0}^{\infty} \begin{Bmatrix} \theta_{mn} \\ p_{mn} \end{Bmatrix} \varphi_m(x) \varphi_n(y), \tag{18}$$

and carry out the Galerkin procedure. In view of $\int_0^1 \varphi_i \varphi_j dx = \delta_j^i$, we have by
inspection

$$\int_0^1 \int_0^1 R_1 \varphi_r(x) \varphi_s(y) dx dy = \rho h \frac{\partial^2 w_{rs}}{\partial t^2} + \rho h \xi \frac{\partial w_{rs}}{\partial t} - p_{rs}. \tag{19}$$

For the biharmonic term we obtain after some algebra

$$\int_0^1 \int_0^1 R_2 \varphi_r(x) \varphi_s(y) dx dy = \frac{D\pi^4}{b^4} \mathcal{R}_1. \tag{20}$$

where $\mathcal{R}_1$ is given by Eq. (E5) of Appendix E. Similary, we have for the
temperature-gradient term

$$\int_0^1 \int_0^1 R_3 \varphi_r(x) \varphi_s(y) dx dy = - \frac{\alpha(1+\mu)D\pi^2}{b^2} \mathcal{R}_2. \tag{21}$$

where

$$\mathcal{R}_2 = - \frac{\rho^2}{8} \sum_{m=1}^{\infty} \theta_{ms} \sum_{I=1}^{m} a_{mI} \sum_{I}' \sum_{J}' JIa_{r(I+I+J)}(I+I)^2 - \frac{1}{8} \sum_{n=1}^{\infty} \theta_{rn} \sum_{j=1}^{n} a_{nj} \sum_{I}' \sum_{J}' JIa_{s(j+I+J)}(j+I)^2.$$

Here, the summation notation $\sum_I' f(I) = f(1) + f(-1)$ of Naekawa [10] was used to
consolidate 8 terms into the 2 terms of $\mathcal{R}_2$. Finally, the integral involving
R_4 is given by Eq. (F6) of Appendix F

$$\int_0^1 \int_0^1 R_4 \varphi_r(x) \varphi_s(y) dx dy = - \frac{\beta^2 \pi^2}{b^4}(P_x b^2 \ell_3 + P_y a^2 \ell_3) - \frac{\beta^2 \pi^4 Eh}{4b^4} \mathcal{F}_{rs}(w_{mn}, F_{pq}). \quad (22)$$

To render Eq. (22) completely determinable, it is necessary to evaluate P_x and P_y under the immovable edge conditions. Using the $<<(\frac{\partial w}{\partial x})^2>>$ and $<<(\frac{\partial w}{\partial y})^2>>$ evaluated in Appendix G, we again rearrange Eq. (22) into linear and cubic contributions

$$\int_0^1 \int_0^1 R_4 \varphi_r(x) \varphi_s(y) dx dy = J_1 + J_2 + J_3 + J_4, \quad (23)$$

where

$$J_1 = - \frac{\pi^2 Eh\alpha t_0}{b^2(1-\mu)}(\beta^2 \ell_3 + \ell_s),$$

$$J_2 = - \frac{\pi^2 \beta^2 \alpha Eh}{4b^2} \mathcal{F}_{rs}(w_{mn}, \frac{t_{pq}}{(\beta^2 p^2 + q^2)}),$$

$$J_3 = \frac{\beta^2 \pi^4 Eh}{2b^4(1-\mu^2)}\left\{(\beta^2 \ell_s + \mu \ell_3)\ell_3 + (\mu \ell_3 + \beta^{-2}\ell_s)\ell_s\right\},$$

$$J_4 = - \frac{\pi^4 \beta^2 Eh}{4b^4} \mathcal{F}_{rs}(w_{mn}, \frac{P_{pq}}{(\beta p^2 + q^2/\beta)^2}).$$

The modal equations for a clamped plate are obtained by assembling Eqs. (19-21) and (23) according to Eq. (7).

For completeness, attempts were made in Appendix I to compare $\mathcal{F}_{rs}$ with the corresponding formulas derived by Paul [6]. However, we can provide only a partial comparison because the orthogonality of Eq. (14), which plays an important role in our formulation, is completely absent in Paul's formulation.

IV. Lowest-Order Modal Equations of Even Mode Shape

The complexity of Eqs. (3.13) and (3.23) prevents us from seeing the overall structure of modal equations. Even more, it is very difficult to assess the role played by each term and thereby demonstrate any inter-relations among the terms of modal equations. To this end, we shall in this section enumerate the lowest-order modal equations which include only the four modes w_{11}, w_{13}, w_{31} and w_{33}. For a unified representation, however, it is necessary to put the modal equations in dimensionless form. As in Ref. [15], we first choose the length scale h, the time scale $\gamma = [\rho h b^4 / \pi^4 D]^{1/2}$, and the force scale $(\rho h^2 / \gamma^2)$. We then introduce the temperature scale T*, which will be defined later for the simply-supported and clamped plates. Using these scales, we form the dimensionless mechanical variables

$$\tau = t/\gamma, \quad P_{rs} = (\gamma^2/\rho h^2) p_{rs}, \quad W_{rs} = w_{rs}/h, \tag{1}$$

and thermal variables

$$T_0 = t_0/T^*, \quad T_{pq} = t_{pq}/T^*, \quad \theta_{rs} = h\theta_{rs}/T^*. \tag{2}$$

Because of the factor h, the θ_{rs} now represents temperature differential rather than gradient across the plate.

A. Simply-Supported Plate

According to Eq. (3.7), the modal equation follows by equating the sum of Eqs. (3.8-3.10) and (3.13) to zero. For the simply-supported plate, the appropriate T* is the critical buckling temperature $T_s^* = \pi^2 h^2 (\beta^2 + 1)/12\alpha b^2 (1+\mu)$, at which the global thermal expansion cancels out the mechanical stiffness for w_{11} [3,16]. Then, the dimensionless modal equations becomes

$$\underbrace{\frac{\partial^2 W_{rs}}{\partial \tau^2}}_{(SSP-1)} + \underbrace{\gamma\xi\frac{\partial W_{rs}}{\partial \tau}}_{(SSP-2)} - \underbrace{P_{rs}}_{(SSP-3)} + \underbrace{(\beta^2 r^2 + s^2)^2 W_{rs}}_{(SSP-4)}$$

$$+6\beta^2\left\{r^2\left(\beta^2\sum_{m,n=1}^{\infty} m^2 W_{mn}^2 + \mu\sum_{m,n=1}^{\infty} n^2 W_{mn}^2\right) + s^2\left(\mu\sum_{m,n=1}^{\infty} m^2 W_{mn}^2 + \beta^{-2}\sum_{m,n=1}^{\infty} n^2 W_{mn}^2\right)\right\}W_{rs}$$

(SSP-5a)

$$-3\beta^2(1-\mu^2)\mathcal{F}_{rs}\left(W_{mn}, \frac{g_{pq}}{(\beta p^2 + q^2/\beta)^2}\right).$$

(SSP-5b)

$$\underbrace{-(\beta^2+1)(\beta^2 r^2 + s^2)T_0 W_{rs}}_{(SSP-6)} - \underbrace{\frac{(1-\mu)\beta^2(\beta^2+1)}{4}\mathcal{F}_{rs}\left(W_{mn}, \frac{T_{pq}}{(\beta^2 p^2 + q^2)}\right)}_{(SSP-7)}$$

$$\underbrace{-\frac{(\beta^2+1)(\beta^2 r^2 + s^2)}{12}\theta_{rs}}_{(SSP-8)} = 0. \tag{3}$$

We may interpret the terms labeled by SSP (simply-supported plate) 1 - 8 as
follows: SSP-1 is the inertial term, SSP-2 represents viscous damping, SSP-3
is the external forcing, SSP-4 is the usual stiffness term, and terms SSP-5a
and 5b represent the cubic nonlinearity. Note that SSP-5a is contribution
from the immovable edge conditions, whereas SSP-5b is derived from the product
terms of w and F. Thermal effects are embodied by the last three terms. That
is, SSP-6 is the global thermal expansion owing to uniform temperature, SSP-7
is the local thermal expansion by temperature variation over the plate, and
SSP-8 represents the thermal moment induced by temperature gradient across the
plate.

Using the $\mathscr{E}_{pq}$ and $\mathscr{F}_{rs}$ tabulated in Appendices A and B, respectively, Eq.
(3) for r and s $=1$ or 3 yields

$$\ddot{W}_{rs} + \gamma\xi\dot{W}_{rs} - P_{rs} + a_{rs}W_{rs} + (SSP-5)_{rs} - (\beta^2+1)T_0 b_{rs}W_{rs}$$

$$- \frac{(1-\mu)\beta^2(\beta^2+1)}{4}\,\mathscr{F}_{rs}(\frac{T_{pq}}{\beta^2 p^2+q^2}) - \frac{(\beta^2+1)}{12}b_{rs}\Theta_{rs} = 0, \qquad (4)$$

where the overhead dot denotes $\partial/\partial\tau$. No sum is implied in Eq. (4) by the
repeated indices, and

$$a_{11}=(\beta^2+1)^2, \quad a_{13}=(\beta^2+9)^2, \quad a_{31}=(9\beta^2+1)^2, \quad a_{33}=81(\beta^2+1)^2, \qquad (5)$$

$$b_{11}=(\beta^2+1), \quad b_{13}=(\beta^2+9), \quad b_{31}=(9\beta^2+1), \quad b_{33}=9(\beta^2+1). \qquad (6)$$

The $\mathscr{F}_{rs}$ given by Eq. (B6) of Appendix B are

$$\mathscr{F}_{11}(\frac{T_{pq}}{\beta^2 p^2+q^2}) = h_1 W_{11} + h_2 W_{13} + h_3 W_{31} + h_4 W_{33},$$

$$\mathscr{F}_{13}(\frac{T_{pq}}{\beta^2 p^2+q^2}) = h_2 W_{11} + h_5 W_{13} + h_6 W_{31} + h_7 W_{33},$$

$$\mathscr{F}_{31}(\frac{T_{pq}}{\beta^2 p^2+q^2}) = h_3 W_{11} + h_6 W_{13} + h_8 W_{31} + h_9 W_{33},$$

$$\mathscr{F}_{33}(\frac{T_{pq}}{\beta^2 p^2+q^2}) = h_4 W_{11} + h_7 W_{13} + h_9 W_{31} + h_{10} W_{33}, \qquad (7)$$

where

$$h_1 = -2(T_{02}+T_{20}/\beta^2), \qquad h_2 = 2T_{02}-4T_{22}/(\beta^2+1)-2T_{04}+T_{24}/(\beta^2+4),$$

$$h_3 = 2T_{20}/\beta^2-4T_{22}/(\beta^2+1)-2T_{40}/\beta^2+T_{42}/(4\beta^2+1),$$

$$h_4 = -9T_{24}/(\beta^2+4)-9T_{42}/(4\beta^2+1), \qquad h_5 = -18(T_{20}/\beta^2+T_{06}/9),$$

$$h_6 = -25T_{24}/(\beta^2+4)-25T_{42}/(4\beta^2+1)+16T_{22}/(\beta^2+1)+4T_{44}/(\beta^2+1),$$

$$h_7 = 18T_{20}/\beta^2 - 18T_{40}/\beta^2 - 36T_{26}/(\beta^2+9) + 9T_{45}/(4\beta^2+9), \quad h_8 = -18(T_{02}+T_{60}/9\beta^2),$$

$$h_9 = 18T_{02} - 18T_{04} - 36T_{62}/(9\beta^2+1) + 9T_{64}/(9\beta^2+4), \quad h_{10} = -18(T_{06}+T_{60}/\beta^2). \tag{8}$$

Finally, the components of SSP-5 are

$$(SSP\text{-}5)_{11} = 4a_1 W_{11}^3 + 2a_2 W_{11} W_{33}^2 + 3a_3 W_{11}^2 W_{13} + 3a_4 W_{11}^2 W_{31} + 2a_5 W_{11} W_{31}^2 + 2a_6 W_{11} W_{13}^2$$
$$+ 2a_7 W_{11} W_{31} W_{33} + 2a_8 W_{11} W_{13} W_{33} + a_9 W_{13} W_{31}^2 + a_{10} W_{13}^2 W_{31} + 2a_{11} W_{11} W_{13} W_{31} + a_{12} W_{13} W_{31} W_{33},$$

$$(SSP\text{-}5)_{13} = a_3 W_{11}^3 + 2a_6 W_{11}^2 W_{13} + a_8 W_{11}^2 W_{33} + a_9 W_{11} W_{31}^2 + 2a_{10} W_{11} W_{13} W_{31} + a_{11} W_{11}^2 W_{31}$$
$$+ a_{12} W_{11} W_{31} W_{33} + 4a_{13} W_{13}^3 + 2a_{14} W_{13} W_{33}^2 + 3a_{15} W_{13}^2 W_{33} + 2a_{16} W_{13} W_{31}^2,$$

$$(SSP\text{-}5)_{31} = a_4 W_{11}^3 + 2a_5 W_{11}^2 W_{31} + a_7 W_{11}^2 W_{33} + 2a_9 W_{11} W_{13} W_{31} + a_{10} W_{11} W_{13}^2 + a_{11} W_{11}^2 W_{13}$$
$$+ a_{12} W_{11} W_{13} W_{33} + 2a_{16} W_{13}^2 W_{31} + 4a_{17} W_{31}^3 + 3a_{18} W_{31}^2 W_{33} + 2a_{19} W_{31} W_{33}^2,$$

$$(SSP\text{-}5)_{33} = 2a_2 W_{11}^2 W_{33} + a_7 W_{11}^2 W_{31} + a_8 W_{11}^2 W_{13} + a_{12} W_{11} W_{13} W_{31} + 2a_{14} W_{13}^2 W_{33} + a_{15} W_{13}^3$$
$$+ a_{18} W_{31}^3 + 2a_{19} W_{31}^2 W_{33} + 4a_{20} W_{33}^3, \tag{9}$$

where the coefficients $a_1 - a_{20}$ involving β and μ are listed in Appendix J. When $\beta = 1$ the expressions for $a_1 - a_{20}$ simplify greatly and reduce to the coefficients $C_1 - C_{12}$ already used in Ref [15]. For r and s>3, it is best to carry out the tedious enumeration by a computer, and a sample listing of such computer enumeration for $\beta = 1.2$ and $\mu^2 = 0.1$ is presented in Appendix K.

B. Clamped Plate

For the clamped plate, using $T_c^* = \pi^2 h^2 (\beta^4 + 2\beta^2/3 + 1)/3 \pi b^2 (1+\mu)(\beta^2+1)$ as the T^*, the modal equations obtained from Eqs. (3.19-3.21) and (3.23) have the dimensionless form in parallel to Eq. (3)

$$\underbrace{\frac{\partial^2 W_{rs}}{\partial \tau^2}}_{(CP\text{-}1)} + \underbrace{\gamma \xi \frac{\partial W_{rs}}{\partial \tau}}_{(CP\text{-}2)} - \underbrace{P_{rs}}_{(Cp\text{-}3)} + \underbrace{[\ell_1(W_{mn})]_{rs}}_{(CP\text{-}4)}$$

$$+ \underbrace{6\beta^2[(\beta^2 \ell_8 + \mu \ell_9)\ell_3 + (\mu \ell_8 + \beta^{-2}\ell_9)\ell_5]_{rs}}_{(CP\text{-}5a)} - \underbrace{3\beta^2(1-\mu^2)\mathcal{J}_{rs}(W_{mn}, \frac{P_{pq}}{(\beta p^2 + q^2/\beta)^2})}_{(CP\text{-}5b)}$$

$$- \underbrace{\frac{4(\beta^4 + 2\beta^2/3 + 1)}{(\beta^2+1)}T_0[\beta^2 \ell_3(W_{mn}) + \ell_5(W_{mn})]_{rs}}_{(CP\text{-}6)}$$

$$- \underbrace{\frac{(1-\mu)\beta^2(\beta^4 + 2\beta^2/3 + 1)}{(\beta^2+1)}\mathcal{J}_{rs}(W_{mn}, \frac{T_{pq}}{(\beta^2 p^2 + q^2)})}_{(CP\text{-}7)}$$

$$- \frac{(\beta^4 + 2\beta^2/3 + 1)}{3(\beta^2 + 1)} [\ell_2(\Theta_{mn})]_{rs} = 0. \qquad (10)$$
$$(CP\text{-}8)$$

Because of the parallelism, Eq. (10) has exactly eight terms CP (clamped plate) 1-8 with the same physical interpretation as SSP 1-8.

In reality, however, the enumeration of Eq. (10) would generate many more terms than Eq. (3) because the terms CP-4, CP-6, and CP-8 are non-diagonal. In any event, the lowest-order components for r and s=1 or 3 are given by

$$\ddot{W}_{rs} + \gamma \xi \dot{W}_{rs} - P_{rs} + [\ell_1]_{rs} + (CP\text{-}5)_{rs} - \frac{4(\beta^4 + 2\beta^2/3 + 1)}{(\beta^2 + 1)} T_0 [\beta^2 \ell_3 + \ell_5]_{rs}$$
$$- \frac{(1-\mu)\beta^2(\beta^4 + 2\beta^2/3 + 1)}{(\beta^2 + 1)} \mathcal{F}_{rs}\left(\frac{T_{pq}}{\beta^2 p^2 + q^2}\right) - \frac{(\beta^4 + 2\beta^2/3 + 1)}{3(\beta^2 + 1)} [\ell_2]_{rs} = 0. \qquad (11)$$

First, the components of CP-4 are

$$[\ell_1]_{11} = \frac{16}{3}(\beta^4 + \frac{2}{3}\beta^2 + 1)W_{11} - \frac{32}{3\sqrt{5}}(\frac{2}{3}\beta^2 + 1)W_{13} - \frac{32\beta}{3\sqrt{5}}(\beta^2 + \frac{2}{3})W_{31} + \frac{128\beta}{45}W_{33},$$

$$[\ell_1]_{13} = -\frac{32}{3\sqrt{5}}(\frac{2}{3}\beta^2 + 1)W_{11} + \frac{16}{3}(\beta^4 + \frac{16}{3}\beta^2 + \frac{148}{5})W_{13} + \frac{128\beta^2}{45}W_{31} - \frac{32\beta^2}{3\sqrt{5}}(\beta^2 + \frac{16}{3})W_{33},$$

$$[\ell_1]_{31} = -\frac{32\beta^2}{3\sqrt{5}}(\beta^2 + \frac{2}{3})W_{11} + \frac{128\beta^2}{45}W_{13} + \frac{16}{3}(\frac{148}{5}\beta^4 + \frac{16}{3}\beta^2 + 1)W_{31} - \frac{32}{3\sqrt{5}}(\frac{16}{3}\beta^2 + 1)W_{33},$$

$$[\ell_1]_{33} = \frac{128\beta^2}{45}W_{11} - \frac{32\beta^2}{3\sqrt{5}}(\beta^2 + \frac{16}{3})W_{13} - \frac{32}{3\sqrt{5}}(\frac{16}{3}\beta^2 + 1)W_{31} + \frac{64}{3}(\frac{37}{5}\beta^4 + \frac{32}{3}\beta^2 + \frac{37}{5})W_{33}. \qquad (12)$$

Second, the components of CP-6 are

$$[\beta^2 \ell_3 + \ell_5]_{11} = \frac{4}{3}(\beta^2 + 1)W_{11} - \frac{8}{3\sqrt{5}}W_{13} - \frac{8\beta^2}{3\sqrt{5}}W_{31},$$

$$[\beta^2 \ell_3 + \ell_5]_{13} = -\frac{8}{3\sqrt{5}}W_{11} + \frac{4}{3}(\beta^2 + 2)W_{13} - \frac{8\beta^2}{3\sqrt{5}}W_{33},$$

$$[\beta^2 \ell_3 + \ell_5]_{31} = -\frac{8\beta^2}{3\sqrt{5}}W_{11} + \frac{8}{3}(2\beta^2 + 1)W_{31} - \frac{8}{3\sqrt{5}}W_{33},$$

$$[\beta^2 \ell_3 + \ell_5]_{33} = -\frac{8\beta^2}{3\sqrt{5}}W_{13} - \frac{8}{3\sqrt{5}}W_{31} + \frac{32}{3}(\beta^2 + 1)W_{33}. \qquad (13)$$

Third, the components of CP-8 are also given by Eq. (13) but with W_{mn} replaced by Θ_{mn} are

$$[\ell_2]_{11} = \frac{4}{3}(\beta^2 + 1)\Theta_{11} - \frac{8}{3\sqrt{5}}\Theta_{13} - \frac{8\beta}{3\sqrt{5}}\Theta_{31},$$

$$[\ell_2]_{13} = -\frac{8}{3\sqrt{5}}\Theta_{11} + \frac{4}{3}(\beta^2 + 2)\Theta_{13} - \frac{8\beta^2}{3\sqrt{5}}\Theta_{33},$$

$$[\mathcal{A}_2]_{31} = -\frac{8\beta^2}{3\sqrt{5}}\theta_{11} + \frac{8}{3}(2\beta^2+1)\theta_{31} - \frac{8}{3\sqrt{5}}W_{33},$$

$$[\mathcal{A}_2]_{33} = -\frac{8\beta^2}{3\sqrt{5}}\theta_{13} - \frac{8}{3\sqrt{5}}\theta_{31} + \frac{32}{3}(\beta^2+1)\theta_{33}. \tag{14}$$

Fourth, the components CP-7 are

$$\mathcal{J}_{11}\left(\frac{T_{pq}}{\beta^2 p^2 + q^2}\right) = g_1 W_{11} + g_2 W_{13} + g_3 W_{31} + g_4 W_{33},$$

$$\mathcal{J}_{13}\left(\frac{T_{pq}}{\beta^2 p^2 + q^2}\right) = g_2 W_{11} + g_5 W_{13} + g_6 W_{31} + g_7 W_{33},$$

$$\mathcal{J}_{31}\left(\frac{T_{pq}}{\beta^2 p^2 + q^2}\right) = g_3 W_{11} + g_6 W_{13} + g_8 W_{31} + g_9 W_{33},$$

$$\mathcal{J}_{33}\left(\frac{T_{pq}}{\beta^2 p^2 + q^2}\right) = g_4 W_{11} + g_7 W_{13} + g_8 W_{31} + g_{10} W_{33}, \tag{15}$$

where g's are given by Eq. (F8) of Appendix F. For instance, we see that

$$g_1 = -14.222(T_{02}+T_{20}\beta^{-2})/4 + 14.222(T_{04}+T_{40}\beta^{-2})/16 + 14.222T_{22}/4(\beta^2+1)$$
$$- 7.111\{T_{24}(\beta^2+4)^{-1}+T_{42}(4\beta^2+1)^{-1}\}/4, \tag{16}$$

and the remaining g's are expressed similarly. Lastly, instead of the analytical expressions, we present here the computer listing of CP-5 with the coefficients evaluated for $\beta=1.2$ and $\mu^2=0.1$

```
(CP-5)₁₁ = 0.76804E+02xW(1,1)W(1,1)W(1,1)-0.14892E+03xW(1,1)W(1,1)W(1,3)
           -0.18330E+03xW(1,1)W(1,1)W(3,1)+0.43305E+02xW(1,1)W(1,1)W(3,3)
           +0.38925E+03xW(1,1)W(1,3)W(1,3)+0.33102E+03xW(1,1)W(1,3)W(3,1)
           -0.28888E+03xW(1,1)W(1,3)W(3,3)+0.55192E+03xW(1,1)W(3,1)W(3,1)
           -0.36109E+03xW(1,1)W(3,1)W(3,3)+0.46008E+03xW(1,1)W(3,3)W(3,3)
           -0.17082E+03xW(1,3)W(1,3)W(1,3)-0.42937E+03xW(1,3)W(1,3)W(3,1)
           +0.17620E+03xW(1,3)W(1,3)W(3,3)-0.45437E+03xW(1,3)W(3,1)W(3,1)
           +0.88712E+03xW(1,3)W(3,1)W(3,3)-0.27129E+03xW(1,3)W(3,3)W(3,3)
           -0.32645E+03xW(3,1)W(3,1)W(3,1)+0.35047E+03xW(3,1)W(3,1)W(3,3)
           -0.54223E+03xW(3,1)W(3,3)W(3,3)-0.92581E+01xW(3,3)W(3,3)W(3,3),

(CP-5)₁₃ =-0.49640E+02xW(1,1)W(1,1)W(1,1)+0.38925E+03xW(1,1)W(1,1)W(1,3)
           +0.16551E+03xW(1,1)W(1,1)W(3,1)-0.14444E+03xW(1,1)W(1,1)W(3,3)
           -0.51247E+03xW(1,1)W(1,3)W(1,3)-0.85874E+03xW(1,1)W(1,3)W(3,1)
           +0.35241E+03xW(1,1)W(1,3)W(3,3)-0.45437E+03xW(1,1)W(3,1)W(3,1)
           +0.88712E+03xW(1,1)W(3,1)W(3,3)-0.27129E+03xW(1,1)W(3,3)W(3,3)
           +0.14310E+04xW(1,3)W(1,3)W(1,3)+0.33868E+03xW(1,3)W(1,3)W(3,1)
```

$$-0.16894E+04xW(1,3)W(1,3)W(3,3)+0.17030E+04xW(1,3)W(3,1)W(3,1)$$
$$-0.78637E+03xW(1,3)W(3,1)W(3,3)+0.31710E+04xW(1,3)W(3,3)W(3,3)$$
$$+0.18257E+03xW(3,1)W(3,1)W(3,1)-0.75391E+03xW(3,1)W(3,1)W(3,3)$$
$$-0.28530E+02xW(3,1)W(3,3)W(3,3)-0.32311E+03xW(3,3)W(3,3)W(3,3)\},$$

$$(CP-5)_{32}=-0.61101E+02xW(1,1)W(1,1)W(1,1)+0.16551E+03xW(1,1)W(1,1)W(1,3)$$
$$+0.55192E+03xW(1,1)W(1,1)W(3,1)-0.18055E+03xW(1,1)W(1,1)W(3,3)$$
$$-0.42937E+03xW(1,1)W(1,3)W(1,3)-0.90874E+03xW(1,1)W(1,3)W(3,1)$$
$$+0.88712E+03xW(1,1)W(1,3)W(3,3)-0.97935E+03xW(1,1)W(3,1)W(3,1)$$
$$+0.70094E+03xW(1,1)W(3,1)W(3,3)-0.54223E+03xW(1,1)W(3,3)W(3,3)$$
$$+0.11289E+03xW(1,3)W(1,3)W(1,3)+0.17030E+04xW(1,3)W(1,3)W(3,1)$$
$$-0.39318E+03xW(1,3)W(1,3)W(3,3)+0.54770E+03xW(1,3)W(3,1)W(3,1)$$
$$-0.15078E+04xW(1,3)W(3,1)W(3,3)-0.28530E+02xW(1,3)W(3,3)W(3,3)$$
$$+0.27674E+04xW(3,1)W(3,1)W(3,1)-0.30167E+04xW(3,1)W(3,1)W(3,3)$$
$$+0.52367E+04xW(3,1)W(3,3)W(3,3)-0.13402E+03xW(3,3)W(3,3)W(3,3),$$

$$(CP-5)_{33}= 0.14435E+02xW(1,1)W(1,1)W(1,1)-0.14444E+03xW(1,1)W(1,1)W(1,3)$$
$$-0.18055E+03xW(1,1)W(1,1)W(3,1)+0.46008E+03xW(1,1)W(1,1)W(3,3)$$
$$+0.17620E+03xW(1,1)W(1,3)W(1,3)+0.88712E+03xW(1,1)W(1,3)W(3,1)$$
$$-0.54259E+03xW(1,1)W(1,3)W(3,3)+0.35047E+03xW(1,1)W(3,1)W(3,1)$$
$$-0.10845E+04xW(1,1)W(3,1)W(3,3)-0.27774E+02xW(1,1)W(3,3)W(3,3)$$
$$-0.56313E+03xW(1,3)W(1,3)W(1,3)-0.39318E+03xW(1,3)W(1,3)W(3,1)$$
$$+0.31710E+04xW(1,3)W(1,3)W(3,3)-0.75391E+03xW(1,3)W(3,1)W(3,1)$$
$$-0.57060E+02xW(1,3)W(3,1)W(3,3)-0.96934E+03xW(1,3)W(3,3)W(3,3)$$
$$-0.10062E+04xW(3,1)W(3,1)W(3,1)+0.52367E+04xW(3,1)W(3,1)W(3,3)$$
$$-0.40205E+03xW(3,1)W(3,3)W(3,3)+0.42215E+04xW(3,3)W(3,3)W(3,3). \quad (17)$$

This therefore completes specification of Eq. (11) for r and s=1 or 3, which clearly involves a lot more terms than Eq. (4) for the simply-supported plate.

V. Hamiltonians for The Modal Equations

Even for only four components of W_{rs}, the modal equations have a bewildering number of constant, linear, and cubic terms. Hence, one cannot help but wonder if the modal equations have included only those terms which rightfully belong to them and left out none inadvertently. The purpose of this section is to show the internal consistency of modal equations. We do this by way of constructing the Hamiltonians for simply-supported and clamped plates, from which Eqs. (4.4) and (4.11) can be recovered by the Hamiltonian equations of motion. Therefore, the readers who have sufficient faith in the accuracy of Sec. IV may skip this section without loss in continuity.

A. Simply-Supported Plate

We define the column vectors $W=(W_{11}, W_{13}, W_{31}, W_{33})$, $T=(\Theta_{11}, \Theta_{13}, \Theta_{31}, \Theta_{33})$, $F=(P_{11}, P_{13}, P_{31}, P_{33})$, the diagonal matrices

$$S_4 = \begin{bmatrix} a_{11} & & & 0 \\ & a_{13} & & \\ & & a_{31} & \\ 0 & & & a_{33} \end{bmatrix}, \quad S_6 = \begin{bmatrix} b_{11} & & & 0 \\ & b_{12} & & \\ & & b_{31} & \\ 0 & & & b_{33} \end{bmatrix},$$

where a_{ij} and b_{ij} are given by Eqs. (4.5) and (4.6), and a symmetric matrix

$$S_7 = \begin{bmatrix} h_1 & h_2 & h_3 & h_4 \\ & h_5 & h_6 & h_7 \\ & & h_8 & h_9 \\ (\text{symm}) & & & h_{10} \end{bmatrix},$$

where h_i are given by Eq. (4.8). With the 4x4 unit matrix I Eq. (4.4) can readily be put in matrix form

$$I\ddot{W} + \gamma\xi I\dot{W} - IF + S_4 W + (SSP-5)_{rs} - (\beta^2+1)T_0 S_6 W$$

$$- \frac{(1-\mu)b^2(\beta^2+1)}{4} S_7 \left(\frac{T_{pq}}{\beta^2 p^2+q^2}\right)W - \frac{(\beta^2+1)}{12}S_6 T = 0. \tag{1}$$

except for the term SSP-5. In fact, one can also express SSP-5 in matrix

$$(SSP-5)_{rs} = 3\beta^2\left\{2S_{8a} - (1-\mu^2)S_7\left[\frac{g_{pq}}{(\beta^2 p^2+q^2/\beta^2)^2}\right]\right\}W. \tag{2}$$

Here, S_{8a} is a 4x4 diagonal matrix with the elements

$$\left\{[(\beta^2+2\mu+\beta^{-2})W_{11}^2 + (\beta^2+10\mu+9\beta^{-2})W_{13}^2 + (9\beta^2+10\mu+\beta^{-2})W_{31}^2 + 9(\beta^2+2\mu+\beta^{-2})W_{33}^2],\right.$$

$$[(\beta^2+10\mu+9\beta^{-2})W_{11}^2 + (\beta^2+18\mu+81\beta^{-2})W_{13}^2 + (9\beta^2+82\mu+9\beta^{-2})W_{31}^2 + 9(\beta^2+10\mu+9\beta^{-2})W_{33}^2],$$

$$[(9\beta^2+10\mu+\beta^{-2})W_{11}^2 + (9\beta^2+82\mu+9\beta^{-2})W_{13}^2 + (81\beta^2+18\mu+\beta^{-2})W_{31}^2 + 9(9\beta^2+10\mu+\beta^{-2})W_{33}^2],$$

$$9[(\beta^2+2\mu+\beta^{-2})W_{11}^2+(\beta^2+10\mu+9\beta^{-2})W_{13}^2+(9\beta^2+10\mu+\beta^{-2})W_{31}^2+9(\beta^2+2\mu+\beta^{-2})W_{33}^2]\Big\}.$$

And, $S_7[.]$ denotes a symmetric matrix with the element h_i.

In the absence of viscous damping, it is straightforward to deduce the Hamiltonian for Eq. (1). To do this requires defining a column vector Q with the components $q_1=W_{11}$, $q_2=W_{13}$, $q_3=W_{31}$, $q_4=W_{33}$, and a column vector P with the conjugate variables $p_1=\dot{W}_{11}$, $p_2=\dot{W}_{13}$, $p_3=\dot{W}_{31}$, $p_4=\dot{W}_{33}$. Ignoring the SSP-2, the Hamiltonian H_s of the simply-supported plate is given by

$$H_s=\frac{1}{2}\Big\{P^TIP+Q^TS_4Q-(\beta^2+1)T_0Q^TS_6Q-\frac{(1-\mu)b^2(\beta^2+1)}{4}Q^TS_7(\frac{T_{pq}}{\beta^2p^2+q^2})Q\Big\}$$

$$-Q^TIF-\frac{(\beta^2+1)}{12}Q^TS_6I+h_s. \tag{3}$$

Here, h_s denotes contribution by the SSP-5, to be determined presently. Although it is tempting to formally define h_s by premultiplying Eq. (2) by Q^T, the resulting quartic expression, though correct in form, does not have the correct coefficients. This is because the quartic form, unlike a quadratic form, generate nonuniform numerical factors under differentiation. We shall therefore deduce h_s directly from Eq. (4.9) [15]

$$h_s=a_1q_1^4+a_2q_1^2q_4^2+a_3q_1^3q_2+a_4q_1^3q_3+a_5q_1^2q_3^3+a_6q_1^2q_2^2+a_7q_1^2q_3q_4+a_8q_1^2q_2q_4$$

$$+a_9q_1q_2q_3^2+a_{10}q_1q_3^2q_3+a_{11}q_1^2q_2q_3+a_{12}q_1q_2q_3q_4+a_{13}q_2^4+a_{14}q_2^2q_4^2$$

$$+a_{15}q_2^3q_4+a_{16}q_2^2q_3^2+a_{17}q_3^4+a_{18}q_3^3q_4+a_{19}q_3^2q_4^2+a_{20}q_4^4. \tag{4}$$

It is simple to checked that Eq. (4.4) is recovered from the Hamiltonian equations of motion

$$\dot{q}_i=\partial H/\partial p_i, \quad \dot{p}_i=-\partial H/\partial q_i, \tag{5}$$

when $H=H_s$ is given by Eqs. (3-4).

B. Clamped Plate

Similarly, Eq. (4.11) can also be put in matrix form

$$I\ddot{W}+\xi I\dot{W}-IF+C_4W+(CP-5)_{rs}-\frac{4(\beta^4+2\beta^2/3+1)}{(\beta^2+1)}T_0C_6W$$

$$-\frac{(1-\mu)\beta^2(\beta^4+2\beta^2/3+1)}{(\beta^2+1)}C_7(\frac{T_{pq}}{\beta^2p^2+q^2})W-\frac{(\beta^4+2J^2/3+1)}{3(\beta^2+1)}C_6I=0, \tag{S}$$

where

$$C_4 = \begin{bmatrix} \frac{16}{3}(\beta^4+\frac{2}{3}\beta^2+1) & \frac{-32}{3\sqrt{5}}(\frac{2}{3}\beta^2+1) & \frac{-32\beta^2}{3\sqrt{5}}(\beta^2+\frac{2}{3}) & \frac{128\beta^2}{45} \\[6pt] & \frac{16}{3}(\beta^4+\frac{16}{3}\beta^2+\frac{148}{5}) & \frac{128\beta^2}{45} & \frac{-32\beta^2}{3\sqrt{5}}(\beta^2+\frac{16}{3}) \\[6pt] & & \frac{16}{3}(\frac{148}{5}\beta^4+\frac{16}{3}\beta^2+1) & \frac{-32}{3\sqrt{5}}(\frac{16}{3}\beta^2+1) \\[6pt] (\text{sym}) & & & \frac{64}{3}(\frac{37}{5}\beta^4+\frac{32}{3}\beta^2+\frac{37}{5}) \end{bmatrix},$$

$$C_6 = \begin{bmatrix} \frac{4}{3}(\beta^2+1) & \frac{-8}{3\sqrt{5}} & \frac{-8\beta^2}{3\sqrt{5}} & 0 \\[6pt] & \frac{4}{3}(\beta^2+2) & 0 & \frac{-8\beta^2}{3\sqrt{5}} \\[6pt] & & \frac{8}{3}(2\beta^2+1) & \frac{-8}{3\sqrt{5}} \\[6pt] (\text{sym}) & & & \frac{32}{3}(\beta^2+1) \end{bmatrix}, \qquad C_7 = \begin{bmatrix} g_1 & g_2 & g_3 & g_4 \\ & g_5 & g_6 & g_7 \\ & & g_8 & g_9 \\ (\text{sym}) & & & g_{10} \end{bmatrix},$$

where g_i are given by Eq. (4.15). Hence, the Hamiltonian H_c for the clamped plate becomes

$$H_c = \frac{1}{2}\left\{ P^T I P + Q^T C_4 Q - \frac{4(\beta^4+2\beta^2/3+1)}{(\beta^2+1)}T_0 Q^T C_6 Q - \frac{(1-\mu)\beta^2(\beta^4+2\beta^2/3+1)}{(\beta^2+1)}Q^T C_7(\frac{T_{pq}}{\beta^2 p^2+q^2})Q\right\}$$

$$- Q^T I F - \frac{(\beta^4+2\beta^2/3+1)}{3(\beta^2+1)}Q^T C_6 T + h_c. \tag{7}$$

And, the contribution by CP-5 deduced from Eq. (4.17) is

$h_c=$ 0.19201E+02xq(1)q(1)q(1)q(1)   -0.49640E+02xq(1)q(1)q(1)q(2)
-0.61101E+02xq(1)q(1)q(1)q(3)   +0.14435E+02xq(1)q(1)q(1)q(4)
+0.19463E+03xq(1)q(1)q(2)q(2)   +0.16351E+03xq(1)q(1)q(2)q(3)
-0.14444E+03xq(1)q(1)q(2)q(4)   +0.27596E+03xq(1)q(1)q(3)q(3)
-0.18055E+03xq(1)q(1)q(3)q(4)   +0.23004E+03xq(1)q(1)q(4)q(4)
-0.17082E+03xq(1)q(2)q(2)q(2)   -0.42937E+03xq(1)q(2)q(2)q(3)
+0.17620E+03xq(1)q(2)q(2)q(4)   -0.45437E+03xq(1)q(2)q(3)q(3)
+0.88712E+03xq(1)q(2)q(3)q(4)   -0.27129E+03xq(1)q(2)q(4)q(4)
-0.32645E+03xq(1)q(3)q(3)q(3)   +0.35047E+03xq(1)q(3)q(3)q(4)
-0.54223E+03xq(1)q(3)q(4)q(4)   -0.92581E+01xq(1)q(4)q(4)q(4)
+0.35776E+03xq(2)q(2)q(2)q(2)   +0.11289E+03xq(2)q(2)q(2)q(3)
-0.56313E+03xq(2)q(2)q(2)q(4)   +0.85149E+03xq(2)q(2)q(3)q(3)
-0.39318E+03xq(2)q(2)q(3)q(4)   +0.15855E+04xq(2)q(2)q(4)q(4)
+0.18257E+03xq(2)q(3)q(3)q(3)   -0.75391E+03xq(2)q(3)q(3)q(4)

$$-0.28530E+02xq(2)q(3)q(4)q(4) \quad -0.32311E+03xq(2)q(4)q(4)q(4)$$
$$+0.69186E+03xq(3)q(3)q(3)q(3) \quad -0.10062E+04xq(3)q(3)q(3)q(4)$$
$$+0.26183E+04xq(3)q(3)q(4)q(4) \quad -0.13402E+03xq(3)q(4)q(4)q(4)$$
$$+0.10554E+04xq(4)q(4)q(4)q(4). \tag{8}$$

Again, the Hamiltonian equations of motion rederive Eq. (4.11) when $H=H_c$.

Summing up, the existence of H_s and H_c strongly suggests the internal consistency of modal equations for the simply-supported and clamped plates, whereby no terms have been added or left out inadvertently. Unfortunately, this does not prove the absolute correctness of the modal equations derived in Sec. III. The reason is that the Hamiltonians are deduced, in part, from the modal equations. Hence, errors that are consistent with the Hamiltonian formulation can remain undetected.

VI. Mid-Plate Temperature Variation and Gradient

To proceed further with the modal equations, it is necessary to specify T_{pq} and Θ_{rs} which appear in Eqs. (4.4) and (4.11). Returning to Eq. (2.3), we first split $T(x,y)$ into the uniform temperature t_0 and temperature variation $t_v(x,y)$ over the plate

$$T = t_0 + t_v(x,y), \tag{1}$$

as in Eq. (3.2). We then convert θ to the corresponding temperature differential Θ (see, Eq. (4.2))

$$\Theta = h\theta. \tag{2}$$

In view of Eqs. (1-2), we may put Eq. (2.3) in the following form

$$T = t_0 + t_v(x,y) + z\Theta(x,y), \tag{3}$$

where $Z=z/h$ ranges over $(1/2,-1/2)$. Since t_0 will be assumed nonzero, we use it as the main thermal parameter to express the magnitudes of t_v and Θ

$$t_v = \delta_v t_0 f_v(x,y), \quad \Theta = \delta_g t_0 f_g(x,y). \tag{4}$$

Here, the scaling factor δ_v defines the magnitude $\delta_v t_0$ of temperature variation whose profile over the plate is given by $f_v(x,y)$. Similarly, $\delta_g t_0$ is the magnitude of temperature gradient through the plate thickness and $f_g(x,y)$ represents its distribution over the plate. Upon introducing Eq. (4) into Eq. (3), we have the dimensionless temperature $\hat{T} = T/T^*$

$$\hat{T} = T_0 + (\delta_v T_0)f_v(x,y) + Z(\delta_g T_0)f_g(x,y), \tag{5}$$

where T^* is T_s^* for a simply-supported plate and T_c^* for a clamped plate.

First of all, for the temperature variation over the plate, we find by comparing Eq. (5) with Eq. (3.2) that

$$(\delta_v T_0)f_v(x,y) = \sum_{p=0}^{\infty} \sum_{q=0}^{\infty} T_{pq} \cos p\pi x \cos q\pi y, \tag{6}$$

which holds for both the simply-supported and clamped plates. Let us examine two examples of $f_v(x,y)$ which are neither constant nor linear. As a first example, we let $f_v = \sin \pi x \sin \pi y$ and find from Eq. (6) that

$$T_{pq} = \frac{16\delta_v T_0}{\pi^2(p^2-1)(q^2-1)(1-\delta_p^0)(1-\delta_q^0)} . \quad (p=q=0 \text{ excluded}) \tag{7}$$

Now, for the second example $f_v = \sin^2 \pi x \sin^2 \pi y$, the sum of Eq. (6) reduces to a finite sum $(1/4)(1-\cos 2\pi x)(1-\cos 2\pi y)$. Hence, we have by inspection

$$T_{20} = T_{02} = -T_{22} = -\delta_v T_0/4, \quad T_{pq} = 0 \text{ (for other p and q).} \tag{8}$$

Since the majority of T_{pq} is zero, Eq. (4.8) reduces to

$$h_1 = \left[\frac{\delta_v T_0}{2}\right](1+\beta^{-2}), \text{ etc.,} \tag{9}$$

for the simply-supported plate, and Eq. (4.16) gives rise to

$$g_1 = \frac{128}{9}\left[\frac{\delta_v T_0}{16}\right][1+\beta^{-2}+\frac{1}{\beta^2+1}], \text{ etc.,} \tag{10}$$

for the clamped plate (Note that the coefficient 14.222 in Eq. (4.16) is 128/9). And, the remaining h's and g's summarized in Appendix L, all have simplified expressions.

Second, for the temperature gradient across the plate thickness we find from Eqs. (3.6) and (3.18)

$$(\delta_g T_0)f_g(x,y) = \sum_{m=0}^{\infty} \sum_{n=0}^{\infty} \Theta_{mn}\eta_m(x)\eta_n(y), \tag{11}$$

where the function η_n is ψ_n for a simply-supported plate and φ_n for the clamped plate case. For maximal simplicity, we shall assume $f_g = \sin\pi x\sin\pi y$ for the simply-supported plate and obtain

$$\Theta_{11} = \delta_g T_0/2 \text{ and } \Theta_{mn} = 0 \text{ (for other m and n).} \tag{12}$$

On the other hand, $f_g = \sin^2\pi x\sin^2\pi y$ gives rise to

$$\Theta_{11} = 3\delta_g T_0/8 \text{ and } \Theta_{mn} = 0 \text{ (for other m and n),} \tag{13}$$

for the clamped plate. Clearly, $\Theta_{mn}=0$ for $m=n\neq1$ is generally not observed under different f_g. Using Eq. (12) the last term of Eq. (4.4) has a single nonzero component $-(\beta^2+1)^2\delta_g T_0/24$. And, similarly, Eq. (4.14) simplifies to $[\ell_2]_{11} = (\beta^2+1)\delta_g T_0/2$, $[\ell_2]_{13} = [\ell_2]_{13}/\beta^2 = -\delta_g T_0/\sqrt{5}$, and $[\ell_2]_{33} = 0$ under Eq. (13).

The relationship between the magnitudes $\delta_v T_0$ and $\delta_g T_0$ is shown schematically in Fig. 3. Although it appears at first sight that the $t_v(x,y)$ and $\Theta(x,y)$ can be assigned arbitrarily, this is not the case when they have a nonuniform distribution over the plate. First of all, we notice that a nonuniform $\Theta(x,y)$ cannot exist unless $t_v(x,y)$ is also nonuniform. That is, $\delta_v=0$ implies $\delta_g=0$. What is then the maximum value of δ_g, denoted by $(\delta_g)_{max}$, for a given δ_v? This cannot be answered, in general, without knowing the profiles $f_v(x,y)$ and $f_g(x,y)$. However, in the case of $f_v(x,y)=f_g(x,y)$ (i.e., $f_v=f_g=\sin^2\pi x\sin^2\pi y$ for the clamped plate discussed), it is readily seen that $(\delta_g)_{max}=2\delta_v$. Sunakawa and Uemura [13] have used a parabolic temperature

distribution for both f_v and f_g, and consequently prescribed $(\delta_g)_{max}=(4/3)\delta_v$, which implies that the upper surface temperature is half the lower surface temperature (see, Eq. (42) in Ref [13]).

In view of the recent attempts [17,18] to generate various temperature profiles by radiant heating, temperature variation profiles of the sort that we have considered here do not appear at all unrealistic. On the other hand, to the best of our knowledge no attempt has yet been made to either measure or impose certain temperature gradient distribution through the plate thickness.

VII. Single-Mode Equation for W_{11}

Let us examine the simplest case of modal equation for W_{11} when all other W_{rs} are absent. With Eqs. (6.9) and (6.12), Eq. (4.4) for the simply-supported plate becomes after letting r=s=1

$$\ddot{W}_{11} + \gamma\xi\dot{W}_{11} + (\beta^2+1)^2\left\{1-T_0[1+\tfrac{1}{6}(1-\mu)\delta_v]\right\}W_{11} + 4a_1W_{11}^3 - [P_{11} + \tfrac{1}{24}(\beta^2+1)^2\delta_gT_0] = 0, \quad (1)$$

where $a_1(\mu,\beta) = \tfrac{3}{4}[(1-\mu^2)(\beta^4+1) + 2(\beta^4+1+2\mu\beta^2)]$ as shown in Appendix J. Similarly, with the use of Eqs. (6.10) and (6.13), Eq. (4.11) for the clamped plate reduces to

$$\ddot{W}_{11} + \gamma\xi\dot{W}_{11} + \tfrac{16}{3}(\beta^4+2\beta^2/3+1)\left\{1- T_0[1+\tfrac{1}{6}(1-\mu)\delta_v\left(1+ \frac{\beta^2}{(\beta^2+1)^2}\right)]\right\}W_{11}$$
$$+ \tfrac{128}{9}d_1W_{11}^3 - [P_{11} + \tfrac{1}{6}(\beta^4+2\beta^2/3+1)\delta_gT_0] = 0, \quad (2)$$

where

$$d_1(\mu,\beta) = \tfrac{3}{4}\beta^2\left\{(\beta^2+\beta^{-2}+2\mu)+(1-\mu^2)\tfrac{4}{9}\left[\tfrac{17}{8}(\beta^2+\beta^{-2})+ \frac{4}{(\beta+\beta^{-1})^2}+ \frac{1}{(\beta+4\beta^{-1})^2}+ \frac{1}{(4\beta+\beta^{-1})^2}\right]\right\}.$$

Here, $(128/9)d_1(\sqrt{0.1},1.2)=76.804$ is the numerical coefficient for $W(1,1)^3$-term in $(CP-5)_{11}$ as given by Eq. (4.17). The eight terms in Eqs. (4.4) and (4.11) have been regrouped into five in Eqs. (1-2). In particular, note that the third term of Eq. (1) is the combined stiffness which subsumes structural stiffness (SSP-4), global thermal expansion by uniform temperature (SSP-6), and local thermal expansion by temperature variation (SSP-7). And, the last term in Eq. (1) is the combined forcing of both the applied external pressure (SSP-3) and thermal moment owing to temperature gradient across the plate (SSP-8). That the temperature gradient plays the role of external forcing has already been observed by Boley and Weiner [7] and Sunakawa and Uemura [13]. In a parallel fashion, the combined stiffness and forcing terms in Eq. (2) are given by the regrouping of terms in Eq. (4.11).

Since Eqs. (1-2) are qualitatively similar, we may present them in a prototype form by denoting $q=W_{11}$ and $f=P_{11}$

$$\ddot{q} + \omega_0\xi\dot{q} + \omega_0^2(1-s)q + \kappa q^3 = f_0 + f, \quad (3)$$

where $\omega_0 = (\beta^2+1)$, $s = T_0[1+\tfrac{1}{6}(1-\mu)\delta_v]$, $\kappa = 4a_1$, $f_0 = \tfrac{1}{24}(\beta^2+1)^2\delta_gT_0$ for the simply-supported plate; and $\omega_0^2 = \tfrac{16}{3}(\beta^4+2\beta^2/3+1)$, $s = T_0[1+\tfrac{1}{6}(1-\mu)\delta_v\left(1+ \frac{\beta}{(\beta^2+1)^2}\right)]$, $\kappa = \tfrac{128}{9}d_1$, $f_0 = \tfrac{1}{6}(\beta^4+2\beta^2/3+1)\delta_gT_0$ for the clamped plate. Note further that $\gamma=\omega_0$ has been introduced. The combined stiffness $\omega_0^2(1-s)$ remains positive as long

as the thermal loading is weak (pre-buckling for $s<1$), whereas it becomes negative under a strong thermal loading (post-buckling for $s>1$).

The Hamiltonian for Eq. (3) including the kinetic energy and potential (strain) energy can be written down from Eqs. (5.3) and (5.7)

$$H = \frac{1}{2}p^2 + \frac{1}{2}\omega_0^2(1-s)q^2 + \frac{\kappa}{4}q^4. \tag{4}$$

As an illustration, we have shown in Fig. 4a the potential energy $U=\frac{1}{2}\omega_0^2(1-s)q^2+\frac{\kappa}{4}q^4$ of a simply-supported plate for $\beta=1$ and $\mu^2=0.1$, while incrementing s from 0 to 3. More visually, however, Fig. 4b depicts the potential energy surface which is a single well potential for $s<1$, but develops symmetric double-well potential as s becomes larger than unity. Both T_0 and $\delta_v T_0$ contribute to the parameter s. We have shown in Fig. 5 the threshold boundary of thermal buckling ($s=1$), which intersects the T_0-axis at $T_0=1$ and approaches the δ_v-axis asymptotically.

A. Thermally Buckled Modal Amplitude

For the static problem, we retain only the terms which do not involve time differentiation

$$\kappa Q^3 + \omega_0^2(1-s)Q - g = 0, \tag{5}$$

where $g=f_0+f$ is the combined forcing. Under a weak thermal loading, the combined stiffness is positive, hence only one root of Eq. (5)

$$Q_1 = \sqrt[3]{\frac{g}{2\kappa} + \sqrt{\frac{g^2}{4\kappa^2} + \frac{\omega_0^6(1-s)^3}{27\kappa^3}}} - \sqrt[3]{-\frac{g}{2\kappa} + \sqrt{\frac{g^2}{4\kappa^2} + \frac{\omega_0^6(1-s)^3}{27\kappa^3}}}, \tag{6}$$

is real. Note that g must be nonzero in Eq. (6); otherwise, $Q_1=0$ is the only real root. Because of $g=f_0+f$, the temperature gradient alone is sufficient to sustain thermal buckling, even when there is no external pressure imposed. In contrast, for a strong thermal loading the combined stiffness becomes negative, hence one may either include [16] or exclude [6] the combined forcing in computing the buckled amplitude. In the latter case, the thermally buckled modal amplitude is

$$Q_2 = \pm\omega_0\sqrt{(s-1)/\kappa}. \tag{7}$$

B. Dynamic Considerations

In the pre-buckled state, $q_0=0$ is the equilibrium state of Eq. (3), and corresponds to the location of single-well potential energy in Fig. 4. Note that Eq. (3) is a Duffing equation [19]. On the other hand, $q_0=0$ becomes unstable in the post-buckled state. Hence, the stable equilibrium states are now given by $q_0=Q_2$, which corresponds to the locations of double-well

potential energy (Fig. 4). We then rewrite Eq. (3)

$$\ddot{q} + \omega_0 \xi \dot{q} - \omega_0^2 (s-1)q + \kappa q^3 = f_0 + f, \tag{8}$$

which is the so-called *buckled beam* equation originally investigated by Holmes [20,21], the trajectory of which wanders in and out of the potential energy wells in a chaotic fashion. By the change of variable

$$q = \pm Q_2 + \tilde{q}, \tag{9}$$

we obtain from Eq. (8)

$$\ddot{\tilde{q}} + \omega_0 \xi \dot{\tilde{q}} + 2\omega_0^2 (s-1)\tilde{q} \pm 3\kappa Q_2 \tilde{q}^2 + \kappa \tilde{q}^3 = f_0 + f, \tag{10}$$

which now represents oscillation about Q_2. Comparing the linear stiffness terms of Eqs. (3) and (10), Schneider [3] has concluded that the natural frequency increases by the factor $\sqrt{2}$ after a thermal buckling. The dynamical behavior of Eqs. (3) and (8) with respect to s will be investigated elsewhere. At present, however, the more compelling need is to estimate the stochastic response, for acoustic excitations will be used in the high-temperature sonic fatigue test facility being constructed at the Structual Dynamics Branch (WL/FIBG).

VIII. Response Estimation by the Equivalent Linearization Technique

Since f_0 is assumed constant, the combined forcing is a Gaussian process superposed on a nonzero-mean level when $f(t)$ is mean-zero Gaussian. The equivalent linearization as originally formulated by Caughey [22] and Booten [23] was built on the zero-mean Gaussian excitation. Hence, it cannot be applied directly to Eqs. (7.3) and (7.10) when $f_0 \neq 0$. In Sec. VIIIa, we restrict ourselves to $f_0 = 0$ and apply the equivalent linearization in its familiar form. The case of $f_0 \neq 0$ will be presented in Sec. VIIIb, after extending the equivalent linearization technique to Gaussian forcing with a nonzero mean (see, Appendix N).

A. Acoustic Loading

For $s<1$ let us denote by q_{lin} the amplitude of linearized Eq. (7.3). Under $f_0 = 0$ the mean square amplitude is given by Eq. (M12) of Appendix M

$$\langle q_{lin}^2 \rangle \approx \frac{\pi \phi_{ff}(\omega_0 \sqrt{1-s})}{\xi \omega_0^3 (1-s)} , \tag{1}$$

where $\langle \ \rangle$ is the statistical (time) average. Here, $\phi_{ff}(\omega)$ is the power spectral density of Gaussian forcing expressed in angular frequency ω [8]. Assuming that $\phi_{ff}(\omega)$ is more or less flat around the sharp resonance peaks at $\omega \approx \omega_0 \sqrt{1-s}$, Eq. (1) has the alternate form

$$\langle q_{lin}^2 \rangle \approx \frac{g_{ff}}{2 \xi \omega_0^3 (1-s)} , \tag{2}$$

using $\phi_{ff}(\omega) = g_{ff}(f)/2\pi$, where f is frequency. The argument of $g_{ff}(f)$ is suppressed, for g_{ff} is assumed a constant power spectral density. Now, for the full nonlinear Eq. (7.3) the mean square amplitude can be estimated by the equivalent linearization technique

$$\langle q^2 \rangle = \frac{\omega_0^2 (1-s)}{6\kappa} \left[\sqrt{1 + \frac{12\kappa \langle q_{lin}^2 \rangle}{\omega_0^2 (1-s)}} - 1 \right], \tag{3}$$

as given by Eq. (M18) of Appendix M. As expected, for a small κ, i.e., weak nonlinearity, Eq. (3) reduces to

$$\langle q^2 \rangle \approx \langle q_{lin}^2 \rangle, \tag{4}$$

whereas, when the cubic nonlinearity is dominant we find that

$$\langle q^2 \rangle \approx \sqrt{\langle q_{lin}^2 \rangle}. \tag{5}$$

Hence, $\langle q^2 \rangle$ increases more gradually as the square root of the magnitude of forcing power spectral density in Eq. (5), rather than linearly in Eq. (4).

As the nonthermal (s=0) reference case, we have evaluated $\langle q_{1in}^2 \rangle$ and $\langle q^2 \rangle$ from Eqs. (2-3) for $\beta=1$, $\mu^2=0.1$, and $\xi=0.04$, and presented in Fig. 6 the maximum mean square displacements computed by

$$\langle (W_{max}/h)^2 \rangle = b\langle q_{1in}^2 \rangle \text{ or } b\langle q^2 \rangle, \tag{6}$$

where b=4 for a simply-supported plate and b=64/9 for a clamped plate. In the figure, the straight lines originating from the origin are the linear input-output relation given by Eq. (2). In contrast, the mean square displacement predicted by Eq. (3) increases more gradually due to the nonlinear energy sharing provided by the equivalent linearization. For a given g_{ff}, the simply-supported plate has a larger mean square displacement than the corresponding clamped plate, as already pointed out by Mei [11].

In the thermal case (s>0), however, the maximum mean square displacement does increase with s, as indicated by the three values of s=0, 0.5, and 0.9 in Fig. 7. However, we notice that the increase is more pronounced in the clamped plate than in simply-supported plate. In both plate cases, the net thermal contribution diminishes as g_{ff} becomes large, which is supported by

$$\langle q^2 \rangle \approx \sqrt{\frac{g_{ff}}{6\xi\kappa\omega_0}}, \tag{7}$$

obtained from Eqs. (2-3) in the limit as $g_{ff} \to \infty$. Eq. (7) states that the response is essentially independent of thermal effects when acoustic excitations become very intense.

Next, let us examine the pair of Eqs. (7.9-7.10) for s>1. Now, denoting by $\tilde{q}_{1in}$ the amplitude of linearized Eq. (7.10), we have in parallel to Eq. (2)

$$\langle \tilde{q}_{1in}^2 \rangle \approx \frac{g_{ff}}{4\xi\omega_0^3(s-1)}. \tag{8}$$

The difference in num...cal factors of Eqs. (2) and (8) is due to the $\sqrt{2}$ factor associated with the post-buckled natural frequency in Eq. (7.10). It is simple to check that the equivalent linearization goes through just as in the pre-buckled case, for the square term $\pm 3\kappa Q_2 q^2$ in Eq. (7.10) has no effect under the Gaussian assumption. Hence, in analogy to Eq. (3) the mean square amplitude is

$$\langle \tilde{q}^2 \rangle = \frac{\omega_0^2(s-1)}{3\kappa}\left[\sqrt{1+ \frac{6\kappa\langle \tilde{q}_{1in}^2 \rangle}{\omega_0^2(s-1)}} - 1\right]. \tag{9}$$

Because of Eq. (7.9), the total mean square amplitude is sum of the buckled plate position and amplitude fluctuations

$$\langle q^2 \rangle = Q_2^2 + \langle \tilde{q}^2 \rangle, \tag{10}$$

since Q_2 and $\tilde{q}$ are statistically independent.

The total mean square displacement shown in Fig. 8 increases greatly with s. Moreover, the increase is considerably more pronouned in a clamped plate (Fig. 8(b)) than simply-supported plate (Fig. 8(a)). However, this rapid increase is mainly due to the contribution of Q_2^2 in Eq. (10). Hence, to separate the contribution of Q_2^2 from that of $<\tilde{q}^2>$, we presented in Fig. 9 the total mean square displacement over the range of s=(0, 3) for a particular value of $g_{ff}=1$. We see from the figure that not only does Q_2^2 increase linearly with (s-1), but also $<\tilde{q}^2>$ actually decreases steadily in the range of s>1 from its maximum value at s=1. The latter is predicted by the asymptotic form of Eq. (8), $<\tilde{q}^2> \propto 1/s$, as s $\rightarrow\infty$. Hence, the mean square displacement falls off as 1/s in the post-buckled state. This has been borne out by the Monte-Carlo simulation of Choi and Vaicaitis [12], in which the amplitude of displacement fluctuations is considerably small whenever the displacement and stress time-histories jump off to thermally buckled positions.

The composite view of total mean square displacements is shown in Fig 10 over the forcing range of $g_{ff}=(0, 5)$. Notice that the clamped plate builds up the total mean square displacement much more rapidly than a simply-supported plate. However, this rapid buildup in the post-buckled state is mostly due to the contribution of buckled plate displacement, as depicted in Fig. 11.

B. Combined Acoustic and Thermal Loading

The analysis of Sec. VIIIa was restricted to $f_0=0$. Clearly, this is valid when a plate is maintained in uniform temperature or there is no heat flux through the plate thickness. The latter is possible when one side of the plate is heated while the other side is insulated. However, under a nonuniform heat flux, the temperature gradient will have a certain distribution over the plate, which is neither constant nor linear. To incorporate f_0 into the acoustic loading, one must extend the equivalent linearization to the nonzero-mean Gaussian excitations. Let us denote by q_c the amplitude under the combined forcing $f_0+f(t)$ and split it into two parts

$$q_c = \bar{x} + y. \tag{11}$$

The implicit assumption is that $\bar{x}$ is the response to f_0 and y to f(t). We first replace q in Eq. (7.3) by q_c and then introduce (11) to obtain

$$\ddot{y} + \omega_0\xi\dot{y} + \{\omega_0^2(1-s)+3\kappa\bar{x}^2\}y + 3\kappa\bar{x}y^2 + \kappa y^3 + \omega_0^2(1-s)\bar{x} + \kappa\bar{x}^3 - f_0 = f. \tag{12}$$

Applying the equivalent linearization technique to Eq. (12) gives rise to

$$\langle y^2 \rangle = \frac{\omega_0^2(1-s)}{6\kappa}\left[\sqrt{\left\{1+\frac{3\kappa\bar{x}^2}{\omega_0^2(1-s)}\right\}^2 + \frac{12\kappa\langle q_{1in}^2\rangle}{\omega_0^2(1-s)}} - \left\{1+\frac{3\kappa\bar{x}^2}{\omega_0^2(1-s)}\right\}\right], \qquad (13)$$

given by Eq. (N17) of Appendix N. Furthermore, the $\bar{x}$ in Eq. (13) is given by Eq. (N20)

$$\bar{x} = \sqrt[3]{\frac{f_0}{6\kappa}+\sqrt{\left[\frac{f_0}{6\kappa}\right]^2+\left(\frac{\omega_0^2(1-s)+3\kappa\langle y^2\rangle}{9\kappa}\right)^3}} - \sqrt[3]{-\frac{f_0}{6\kappa}+\sqrt{\left[\frac{f_0}{6\kappa}\right]^2+\left(\frac{\omega_0^2(1-s)+3\kappa\langle y^2\rangle}{9\kappa}\right)^3}}. \qquad (14)$$

The pair of Eqs. (13) and (14) can be solved simultaneously for $\langle y^2\rangle$ and $\bar{x}$. Afterwards, the total mean square of q_c is computed by sum of the squared $\bar{x}$ and mean square fluctuations owing to acoustic loading

$$\langle q_c^2\rangle = \bar{x}^2 + \langle y^2\rangle. \qquad (15)$$

This is the amplitude response to the combined acoustic-thermal forcing. Note that when $f_0=0$ Eq. (14) becomes $\bar{x}=0$. Then, Eqs. (13) and (15) degenerate to Eq. (7.13) which was derived in Sec. VIIIa under the assumption of $f_0=0$.

Recall that in Sec. VII both T_0 and $\delta_v T_0$ are represented collectively by a single parameter s. Under the combined forcing, however, one must also specify the magnitude of temperature gradient $\delta_g T_0$, in addition to s. For simplicity, we shall assume $\delta_g=\delta_v$ in what follows. For three values of $T_0 = 0.2$, 0.5, and 0.8, we choose δ_v large enough for s to be about 0.96 and compute the total mean square amplitude by Eqs. (13-15). The results are summarized in Figs. 12 and 13 for the simply-supported and clamped plates, respectively. Three plots are presented in each frame of the figures. The first two plots, referring to the left ordinate, are the maximum mean square displacement $b\langle q_c^2\rangle$ under the combined loading (solid curve) and $b\langle q^2\rangle$ under the acoustic loading alone (dotted curve). Here, b=4 for the simply-supported plate and b=64/9 for the clamped plate. One observes that the thermal loading is generally unimportant, unless acoustic excitations are very weak. Now, to accentuate the difference of the first two plots, the third plot with respect to the right ordinate, shows the difference of the first two in percent, i.e.,
$\Delta\langle(w_{max}/h)^2\rangle=100(\langle q_c^2\rangle-\langle q^2\rangle)/\langle q_c^2\rangle$. All the third plots fall off rapidly from the initial 100% as g_{ff} increases. Even in the most thermal-loading sensitive case (Fig. 13a), we find that $\Delta\langle(w_{max}/h)^2\rangle$ drops down to 4% when g_{ff} approaches unity.

C. RMS stress and strain

The lesson of Sec VIIIb is that the temperature gradient across the plate

which appears as an additional loading, is generally unimportant, as long as the acoustic loading is dominant. Quantitatively, for $g_{ff}>1$ we can ignore the effect of temperature gradient, and hence consider only the uniform temperature and temperature variation over the plate. Nevertheless, since the αT term appears explicitly in Eqs. (2.1-2.2), one suspects that the temperature gradient might contribute to the stress and strain tensors as equally as the uniform temperature and temperature variation. The purpose of this subsection is to substantiate this suspicion.

To this end, we express the normal stress and strain components involving only the W_{11} in the following form

$$\begin{Bmatrix} \sigma_x \\ \sigma_y \end{Bmatrix} = \frac{\pi^2 E h^2}{b^2} \begin{Bmatrix} \hat{\sigma}_x \\ \hat{\sigma}_y \end{Bmatrix},$$ (16)

$$\begin{Bmatrix} \varepsilon_x \\ \varepsilon_y \end{Bmatrix} = \frac{\pi^2 h^2}{b^2} \begin{Bmatrix} \hat{\varepsilon}_x \\ \hat{\varepsilon}_y \end{Bmatrix},$$ (17)

where the dimensionless $\hat{\sigma}_x$, $\hat{\sigma}_y$, $\hat{\varepsilon}_x$, and $\hat{\varepsilon}_y$ are given by Eqs. (012-015) of Appendix 0. It should be pointed out that $\hat{\sigma}_x$ and $\hat{\sigma}_y$ are symmetric in x and y (when one ignores the parameters β and μ), and so are $\hat{\varepsilon}_x$ and $\hat{\varepsilon}_y$. We shall therefore examine here only $\hat{\sigma}_x$ and $\hat{\varepsilon}_x$ as a function of x, under a fixed y=1/2

Simply-supported plate

$$\hat{\sigma}_x = -\frac{(\beta^2+1)T_0}{12(1-\mu^2)}\left\{1 +(1-\mu)(\frac{\delta_v}{4})\left[1 - \frac{1}{(\beta^2+1)}\cos2\pi x\right] +Z\delta_g\sin\pi x\right\}$$
$$+ \frac{2Z(\beta^2+\mu)}{(1-\mu^2)}(\sin\pi x)q + \frac{1}{2}\left\{\frac{(\beta^2+\mu)}{(1-\mu^2)} + \beta^2\right\}q^2 ,$$ (18)

$$\hat{\varepsilon}_x = \frac{(\beta^2+1)}{12(1+\mu)}\delta_v T_0\left\{f_v- \frac{1}{4}\left[(1+\mu\cos2\pi x) - \frac{(1-\mu\beta^2)}{(\beta^2+1)}\cos2\pi x\right]\right\} + 2Z\beta^2(\sin\pi x)q$$
$$+ \frac{1}{2}(2\beta^2+ \mu\cos2\pi x)q^2 .$$ (19)

Clamped plate

$$\hat{\sigma}_x = -\frac{(\beta^4+2\beta^2/3+1)T_c}{3(1-\mu^2)(\beta^2+1)}\left\{1 + (1-\mu)(\frac{\delta_v}{4})\left[1 - \frac{1}{(\beta^2+1)}\cos2\pi x\right] +Z\delta_g\sin^2\pi x\right\}$$
$$- \frac{16Z}{3(1-\mu^2)}[\beta^2\cos2\pi x + \mu\sin^2\pi x]q$$
$$+ \frac{32}{9}\left\{\frac{3(\beta^2+\mu)}{16(1-\mu^2)} + \frac{\beta^2}{4} + \frac{\beta^2}{16} + \frac{\cos2\pi x}{2(\beta+\beta^{-1})^2} - \frac{\cos2\pi x}{(\beta+4\beta^{-1})^2} + \frac{\cos4\pi x}{4(4\beta+\beta^{-1})^2}\right\}q^2 .$$ (20)

$$\hat{\varepsilon}_x = \frac{(\beta^4 + 2\beta^2/3 + 1)}{3(1+\mu)(\beta^2+1)} \delta_v T_0 \left\{ \sin^2\pi x - \frac{1}{4}\left[(1+\mu\cos2\pi x) - \frac{(1-\mu\beta^2)}{(\beta^2+1)}\cos2\pi x \right] \right\} - \frac{16Z\beta^2}{3}(\cos2\pi x)q$$
$$+ \frac{32}{9}\left\{ \frac{3\beta^2}{16} + \frac{1}{4}(\beta^2 + \mu\cos2\pi x) + \frac{1}{16}(\beta^2 - \mu\cos4\pi x) - \frac{\cos2\pi x}{2(\beta+\beta^{-1})^2}(1-\mu\beta^2) \right.$$
$$\left. - \frac{\cos2\pi x}{(\beta+4\beta^{-1})^2}(1-\frac{\mu\beta^2}{4}) + \frac{\cos4\pi x}{(4\beta+\beta^{-1})^2}(\frac{1}{4} - \beta^2\mu) \right\} q^2 . \tag{21}$$

Eqs. (18-21) are quadratic expressions in q, which we shall express in the following skeleton form

$$\Pi = C_0 + C_1 q + C_2 q^2 , \tag{22}$$

where Π represents any one of $\hat{\sigma}_x$, $\hat{\sigma}_y$, $\hat{\varepsilon}_x$, and $\hat{\varepsilon}_y$ and C_0, C_1, and C_2 are the corresponding coefficients involving x and other parameters. Under the assumption that q is zero-mean Gaussian, the mean square Π is given by

$$\langle \Pi^2 \rangle = C_0^2 + (C_1^2 + 2C_0 C_2)\langle q^2 \rangle + 3C_2^2(\langle q^2 \rangle)^2 , \tag{23}$$

in terms of the $\langle q^2 \rangle$ already presented in Figs. 12 and 13.

To be specific, let us choose Figs. 12b and 13b as typical cases of the simply-supported and clamped plates, and also consider $g_{ff} = 1$. As discussed in Sec. VIIIb, at this acoustic loading the effect of thermal loading is negligible on the mean square amplitude. Using the parameter values of Figs. 12b and 13b, we first compute the extreme-fiber stress and strain by setting $Z = 1/2$ in Eqs. (18-21), then estimate the mean square stress and strain by Eq. (23), and finally present in Figs. 14 and 15 the root-mean-square stress and strain distributions in the x coordinate. To quantify the role of thermal terms, four plots are shown in each frame of Figs. 14-15. The first (dotted curve) is the nonthermal reference case ($T_0 = \delta_v = \delta_g = 0$); the second (solid curve with O) includes only the uniform temperature ($T_0 \neq 0$, $\delta_v = \delta_g = 0$); the third (solid curve) involves both the uniform temperature and temperature variation over the plate ($T_0 \neq 0$, $\delta_v \neq 0$, $\delta_g = 0$); and the last (solid curve with X) represents the fully thermal case ($T_0 \neq 0$, $\delta_v \neq 0$, $\delta_g \neq 0$). Figs. 14-15 show that three thermal terms do not contribute additively to the stress and strain tensors. In other words, the thermal terms do not necessarily bring about increased stress and strain over the entire x range. Moreover, the effect of temperature gradient which we have written off as unimportant in Sec. VIIIb, becomes the main contributor to the stress components.

IX. Assessment of Random Single-Mode Dynamics

For a pre-buckled plate (s<1), the three terms of uniform temperature, temperature variation over the plate, and temperature gradient across the plate, all contribute to increasing the mean square displacement, although the increase due to the temperature gradient is insignificant unless the acoustic loading is very weak. On the other hand, the thermal terms do not necessarily bring about increased stress and strain components, as evidenced by the decreased root-mean-square strain and stress tensors in some region of the plate. Moreover, the temperature gradient contributes significantly to the stress tensor, while its effect was negligible on the mean square displacement. The roles played by three thermal terms are briefly summarized in Table 1.

Table 1. Summary of the thermal effects for s<1

	Uniform temperature	Temperature variation over the plate	Temperature gradient across the plate
Displace-ment	In the absence of temperature gradient, the uniform temperature and temperature variation are lumped into the parameter s (Fig. 8). Small increase for a sim-ply-supported plate and moderate in-crease for a clamped plate.		Negligible for both the simply-supported and clamped plates, except when the acous-tic loading is weak (Figs. 12 and 13).
Stress	Very small increase for a simply-sup-ported plate and moderate increase for a clamped plate (Figs. 14 and 15).		Significant for both the simply-supported and clamped plates.
Strain	Moderate increase for both the sim-ply-supported and clamped plates.	Significant in-crease for both the simply-supported and clamped plates.	Negligible for both the simply-supported and clamped plates.

Now, for a post-buckled plate (s>1) we have restricted ourselves to zero temperature gradient, i.e., no thermal loading, so that the uniform tempera-ture and temperature variation can be lumped into the parameter s. In the post-buckled state, the total mean square displacement is sum of the square of buckled plate amplitude and mean square displacement owing to the acoustic loading only. As s becomes large, the former increases linearly with s, whereas the latter falls off by 1/s. Hence, the total mean square displace-ment is dominated by the buckled plate amplitude in the high-temperature limit. It should be pointed that the extended equivalent linearization devel-oped in Appendix N does not work when applied to Eq. (7.10). This, together with the 1/s falloff, is why the post-buckled plate analysis was restricted to zero temperature gradient.

At this juncture, one may ask: "How good is the random dynamics of a single-mode equation?" Clearly, we cannot answer this fully without the detailed study of multi-mode equations. In the nonthermal case, however, Mei has shown that the single-mode dynamics provides an adequate approximation, as long as the external forcing is weak [11,24]. In fact, this is a good news in that the thermal effects are played out quite poigantly in the weak external forcing range. Hence, the peculiarities of three thermal terms might have already been captured by the single-mode equation investigated here. Finally, a redeeming feature of the present analysis is dimensionless representation of the results, thereby freeing the validity of analysis from the lack of knowledge of the precise temperature dependency of parameters involved in the formulation.

X. Directions for Further Work

This report began with the derivation of modal equations for both the simply-supported and clamped plates, under the immovable edge condition. It is this edge condition that gives rise to thermal buckling when the effect of large-amplitude displacements is incorporated into the displacement equation. However, in an attempt to exhibit the interplay of thermal and structural terms, we first obtained the modal equation for W_{11}, W_{13}, W_{31}, and W_{33}, and then reduced it further to the prototype single-mode equation for quantitative comparisons. Clearly, we notice the direction of simplification from multi-mode to the single-mode equation. Hence, the further work must follow the reversed path of generalizing the single-mode dynamics to multi-mode equations.

Some specific proposals for further investigation are then:

(1) Investigate the dynamical behavior of Eqs. (4.4) and (4.11) to exhibit the role of thermally buckled modes on the modal energy exchange. The underlying motivation is that the post-buckled mode has a larger amplitude than the pre-buckled. It is therefore necessary to investigate the sequence of modes undergoing thermal buckling in a multi-mode system.

(2) Validate the random dynamics of single-mode for the multi-mode Eqs. (4.4) and (4.11). This should be carried out in two steps. First, analytically by extending the equivalent linearization to Eqs. (4.4) and (4.11), and then numerically by applying the Monte-Carlo computer simulation to compare with the analytical approximation. It is also suggested that other random dynamic techniques such as, for example, stochastic averaging should be compared with the equivalent linearization used in this report.

(3) Investigate t`e multi-layered composite plates. Although this is doable by the Galerkin type of analysis, it is preferred to formulate an alternative finite element numerical procedure which can easily handle the complex plate geometry, boundary and edge conditions, non-symmetric composite layers, etc.

(4) It is highly desirous to provide some experimental verification for the random dynamic analysis presented in this report. Perhaps, it may be necessary to begin with investigation of a system simpler than the plate, and a deterministic excitation rather than the acoustic loading considered here.

REFERENCES

1. Barthelemy, R. R., "The National Aero-Space Plane Program--A Revolutionary Concept", Structural Testing Technology at High Temperature Conference, Society for Experimental Mechanics, Dayton, OH, Nov 4-6, 1991.

2. Seide, P. and C. Adami, Dynamic Stability of Beams in a Combined Thermal-Acoustic Environment, AFWAL-TR-83-3072, Flight Dynamics Lab., Wright-Patterson AFB, OH, 1983

3. Schneider, C. W., Acoustic Fatigue of Aircraft Structures at Elevated Temperatures. AFFDL-TR-73-155, Flight Dynamics Lab., Wright-Patterson AFB, OH, 1974

4. Bolotin, V.V., Nonconservative Problems of the Theory of Elastic Stability, MacMillan, New York, 1963.

5. Levy, S., Bending of Rectangular Plates with Large Deflections, NACA Report No. 737, 1942.

6. Paul, D. B., Large Deflections of Clamped Rectangular Plates with Arbitrary Temperature Distributions, AFWAL-TR-81-3003, Vol. 1, Flight Dynamics Lab., Wright-Patterson AFB, OH, 1982.

7. Boley, B. A. and J. H. Weiner, Theory of Thermal Stresses, Wiley, New York, 1960.

8. Lin, Y. K., Probabilistic Theory of Structural Dynamics, Robert E. Krieger Publishing, Huntington, New York, 1976.

9. Caughey, T. K., "Equivalent Linearization Techniques", Journal of Acoustic Society of America, Vol. 35, pp.1706-1711, 1963.

10. Maekawa, S., "On the Sonic Fatigue Life Estimation of Skin Structures at Room and Elevated Temperatures", Journal of Sound and Vibration, Vol. 80, pp.41-59, 1982.

11. Mei, C., Response of Nonlinear Structural Panels Subjected to High Intensity Noise, AFWAL-TR-80-3018, Flight Dynamics Lab., Wright-Patterson AFB, OH, 1980.

12. Choi, S. T. and R. Vaicaitis, "Nonlinear Response and Fatigue of Stiffened Panels", Probabilistic Engineering Mechanics, Vol. 4, pp.150-160, 1989.

13. Sunakawa, M. and M. Uemura, Deformation and Thermal Stress in a Rectangular Plate Subjected to Aerodynamic Heating, Report No. 359, Aeronautical Research Institute, University of Tokyo, 1960.

14. Luenberger, D. G., Optimization by Vector Space Methods, Wiley, New York, 1969.

15. Lee, J., "Free Vibration of a Large-Amplitude Deflected Plate-- Reexamination by the Dynamical Systems Theory", ASME Journal of Applied Mechanics, Vol. 53, pp.633-640, 1986.

16. Wilcox, M. W. and L. R. Clemmer, "Large Deflection Analysis of Heated Plates", Journal of Engineering Mechanics Division Proceedings, ASCE, Vol. 90, pp.165-189, 1964.

17. Kehoe, M. W. and H. T. Synder, "High Temperature Ground Vibration Test Techniques", Structural Testing Technology at High Temperature Conference, Society for Experimental Mechanics, Dayton, OH, Nov 4-6, 1991.

18. Richards, W. L. and R. C. Thompson, "Titanium Honeycomb Panel Testing", Structural Testing Technology at High Temperature Conference, Society for Experimental Mechanics, Dayton, OH, Nov 4-6, 1991.

19. Nayfeh, A. H. and D.T. Mook, Nonlinear Oscillations, John Wiley and Sons, New York, 1979.

20. Guckenheimer, J. and P. Holmes, Nonlinear Oscillations, Dynamical Systems, and Bifurcation of Vector Fields, Applied Mathematical Sciences, No. 42, Springer-Verlag, New York, 1963.

21. Holmes, P., "A Nonlinear Oscillator with a Strange Attractor", Philosophical Transaction, Royal Society of London, Vol. 292A, pp.419-448, 1979.

22. Booten, R. C., "The Analysis of Nonlinear Control Systems with Random Inputs", Proceedings of Symposium on Nonlinear Circuit Analysis, Polytechnical Institute of Brooklyn, Vol. 2, 1953.

23. Caughey, T. K., "Response of Nonlinear Systems to Random Excitation", Lecture Note, California Institute of Technology, 1953.

24. Mei, C. and D. B. Paul, "Nonlinear Multimord Response of Clamped Rectangular Plates to Acoustic Loading", AIAA Journal, Vol. 24, pp.643-648, 1986.

25. Bendat, J. S., Principles and Applications of Random Noise Theory, Wiley, New York, 1958.

26. Lee. J., "A New Formulation of the Linear Dynamic Response to Random Excitations", Journal of Sound and Vibration, Vol. 35, pp.47-53, 1974.
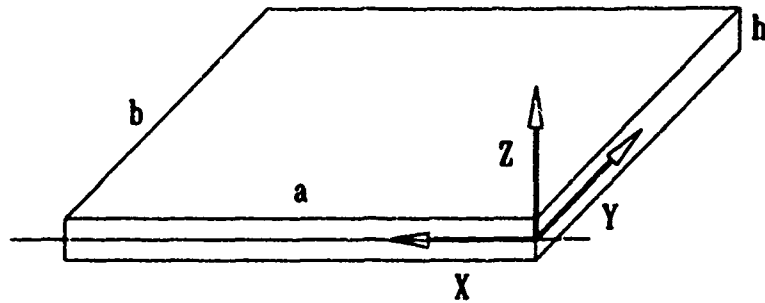
Fig. 1 Plate configuration.
The x-y plane is at the mid-plate and z-axis is across the plate
thickness. The Top and bottom of plate are located at h/2 and –h/2,
respectively.
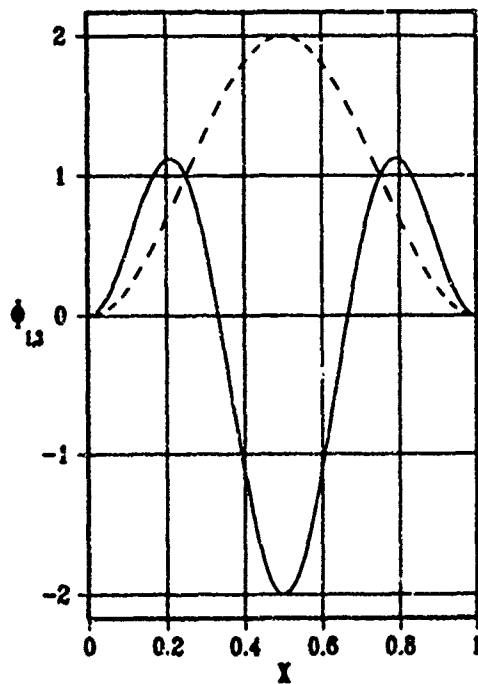
(a)
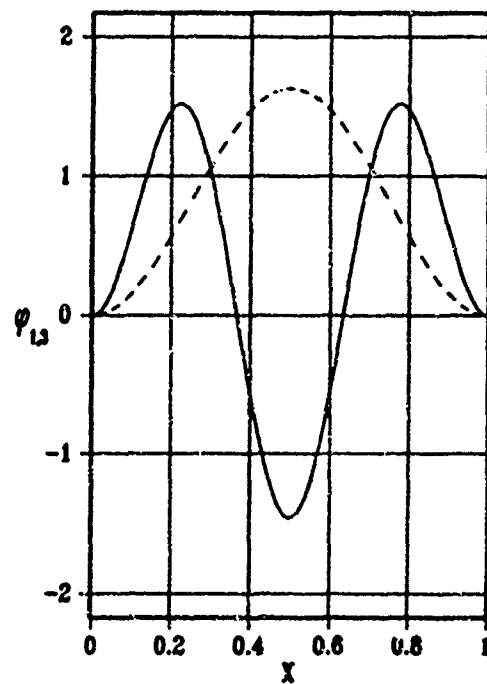
(b)

Fig. 2 Comparison of basis functions for clamped plate.
(a) Nonorthogonal expansion functions of even mode shape
 ---- $\phi_1 = 2S_1(x)$; ——— $\phi_3 = 2S_3(x)$.
(b) Orthonormal expansion functions of even mode shape
 ---- $\varphi_1 = \sqrt{8/3}S_1(x)$; ——— $\varphi_3 = \sqrt{24/5}S_2(x) + \sqrt{8/15}S_4(x)$.
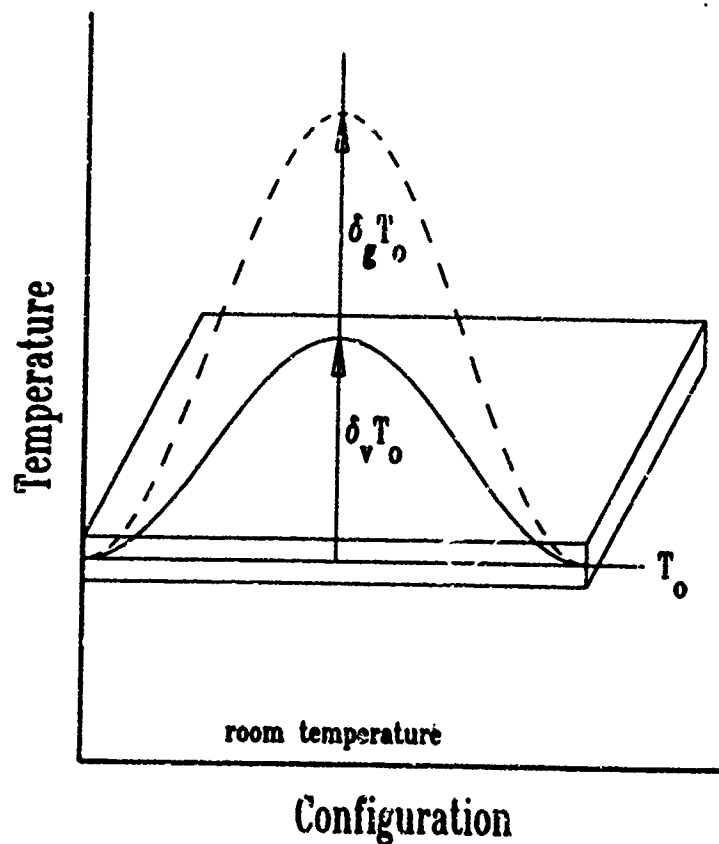
Fig. 3 Typical distributions of temperature variation and gradient.
T_0 is dimensionless uniform temperature above the room temperature;
$T_0 \delta_v$ is the magnitude of temperature variation over the plate;
$T_0 \delta_g$ is the magnitude of temperature gradient through the plate thickness.
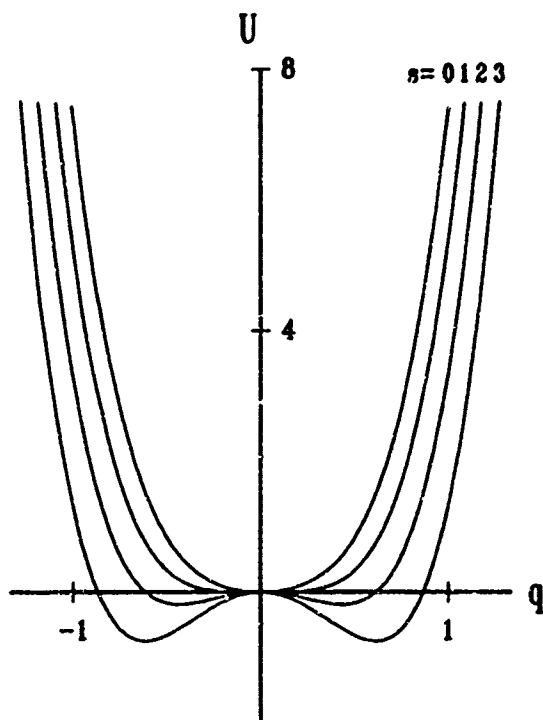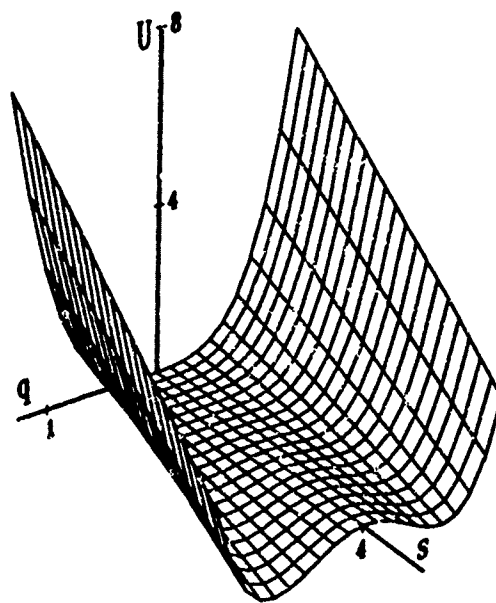
Fig. 4 The potential energy U of simply-supported plate.

(a) $U = \frac{(\beta^2+1)^2}{2}(1-s)q^2 + \frac{3}{4}[(1-\mu^2)(\beta^4+1)+2(\beta^4+1+2\mu\beta^2)]$ under $\beta=1$ and $\mu^2=0.1$.

(b) Potential energy surface developing a symmetric double-well.
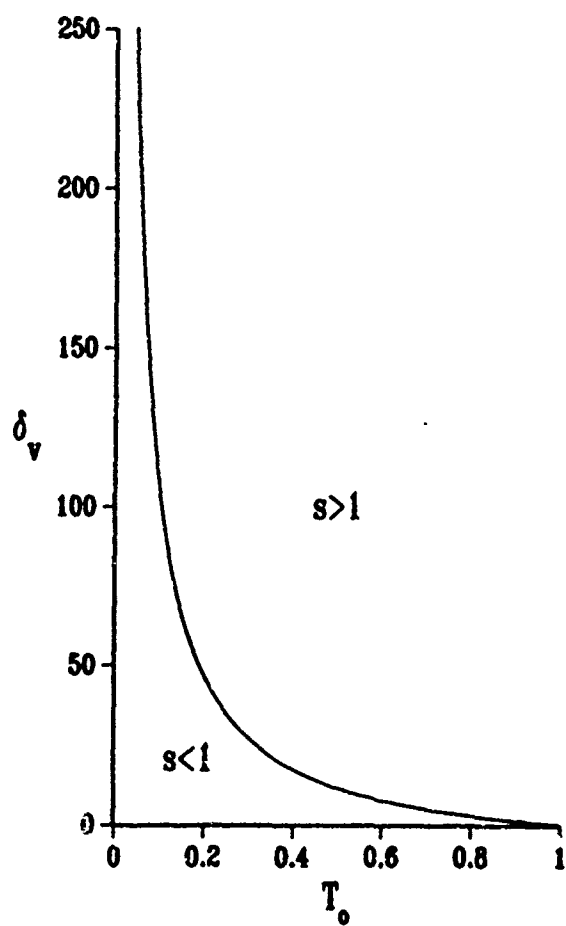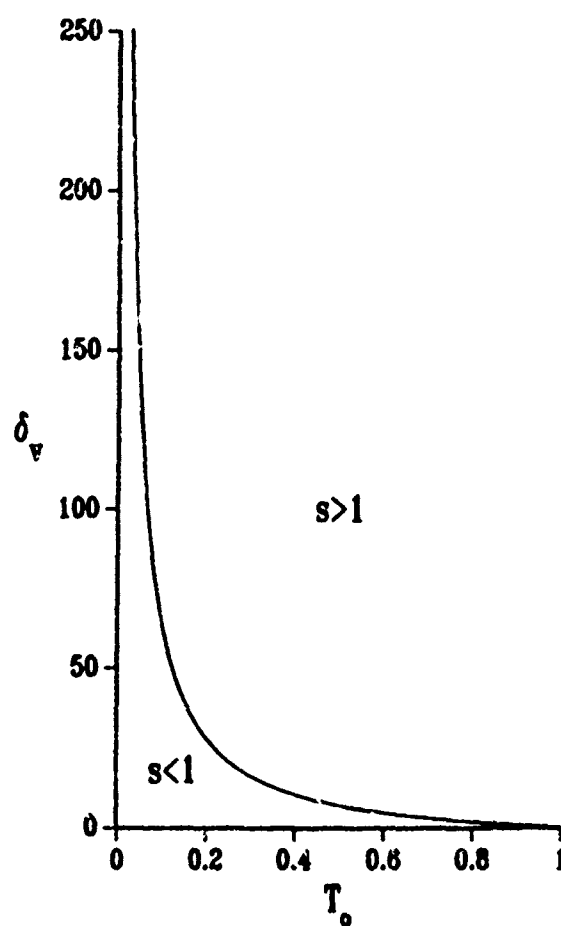
Fig. 5 The threshold boundary for thermal buckling.
(a) Simply-suppported plate. (b) Clamped plate.
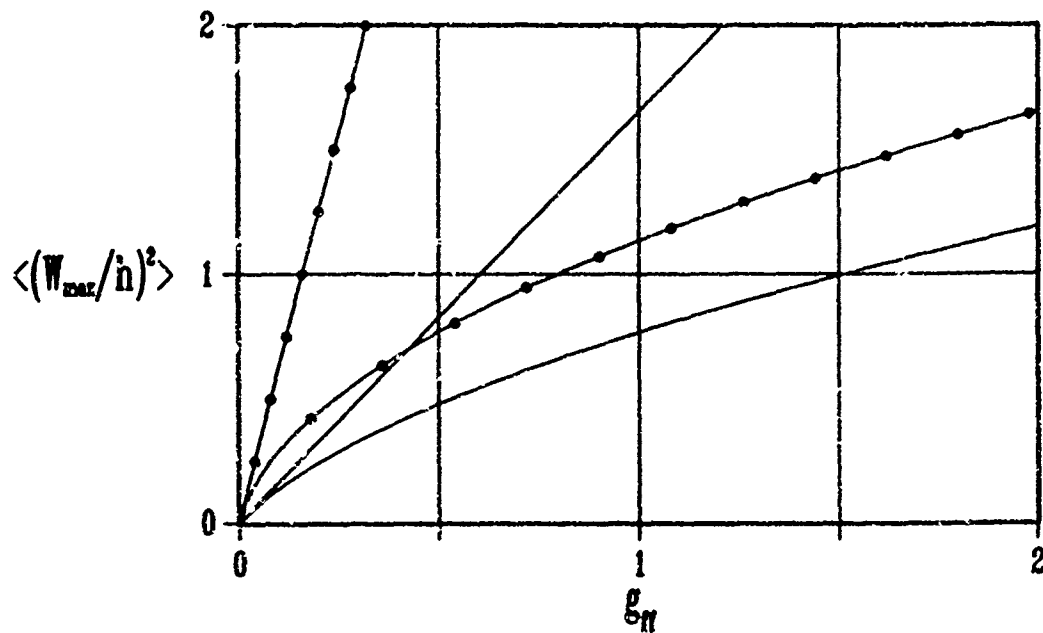
Fig. 6 Linear and nonlinear estimates of the maximum mean square displacement. Nonthermal case (s=0). ——O—— simply-supported plate; ———— clamped plate.
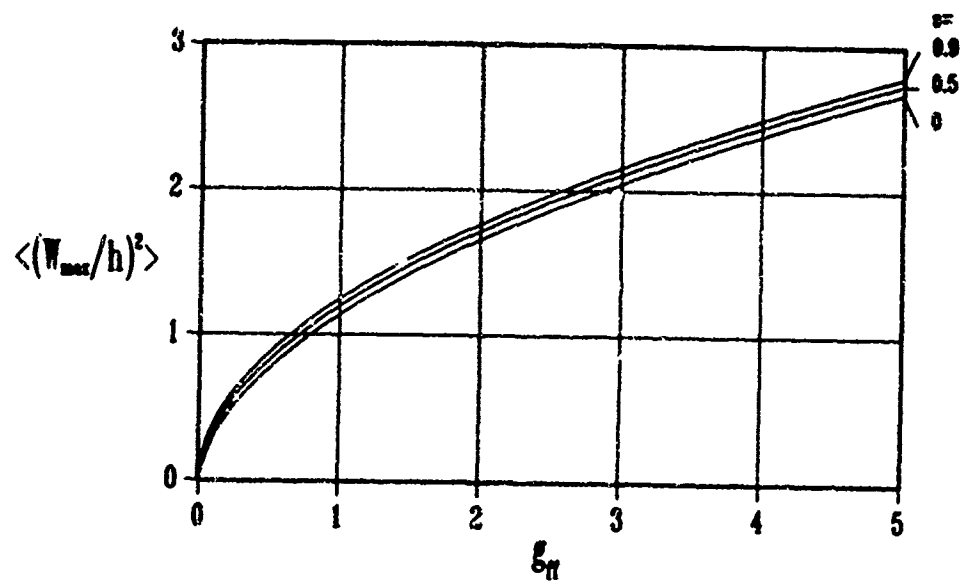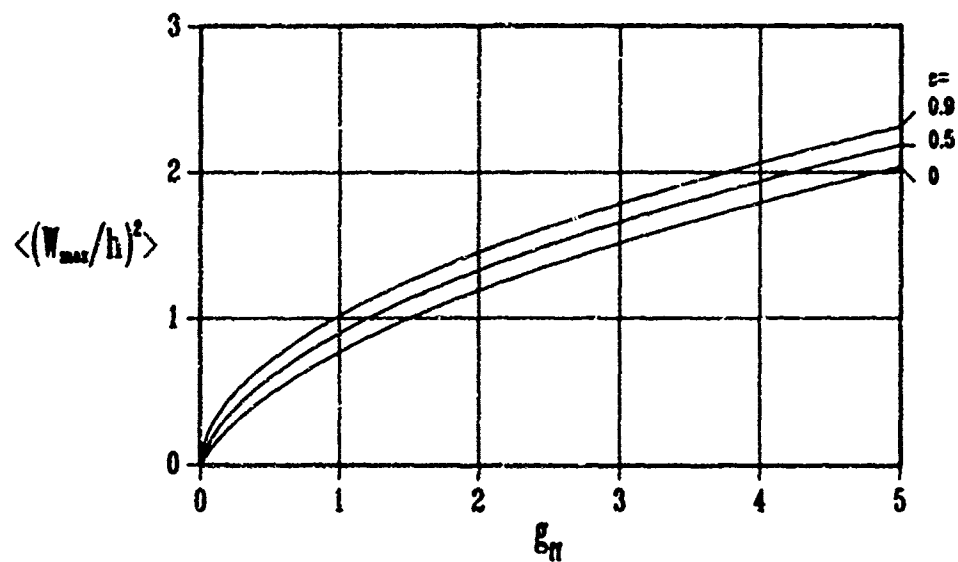
Fig. 7 Maximum mean square displacement of pre-buckled plate ($s<1$).
(a) Simply-supported plate. (b) Clamped plate.
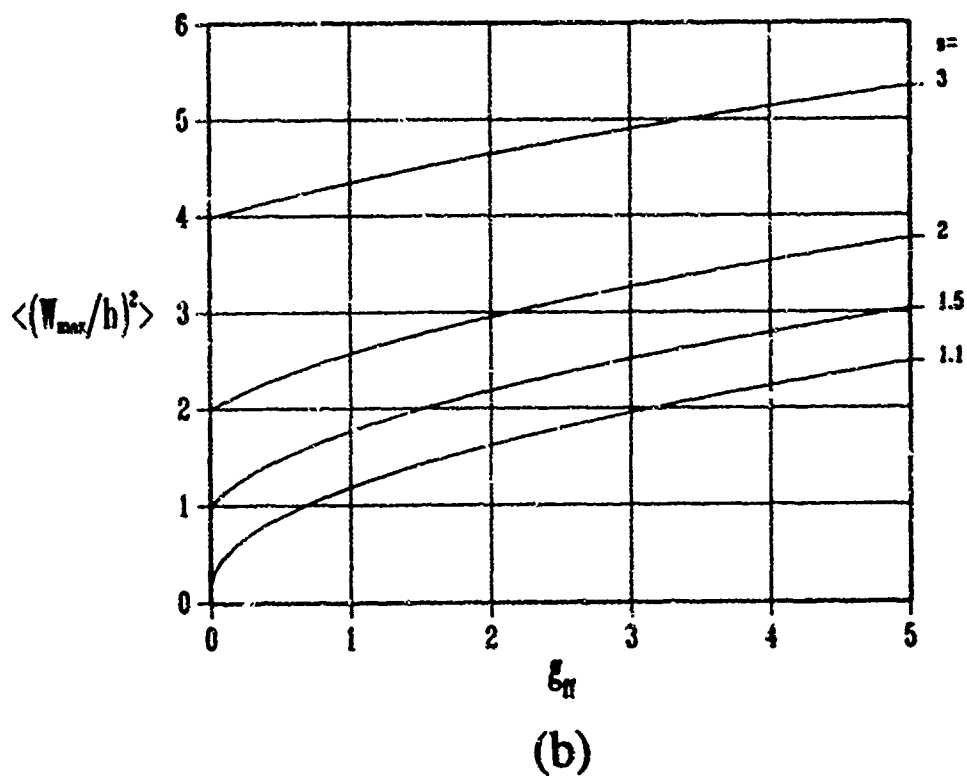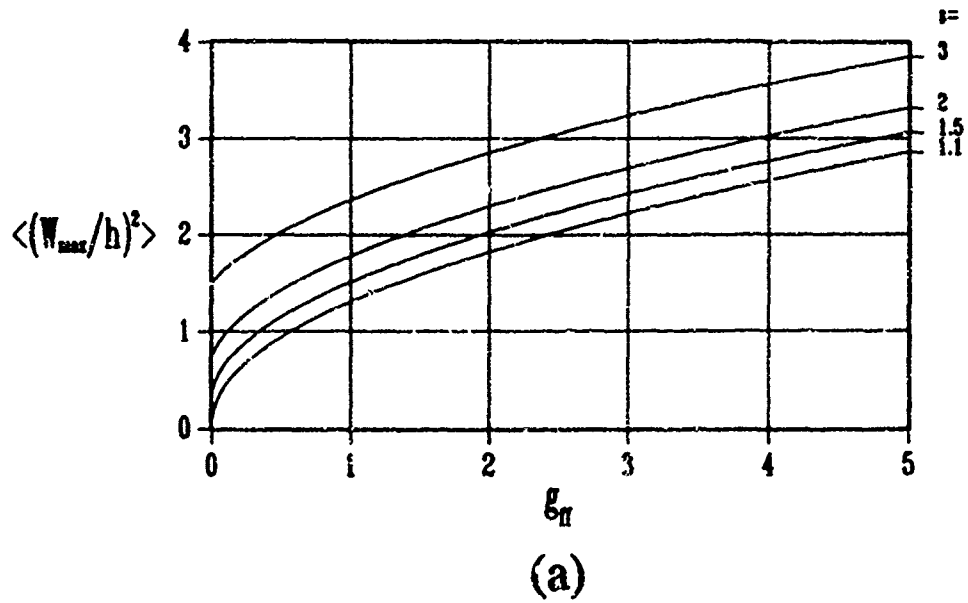
Fig. 8 Maximum mean square displacement of post-buckled plate (a>1).
The level of mean square displacement is raised y the square of buckled
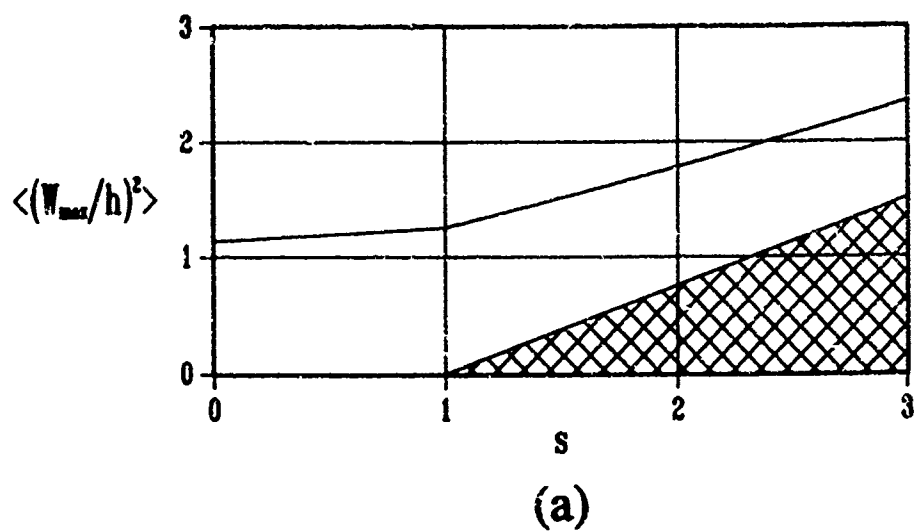plate amplitudes. (a) Simply-supported plate. (b) Clamped plate.
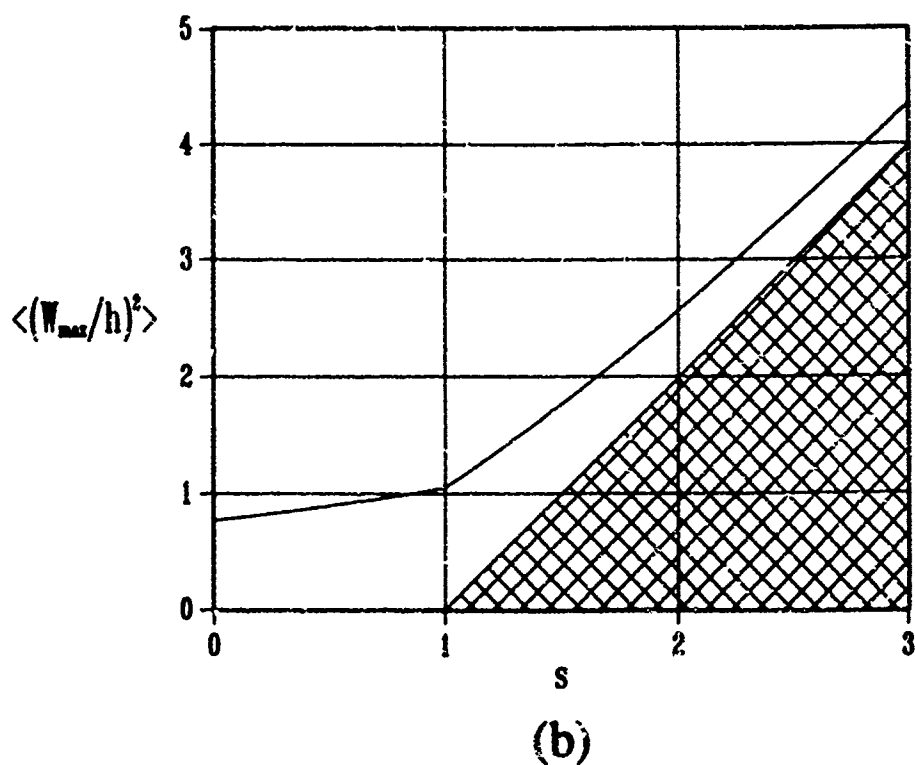
Fig. 9 Maximum mean square displacement under $g_{rf}=1$.
The cross-hatched triangle represents the contribution of buckled plate
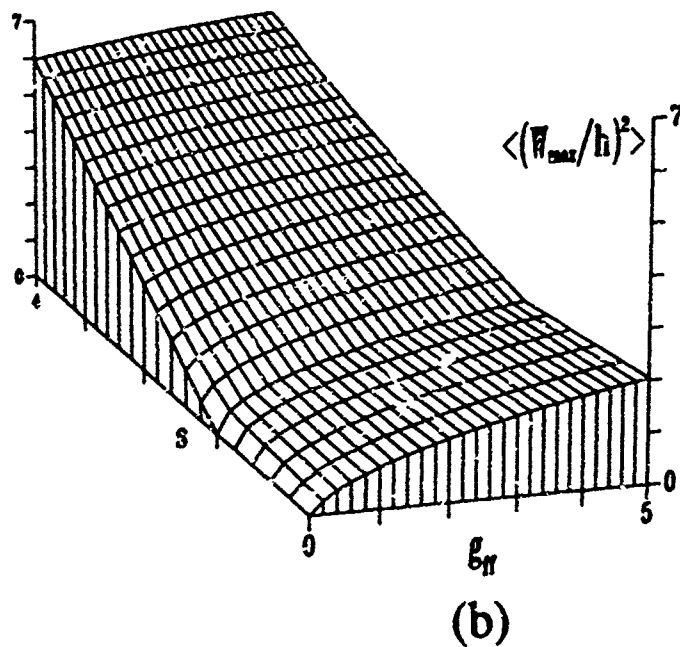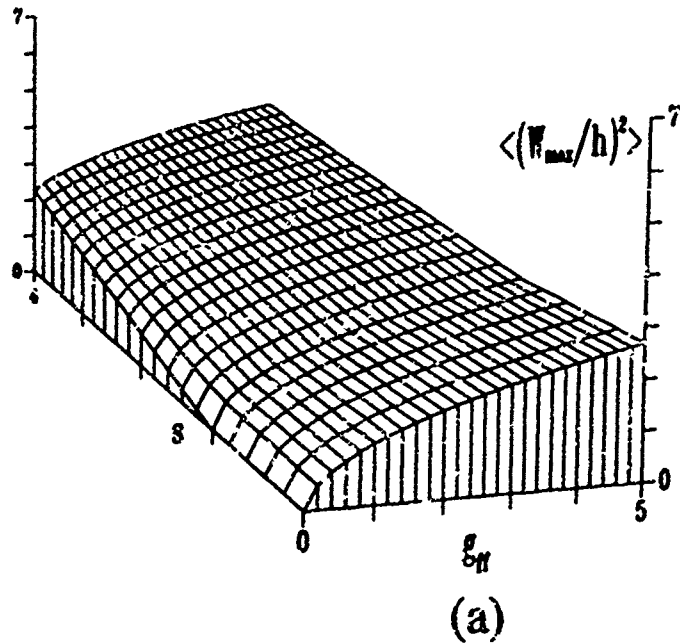amplitude. (a) Simply-supported plate. (b) Clamped plate.

Fig. 10 Total mean square displacement.
The mean square displacement is entirely due to the fluctuations for s<1,
whereas the contribution of buckled plate amplitude increases linearly
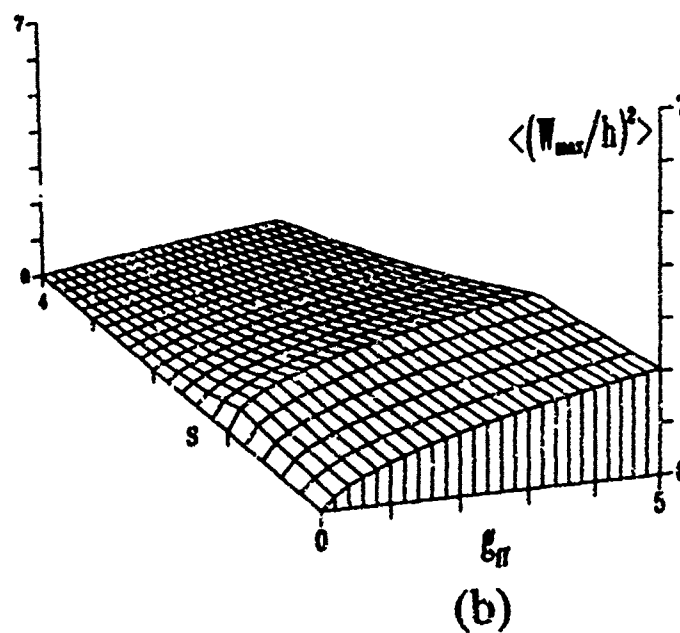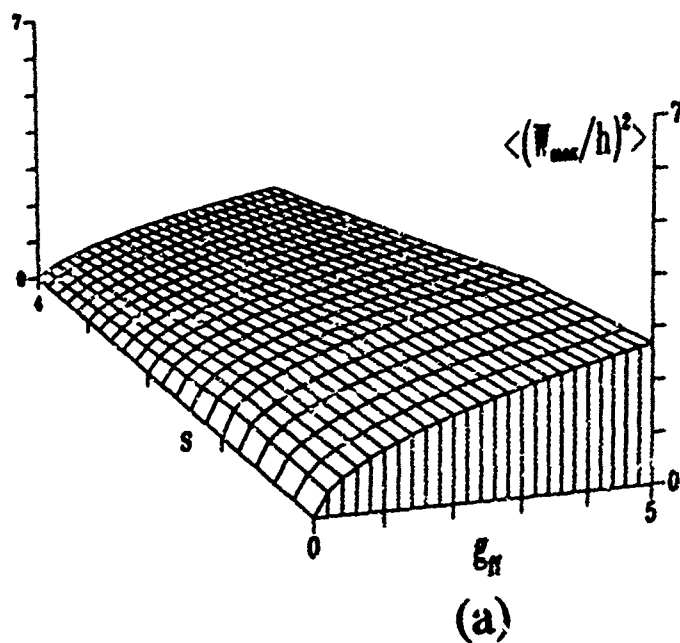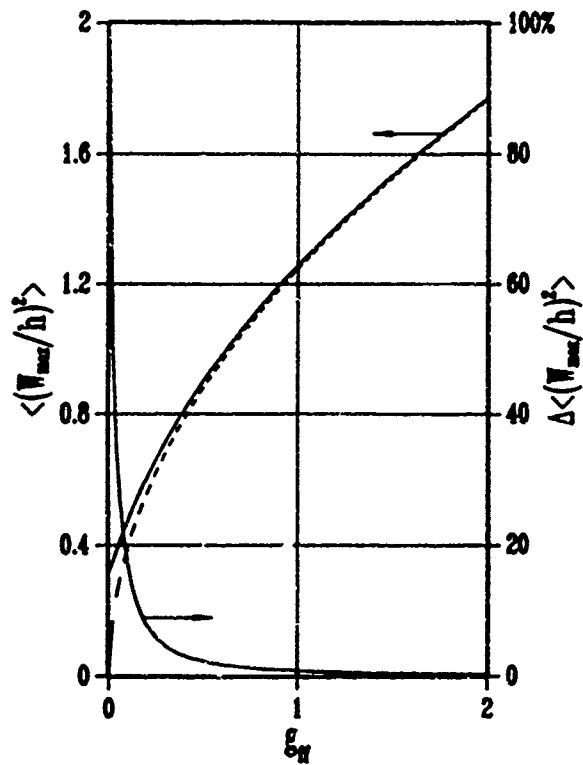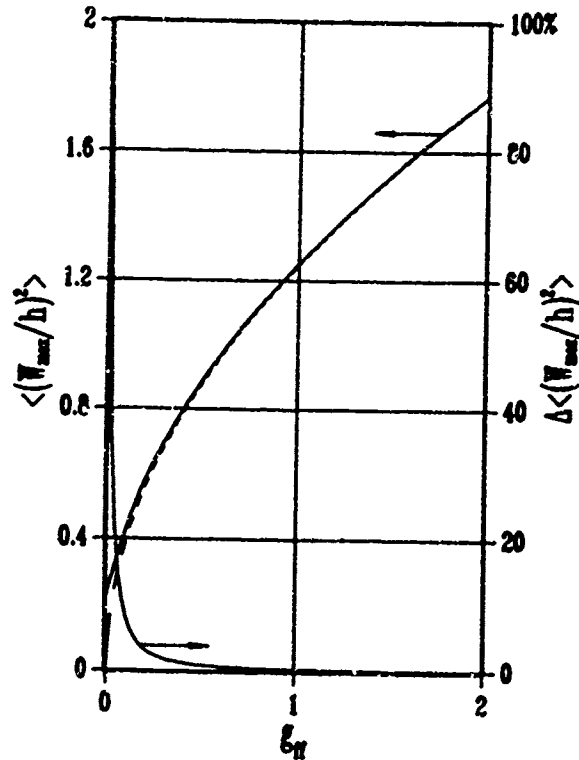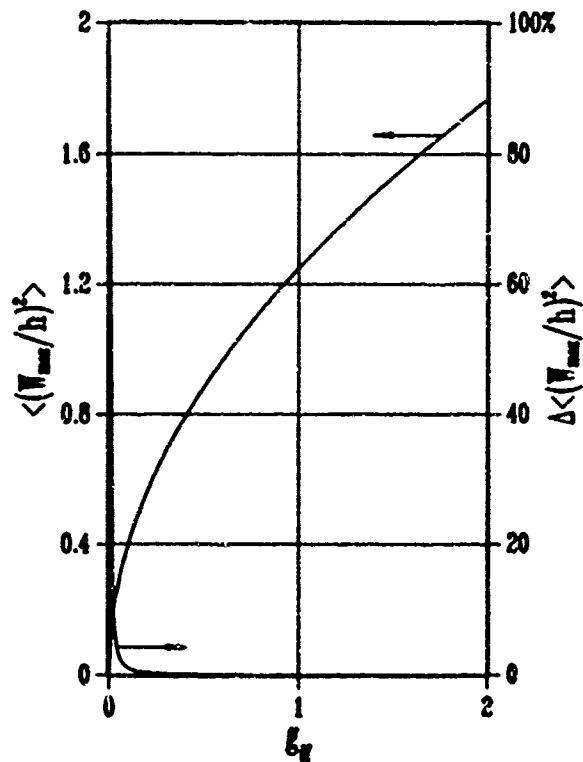with s for s>>1. (a) Simply-supported plate. (b) Clamped plate.

Fig. 11 Mean square displacement due to acoustic loading.
Up to s=1, the mean square displacements are identical to Fig. 10.
However, only the contribution by acoustic loading is displayed for s>1.
(a) Simply-supported plate. (b) Clamped plate.

Fig. 12 Maximum mean square displacement of simply-supported plate. The left ordinate refers to ——— $4\langle q_C^2 \rangle$ and - - - - $4\langle q^2 \rangle$; the right ordinate represents $(\langle q_C^2 \rangle - \langle q^2 \rangle)/\langle q_C^2 \rangle$ in percent.

(a) T_0=0.2, δ_v=δ_g=44 (s=0.952).

(b) T_0=0.5, δ_v=δ_g=10.8 (s=0.962).

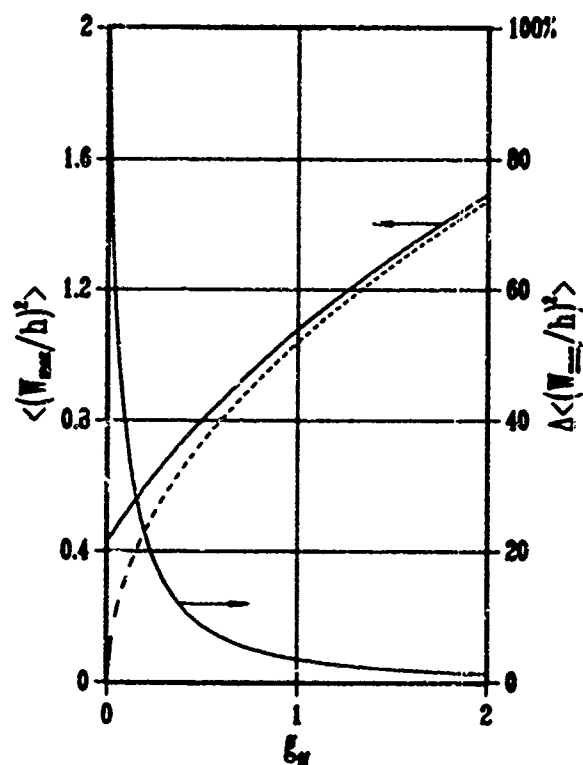(a) T_0=0.8, δ_v=δ_g=2.3 (s=0.957).

(a)
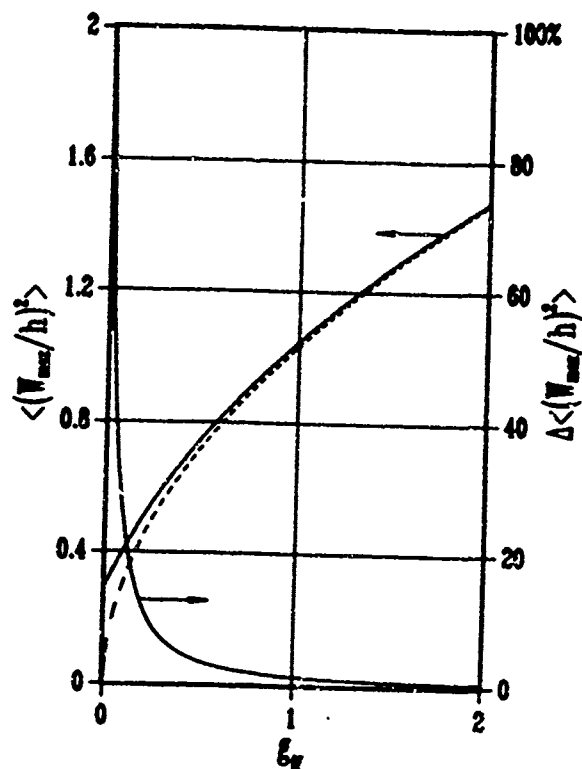
(b)
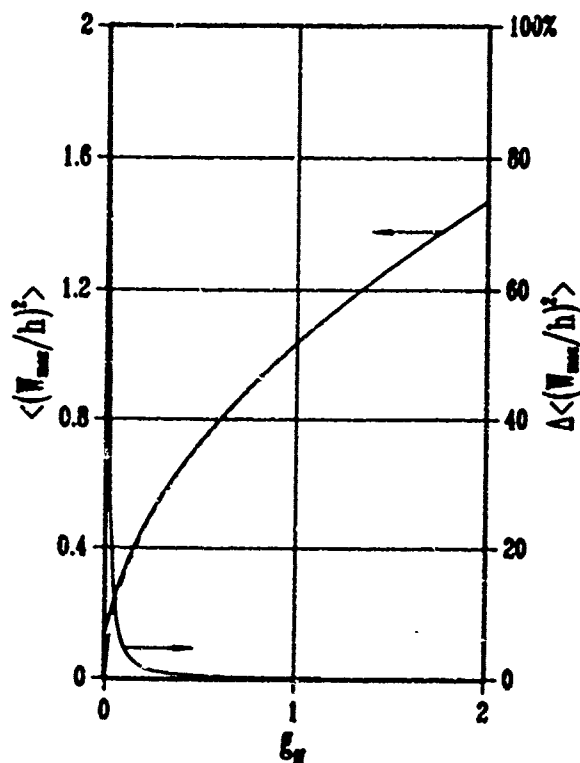
(c)

Fig. 13 Maximum mean square displacement of clamped plate. The left ordinate refers to

——— $64\langle q_C^2\rangle/9$ and – – – $64\langle q^2\rangle/9$; the right ordinate represents $(\langle q_C^2\rangle - \langle q^2\rangle)/\langle q_C^2\rangle$ in percent.

(a) $T_0 = 0.2$, $\delta_v = \delta_g = 27$ (s=0.969).
(b) $T_0 = 0.5$, $\delta_v = \delta_g = 6.4$ (s=0.956).
(a) $T_0 = 0.8$, $\delta_v = \delta_g = 1.4$ (s=0.9600.
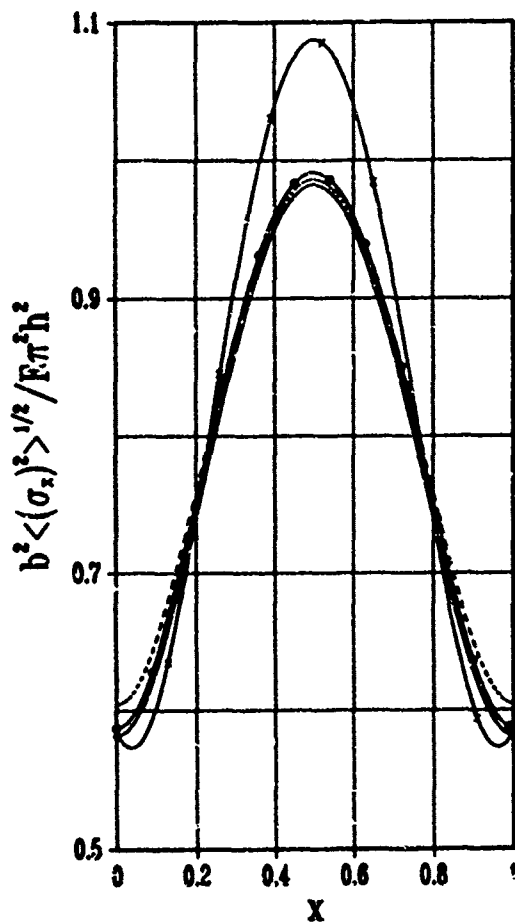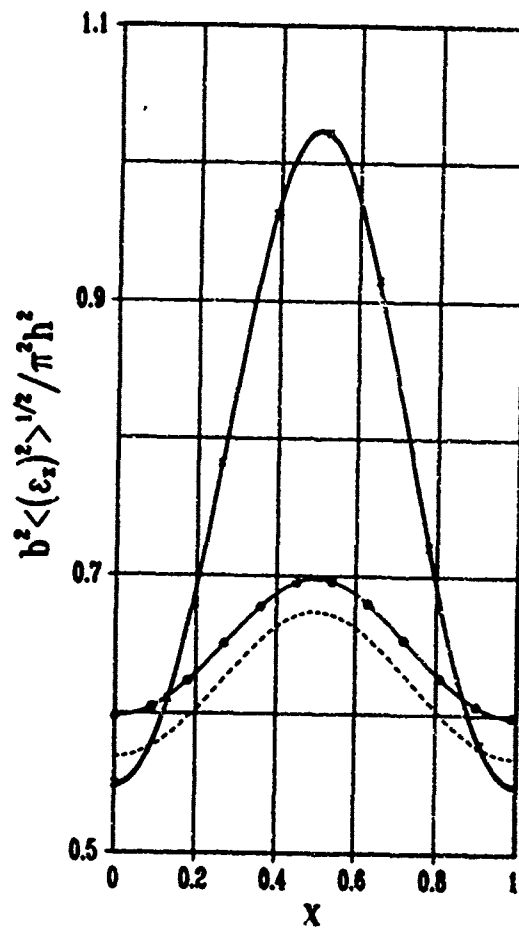
Fig. 14 Root-mean-square of extreme-fiber stress and strain for simply-supported plate under $g_{ff} = 1$.

------- $T_0 = \delta_v = \delta_g = 0$; ——O—— $T_0 = 0.5$, $\delta_v = \delta_g = 0$;

——— $T_0 = 0.5$, $\delta_v = 10.8$, $\delta_g = 0$; ——X—— $T_0 = 0.5$, $\delta_v = \delta_g = 10.8$

Fig. 15 Root-mean-square of extreme-fiber stress and strain for clamped plate under $g_{ff}=1$.

- - - - - - $T_0 = \delta_v = \delta_g = 0$;   ——O—— $T_0 = 0.5$, $\delta_v = \delta_g = 0$;

——————— $T_0 = 0.5$, $\delta_v = 6.4$, $\delta_g = 0$;   ——X—— $T_0 = 0.5$, $\delta_v = \delta_g = 6.4$

Appendix A: Cosine expansion of $(\frac{\partial^2 w}{\partial x \partial y})^2$ and $(\frac{\partial^2 w}{\partial x^2})(\frac{\partial^2 w}{\partial y^2})$ expressed by Eq. (3.3)

The term $(\frac{\partial^2 w}{\partial x \partial y})^2$: Using Eq. (3.3) we have by the trigonometric identities

$$(w_{xy})^2 = \pi^4 \sum_{n=0}^{\infty} \sum_{j=0}^{\infty} nj$$

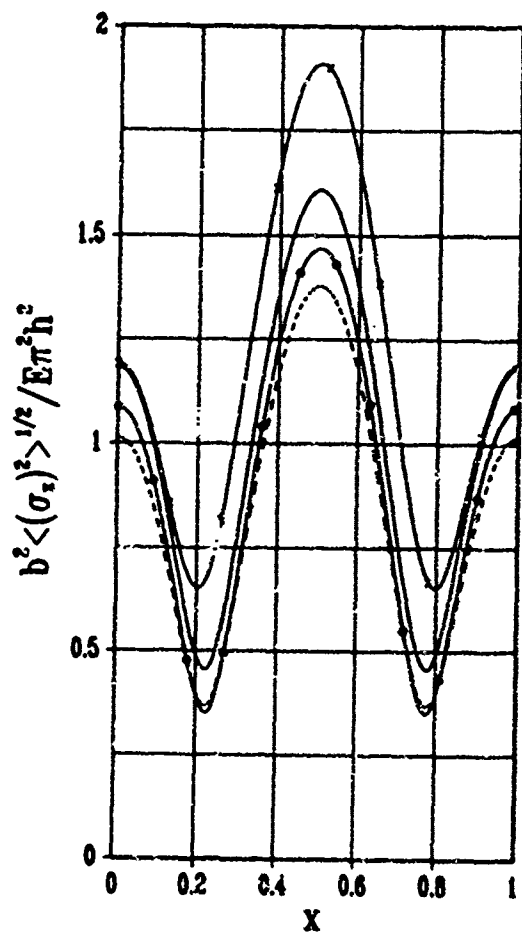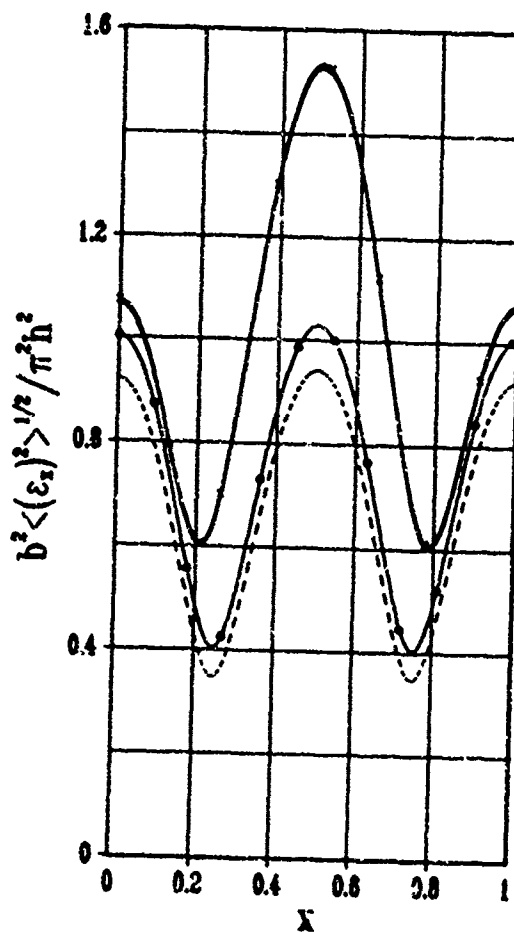$$\times \left\{ \sum_{m=0}^{\infty} \sum_{i=0}^{\infty} w_{mn} w_{ij} mi (\cos(m+i)\pi x + \cos(m-i)\pi x) \right\} (\cos(n+j)\pi y + \cos(n-j)\pi y), \quad (A1)$$

By interchanging the order of summations, the $\{..\}$ in Eq. (A1) becomes

$$\left\{..\right\} = \sum_{p=0}^{\infty} \alpha_{pnj} \cos p\pi x. \quad (A2)$$

Here

$$\alpha_{pnj} = \sum_{m=0}^{p} w_{mn} w_{(p-m)j} m(p-m) + \sum_{m=p}^{\infty} w_{mn} w_{(m-p)j} m(m-p) + \sum_{m=0}^{\infty} w_{mn} w_{(m+p)j} m(m+p)\Delta(p),$$

where $\Delta(p) = 1 - \delta_p^0$ excludes the term for $p=0$. (Note that the factor $\Delta(p)$ can be applied to either the second or third term to avoid double counting.) Now, inserting Eq. (A2) into Eq. (A1) and interchanging the order of summations, we obtain the double cosine expansion

$$(w_{xy})^2 = \pi^4 \sum_{p=0}^{\infty} \sum_{q=0}^{\infty} \beta_{pq} \cos p\pi x \cos q\pi y, \quad (A3)$$

where $\beta_{pq} = \sum_{n=0}^{q} \alpha_{pn(q-n)} n(q-n) + \sum_{n=q}^{\infty} \alpha_{pn(n-q)} n(n-q) + \sum_{n=0}^{\infty} \alpha_{pn(n+q)} n(n+q)\Delta(q).$

The term $(\frac{\partial^2 w}{\partial x^2})(\frac{\partial^2 w}{\partial y^2})$: In parallel to Eq. (A1), we have

$$w_{xx} w_{yy} = \pi^4 \sum_{n=0}^{\infty} \sum_{j=0}^{\infty} j^2$$

$$\times \left\{ \sum_{m=0}^{\infty} \sum_{i=0}^{\infty} w_{mn} w_{ij} m^2 (-\cos(m+i)\pi x + \cos(m-i)\pi x) \right\} (-\cos(n+j)\pi y + \cos(n-j)\pi y). \quad (A4)$$

After expressing the $\{..\}$ in Eq. (A4)

$$\left\{..\right\} = \sum_{p=0}^{\infty} C_{pnj} \cos p\pi x, \quad (A5)$$

where

$$C_{pnj} = -\sum_{m=0}^{p} w_{mn} w_{(p-m)j} m^2 + \sum_{m=p}^{\infty} w_{mn} w_{(m-p)j} m^2 + \sum_{m=0}^{\infty} w_{mn} w_{(m+p)j} m^2 \Delta(p),$$

the interchange of the order of summations gives

$$w_{xx} w_{yy} = \pi^4 \sum_{p=0}^{\infty} \sum_{q=0}^{\infty} D_{pq} \cos p\pi x \cos q\pi y, \quad (A6)$$

where

$$D_{pq} = -\sum_{n=0}^{q} C_{pn(q-n)}(q-n)^2 + \sum_{n=q}^{\infty} C_{pn(n-q)}(n-q)^2 + \sum_{n=0}^{\infty} C_{pn(n+q)}(n+q)^2 \Delta(q).$$

Therefore, by combining Eqs. (A3) and (A6) we obtain the final expression

$$(w_{xy})^2 - w_{xx}w_{yy} = \pi^4 \sum_{p=0}^{\infty} \sum_{q=0}^{\infty} \mathcal{E}_{pq} \cos p\pi x \cos q\pi y, \qquad (A7)$$

where $\mathcal{E}_{pq} = \mathcal{B}_{pq} - D_{pq}$.

For later reference, we shall enumerate $\mathcal{E}_{pq}$ which involve only w_{11}, w_{13}, w_{31} and w_{33};

$\mathcal{E}_{02} = 2[w_{11}^2 - 2w_{11}w_{13} + 9w_{31}^2 - 18w_{31}w_{33}]$, $\mathcal{E}_{20} = 2[w_{11}^2 - 2w_{11}w_{31} + 9w_{13}^2 - 16w_{13}w_{33}]$,

$\mathcal{E}_{22} = 16[w_{11}(w_{13} + w_{31}) - 4w_{13}w_{31}]$,

$\mathcal{E}_{04} = 16[w_{11}w_{13} + 9w_{31}w_{33}]$, $\mathcal{E}_{40} = 16[w_{11}w_{31} + 9w_{13}w_{33}]$,

$\mathcal{E}_{24} = 4[-w_{11}w_{13} + 9w_{11}w_{33} + 25w_{13}w_{31}]$, $\mathcal{E}_{42} = 4[-w_{11}w_{31} + 9w_{11}w_{33} + 25w_{13}w_{31}]$,

$\mathcal{E}_{06} = 18[w_{13}^2 + 9w_{33}^2]$, $\mathcal{E}_{60} = 18[w_{31}^2 + 9w_{33}^2]$,

$\mathcal{E}_{26} = 16[9w_{13}w_{33}]$, $\mathcal{E}_{62} = 16[9w_{31}w_{33}]$,

$\mathcal{E}_{46} = 4[-9w_{13}w_{33}]$, $\mathcal{E}_{64} = 4[-9w_{31}w_{33}]$, $\mathcal{E}_{44} = 64[-w_{13}w_{31}]$.

Note that the pattern of quadratic terms in the [..] agrees with Levy's Table 1 in Ref [5].

Appendix B: Evaluation of $\int_0^1\int_0^1 R_4 \psi_r(x)\psi_s(y)dxdy$

Let us evaluate the first term $w_{xx}F_{yy}$ of R_4. In view of Eq. (3.1) and (3.3), we find that

$$\int_0^1\int_0^1 w_{xx}F_{yy}\psi_r(x)\psi_s(y)dxdy = \pi^2 b^2 P_x r^2 w_{rs} + \frac{Eh\pi^4}{4}\mathcal{F}_1, \tag{B1}$$

where

$$\mathcal{F}_1 = \sum_{n=1}^\infty \sum_{q=0}^\infty q^2 \left\{\sum_{m=1}^\infty \sum_{p=0}^\infty w_{mn}F_{pq}m^2(\delta_{r-p}^m - \delta_{p-r}^m + \delta_{p+r}^m)\right\}(\delta_{s-q}^n - \delta_{q-s}^n + \delta_{q+s}^n).$$

The integrations have been carried out with the aid of Eqs. (H1) and (H2) of Appendix H. By expanding the factors of δ, we see there are nine sums in $\mathcal{F}_1$

$$\mathcal{F}_1 = \sum_{q=0}^s q^2 U_{r(s-q)q} - \sum_{q=s}^\infty q^2 U_{r(q-s)q} + \sum_{q=0}^\infty q^2 U_{r(q+s)q}, \tag{B2}$$

where

$$U_{rnq} = \sum_{p=0}^r w_{(r-p)n}F_{pq}(r-p)^2 - \sum_{p=r}^\infty w_{(p-r)n}F_{pq}(p-r)^2 + \sum_{p=0}^\infty w_{(p+r)n}F_{pq}(p+r)^2.$$

Similarly, we have

$$\int_0^1\int_0^1 w_{yy}F_{xx}\psi_r(x)\psi_s(y)dxdy = \pi^2 a^2 P_y s^2 w_{rs} + \frac{Eh\pi^4}{4}\mathcal{F}_2, \tag{B3}$$

where

$$\mathcal{F}_2 = \sum_{n=1}^\infty \sum_{q=0}^\infty n^2 \left\{\sum_{m=1}^\infty \sum_{p=0}^\infty w_{mn}F_{pq}p^2(\delta_{r-p}^m - \delta_{p-r}^m + \delta_{p+r}^m)\right\}(\delta_{s-q}^n - \delta_{q-s}^n + \delta_{q+s}^n).$$

Also,

$$\int_0^1\int_0^1 w_{xy}F_{xy}\psi_r(x)\psi_s(y)dxdy = \frac{Eh\pi^4}{4}\mathcal{F}_3, \tag{B4}$$

where

$$\mathcal{F}_3 = \sum_{n=1}^\infty \sum_{q=0}^\infty nq \left\{\sum_{m=1}^\infty \sum_{p=0}^\infty w_{mn}F_{pq}mp(\delta_{r-p}^m - \delta_{p-r}^m + \delta_{p+r}^m)\right\}(\delta_{s-q}^n - \delta_{q-s}^n + \delta_{q+s}^n).$$

By combining Eqs. (B1), (B3) and (B4), we obtain the final expression

$$\int_0^1\int_0^1 R_4 \psi_r(x)\psi_s(y)dxdy = -\frac{\pi^2\beta^2}{b^4}(b^2 P_x r^2 + a^2 P_y s^2)w_{rs} - \frac{\beta^2 Eh\pi^4}{4b^4}\mathcal{F}_{rs}, \tag{B5}$$

where $\mathcal{F}_{rs} = \mathcal{F}_1 + \mathcal{F}_2 - 2\mathcal{F}_3$. In view of Eq. (B2), we see that $\mathcal{F}_{rs}$ represents the nine sums in Levy's Eq. (9) in Ref [5].

As an illustration, we enumerate $\mathcal{F}_{rs}$ for w_{11}, w_{13}, w_{31} and w_{33}:

$$\mathcal{F}_{11} = h_1 w_{11} + h_2 w_{13} + h_3 w_{31} + h_4 w_{33},$$
$$\mathcal{F}_{13} = h_2 w_{11} + h_5 w_{13} + h_6 w_{31} + h_7 w_{33},$$
$$\mathcal{F}_{31} = h_3 w_{11} + h_6 w_{13} + h_8 w_{31} + h_9 w_{33},$$

$$\mathcal{F}_{33} = h_4 w_{11} + h_7 w_{13} + h_9 w_{31} + h_{10} w_{33} , \tag{b6}$$

where

$$h_1 = -8(F_{02} + F_{20}),$$

$$h_2 = 8F_{02} - 16F_{22} - 32F_{04} + 4F_{24},$$

$$h_3 = 8F_{20} - 16F_{22} - 32F_{40} + 4F_{42},$$

$$h_4 = -36(F_{24} + F_{42}),$$

$$h_5 = -72(F_{20} + F_{06}),$$

$$h_6 = -100(F_{24} + F_{42}) + 34(F_{22} + F_{44}),$$

$$h_7 = 72F_{20} - 288F_{40} - 144F_{26} + 36F_{46},$$

$$h_8 = -72(F_{02} + F_{60}),$$

$$h_9 = 72F_{02} - 288F_{04} - 144F_{62} + 36F_{24},$$

$$h_{10} = -648(F_{06} + F_{60}). \tag{B7}$$

Appendix C: Cosine expansion of $(\frac{\partial^2 w}{\partial x \partial y})^2$ and $(\frac{\partial^2 w}{\partial x^2})(\frac{\partial^2 w}{\partial y^2})$ expressed by Eq. (3.15)

The term $(\frac{\partial^2 w}{\partial x \partial y})^2$: Using the alternate expression for Eq. (3.15)

$$w(x,y) = \Sigma_{r=0}^{\infty} \Sigma_{s=0}^{\infty} \Sigma_{r=m}^{\infty} \Sigma_{s=n}^{\infty} w_{rs} a_{rm} a_{sn} S_m(x) S_n(y),$$

we have

$$(w_{xy})^2 = \pi^4 \Sigma_{n=0}^{\infty} \Sigma_{j=0}^{\infty} \Sigma_{s=n}^{\infty} \Sigma_{d=j}^{\infty} a_{sn} a_{dj}$$
$$\times \Sigma_{m=0}^{\infty} \Sigma_{i=0}^{\infty} \left\{ \Sigma_{r=m}^{\infty} \Sigma_{c=i}^{\infty} w_{rs} w_{cd} a_{rm} a_{ci} A_m(x) A_i(x) \right\} A_n(y) A_j(y), \qquad (C1)$$

where $A_m(x) = m\cos(m\pi x)\sin n\pi x + \sin(m\pi x)\cos n\pi x$. By trigonometric identities, we rewrite the $\{..\}$ in Eq. (C1)

$$\left\{ .. \right\} = \tfrac{1}{8}(Q^+_{misd} \cos(m+i)\pi x + Q^-_{misd} \cos(m-i)\pi x), \qquad (C2)$$

where

$$Q^{\pm}_{misd} = \Sigma_{r=m}^{\infty} \Sigma_{c=i}^{\infty} w_{rs} w_{cd} a_{rm} a_{ci} 2(mi\mp1) - \Sigma_{r=m-2}^{\infty} \Sigma_{c=i}^{\infty} w_{rs} w_{cd} a_{r(m-2)} a_{ci} (m-1)(i\pm1)$$
$$- \Sigma_{r=m+2}^{\infty} \Sigma_{c=i}^{\infty} w_{rs} w_{cd} a_{r(m+2)} a_{ci} (m+1)(i\mp1).$$

By changing the order of summations, we then have

$$\Sigma_{m=0}^{\infty} \Sigma_{i=0}^{\infty} \left\{ .. \right\} = \tfrac{1}{8}\Sigma_{p=0}^{\infty} \left[\Sigma_{m=0}^{p} Q^+_{m(p-m)sd} + \Sigma_{m=p}^{\infty} Q^-_{m(m-p)sd} + \Sigma_{m=0}^{\infty} Q^-_{m(m+p)sd} \Delta(p) \right] \cos p\pi x, \qquad (C3)$$

where $\Delta(p) = (1-\delta_p^0)$. Now, substituting Eq. (C3) into Eq. (C1) yields

$$(w_{xy})^2 = \frac{\pi^4}{8}\Sigma_{p=0}^{\infty} \Sigma_{n=0}^{\infty} \Sigma_{j=0}^{\infty} \left[\Sigma_{s=n}^{\infty} \Sigma_{d=j}^{\infty} a_{sn} a_{dj} \mathcal{H}_{psd} A_n(y) A_j(y) \right] \cos p\pi x, \qquad (C4)$$

where

$$\mathcal{H}_{psd} = \Sigma_{m=0}^{p} Q^+_{m(p-m)sd} + \Sigma_{m=p}^{\infty} Q^-_{m(m-p)sd} + \Sigma_{m=0}^{\infty} Q^-_{m(m+p)sd} \Delta(p).$$

By repeating the same interchange procedures for the $[..]$ in Eq. (C4), we obtain

$$\Sigma_{n=0}^{\infty} \Sigma_{j=0}^{\infty} \left[.. \right] = \tfrac{1}{8}\Sigma_{q=0}^{\infty} \left[\Sigma_{n=0}^{q} X^+_{pn(q-n)} + \Sigma_{n=q}^{\infty} X^-_{pn(n-q)} + \Sigma_{n=0}^{\infty} X^-_{pn(n+q)} \Delta(q) \right] \cos q\pi x, \qquad (C5)$$

where

$$X^{\pm}_{pnj} = \Sigma_{s=n}^{\infty} \Sigma_{d=j}^{\infty} a_{sn} a_{dj} \mathcal{H}_{psd} 2(nj\mp1) - \Sigma_{s=n-2}^{\infty} \Sigma_{d=j}^{\infty} a_{s(n-2)} a_{dj} \mathcal{H}_{psd} (n-1)(j\pm1)$$
$$- \Sigma_{s=n+2}^{\infty} \Sigma_{d=j}^{\infty} a_{s(n+2)} a_{dj} \mathcal{H}_{psd} (n+1)(j\mp1).$$

Hence, the final cosine expansion becomes

$$(w_{xy})^2 = \frac{\pi^4}{8^2} \sum_{p=0}^{\infty} \sum_{q=0}^{\infty} \mathcal{Z}_{pq} \cos p\pi x \cos q\pi y, \qquad (C6)$$

where

$$\mathcal{Z}_{pq} = \sum_{n=0}^{q} \chi_{pn(q-n)}^{+} + \sum_{n=q}^{\infty} \chi_{pn(n-q)}^{-} + \sum_{n=0}^{\infty} \chi_{pn(n+q)}^{-} \Delta(q).$$

The term $(\frac{\partial^2 w}{\partial x^2})(\frac{\partial^2 w}{\partial y^2})$: We begin with the representation

$$w_{xx}w_{yy} = \pi^4 \sum_{n=0}^{\infty} \sum_{j=0}^{\infty} \sum_{s=n}^{\infty} \sum_{d=j}^{\infty} a_{sn}a_{dj}$$

$$\times \sum_{m=0}^{\infty} \sum_{i=0}^{\infty} \left\{ \sum_{r=m}^{\infty} \sum_{c=i}^{\infty} w_{rs}w_{cd}a_{rm}a_{ci}B_m(x)S_i(x) \right\} S_n(y)B_j(y), \qquad (C7)$$

where $B_m(x) = 2m\cos(m\pi x)\cos\pi x + (1+m^2)S_m(x)$. The $\{..\}$ in Eq. (C7) summed over m and i gives

$$\sum_{m=0}^{\infty} \sum_{i=0}^{\infty} \left\{ .. \right\} = \frac{1}{8}\sum_{p=0}^{\infty} \left[\sum_{m=0}^{p} \mathbf{m}_{m(p-m)sd}^{+} + \sum_{m=p}^{\infty} \mathbf{m}_{m(m-p)sd}^{-} + \sum_{m=0}^{\infty} \mathbf{m}_{m(m+p)sd}^{-}\Delta(p) \right] \cos p\pi x, \quad (C8)$$

where

$$\mathbf{m}_{misd}^{\pm} = \pm \sum_{r=m}^{\infty} \sum_{c=i}^{\infty} w_{rs}w_{cd}a_{rm}a_{ci}2(m^2+1) \mp \sum_{r=m-2}^{\infty} \sum_{c=i}^{\infty} w_{rs}w_{cd}a_{r(m-2)}a_{ci}(m-1)^2$$

$$\mp \sum_{r=m+2}^{\infty} \sum_{c=i}^{\infty} w_{rs}w_{cd}a_{r(m+2)}a_{ci}(m+1)^2.$$

Now, insert Eq. (C8) back into Eq. (C7) to obtain

$$w_{xx}w_{yy} = \frac{\pi^4}{8}\sum_{p=0}^{\infty} \sum_{n=0}^{\infty} \sum_{j=0}^{\infty} \left[\sum_{s=n}^{\infty} \sum_{d=j}^{\infty} a_{sn}a_{dj}\eta_{psd}S_n(y)B_j(y) \right] \cos p\pi x, \qquad (C9)$$

where

$$\eta_{psd} = \sum_{m=0}^{p} \mathbf{m}_{m(p-m)sd}^{+} + \sum_{m=p}^{\infty} \mathbf{m}_{m(m-p)sd}^{-} + \sum_{m=0}^{\infty} \mathbf{m}_{m(m+p)sd}^{-}\Delta(p).$$

After interchanging the order of summations for the $[..]$ in Eq. (C9)

$$\sum_{n=0}^{\infty} \sum_{j=0}^{\infty} [..] = \frac{1}{8}\sum_{q=0}^{\infty} \left[\sum_{j=0}^{q} o_{p(q-j)j}^{+} + \sum_{j=q}^{\infty} o_{p(j-q)j}^{-} + \sum_{j=0}^{\infty} o_{p(j+q)j}^{-}\Delta(q) \right] \cos q\pi x, \quad (C10)$$

where

$$o_{pnj}^{\pm} = \pm \sum_{s=n}^{\infty} \sum_{d=j}^{\infty} a_{sn}a_{dj}\eta_{psd}2(j^2+1) \mp \sum_{s=n}^{\infty} \sum_{d=j-2}^{\infty} a_{sn}a_{d(j-2)}\eta_{psd}(j-1)^2$$

$$\mp \sum_{s=n}^{\infty} \sum_{d=j+2}^{\infty} a_{sn}a_{d(j+2)}\eta_{psd}(j+1)^2,$$

the final cosine expansion becomes

$$w_{xx}w_{yy} = \frac{\pi^4}{8^2} \sum_{p=0}^{\infty} \sum_{q=0}^{\infty} \mathcal{J}_{pq}\cos p\pi x \cos q\pi y, \qquad (C11)$$

where

$$\mathcal{g}_{pq} = \sum_{j=0}^{q} \mathcal{O}^{+}_{p(q-j)j} + \sum_{j=q}^{\infty} \mathcal{O}^{-}_{p(j-q)j} + \sum_{j=0}^{\infty} \mathcal{O}^{-}_{p(j+q)j} \Delta(q).$$

Therefore, combining Eqs. (C6) and (C11) gives

$$(w_{xy})^{2} - w_{xx}w_{yy} = \pi^{4} \sum_{p=0}^{\infty} \sum_{q=0}^{\infty} P_{pq} \cos p\pi x \, \cos q\pi y, \tag{C12}$$

where $P_{pq} = (\mathcal{L}_{pq} - \mathcal{g}_{pq})/8^{2}$.

For later reference, we enumerate P_{pq} which involve only w_{11}, w_{13}, w_{21} and w_{33}.

$$P_{02} = 3.556w_{13}^{2} - 3.975w_{11}w_{13} - 6.360w_{11}w_{31} + 3.556w_{11}w_{33} + 0.711w_{13}^{2}$$
$$+ 3.556w_{13}w_{31} - 1.272w_{13}w_{33} + 28.444w_{31}^{2} - 31.802w_{31}w_{33} + 5.689w_{33}^{2},$$

$$P_{20} = 3.556w_{11}^{2} - 6.360w_{11}w_{13} - 3.975w_{11}w_{31} + 3.556w_{11}w_{33} + 28.444w_{13}^{2}$$
$$+ 3.556w_{13}w_{31} - 31.802w_{13}w_{33} + 0.711w_{31}^{2} - 1.272w_{31}w_{33} + 5.689w_{33}^{2},$$

$$P_{22} = -7.111w_{11}^{2} + 27.032w_{11}w_{13} + 27.032w_{11}w_{31} + 14.222w_{11}w_{33} - 18.489w_{13}^{2}$$
$$- 65.778w_{13}w_{31} + 24.487w_{13}w_{33} - 18.489w_{31}^{2} + 24.487w_{31}w_{33} - 7.111w_{33}^{2},$$

$$P_{04} = -3.556w_{11}^{2} + 25.441w_{11}w_{13} + 6.360w_{11}w_{31} - 22.756w_{11}w_{33} + 5.689w_{13}^{2}$$
$$- 22.756w_{13}w_{31} - 10.177w_{13}w_{33} - 28.444w_{31}^{2} + 203.53w_{31}w_{33} + 45.511w_{33}^{2},$$

$$P_{40} = -3.556w_{11}^{2} + 6.360w_{11}w_{13} + 25.441w_{11}w_{31} - 22.756w_{11}w_{33} - 28.444w_{13}^{2}$$
$$- 22.756w_{13}w_{31} + 203.53w_{13}w_{33} + 5.689w_{31}^{2} - 10.177w_{31}w_{33} + 45.511w_{33}^{2},$$

$$P_{06} = -21.466w_{11}w_{13} + 19.20w_{11}w_{33} + 19.20w_{13}^{2} + 19.20w_{13}w_{31} - 34.346w_{13}w_{33}$$
$$- 171.73w_{31}w_{33} + 153.60w_{33}^{2},$$

$$P_{60} = -21.466w_{11}w_{31} + 19.20w_{11}w_{33} + 19.20w_{13}w_{31} - 171.73w_{13}w_{33} + 19.20w_{31}^{2}$$
$$- 34.346w_{31}w_{33} + 153.60w_{33}^{2},$$

$$P_{24} = 3.556w_{11}^{2} - 44.523w_{11}w_{13} - 23.056w_{11}w_{31} + 29.156w_{11}w_{33} - 14.222w_{13}^{2}$$
$$+ 157.16w_{13}w_{31} + 46.431w_{13}w_{33} + 17.778w_{31}^{2} - 131.02w_{31}w_{33} - 30.151w_{33}^{2},$$

$$P_{42} = 3.556w_{11}^{2} - 23.056w_{11}w_{13} - 44.523w_{11}w_{31} + 29.156w_{11}w_{33} + 17.778w_{13}^{2}$$
$$+ 157.16w_{13}w_{31} - 131.02w_{13}w_{33} - 14.222w_{31}^{2} + 46.431w_{31}w_{33} - 30.151w_{33}^{2},$$

$$P_{08} = -25.60w_{13}^{2} + 45.795w_{13}w_{33} - 20.480w_{33}^{2},$$

$$P_{80} = -25.60w_{31}^{2} + 45.795w_{31}w_{33} - 20.480w_{33}^{2},$$

$$P_{26} = 23.851w_{11}w_{13} - 46.933w_{11}w_{33} - 21.333w_{13}^{2} - 94.933w_{13}w_{31} + 126.89w_{13}w_{33}$$
$$+ 107.81w_{31}w_{33} - 96.427w_{33}^{2},$$

$$P_{62} = 23.851w_{11}w_{31} - 46.933w_{11}w_{33} - 94.933w_{12}w_{31} + 107.81w_{12}w_{33} - 21.333w_{31}^2$$
$$+126.89w_{31}w_{33} - 96.427w_{33}^2 \, ,$$

$$P_{44} = 19.081w_{11}w_{12} + 19.081w_{11}w_{31} - 34.133w_{11}w_{33} + 8.533w_{12}^2 - 238.93w_{12}w_{31}$$
$$-91.589w_{12}w_{33} + 8.533w_{31}^2 - 91.589w_{31}w_{33} - 27.307w_{33}^2 \, .$$

$$P_{26} = 25.60w_{12}^2 - 166.01w_{12}w_{33} + 128.0w_{33}^2 \, ,$$

$$P_{62} = 25.60w_{31}^2 - 166.01w_{31}w_{33} + 128.0w_{33}^2 \, ,$$

$$P_{46} = -2.385w_{11}w_{12} + 27.733w_{11}w_{33} \div 2.133w_{12}^2 + 104.53w_{12}w_{31} - 118.30w_{12}w_{33}$$
$$+55.335w_{31}w_{33} - 49 \ 493w_{33}^2 \, ,$$

$$P_{64} = -2.385w_{11}w_{31} + 27.733w_{31}w_{33} + 104.53w_{12}w_{31} + 55.335w_{12}w_{33} + 2.133w_{31}^2$$
$$-118.30w_{31}w_{33} - 49.493w_{33}^2 \, ,$$

$$P_{66} = -28.80w_{12}w_{31} + 25.760w_{12}w_{33} + 25.760w_{31}w_{33} - 23.040w_{33}^2 \, ,$$

$$P_{48} = 137.38w_{12}w_{33} + 61.440w_{33}^2 \, , \qquad P_{84} = 137.38w_{31}w_{33} + 61.440w_{33}^2 \, ,$$

$$P_{68} = -17.173w_{12}w_{33} + 15.360w_{33}^2 \, , \qquad P_{86} = -17.173w_{31}w_{33} + 15.360w_{33}^2 \, ,$$

Appendix D: Complete listing of $\mathcal{L}_{02}-\mathcal{G}_{02}$

The enumeration of $\mathcal{L}_{pq}$ and $\mathcal{G}_{pq}$ becomes simpler when only w_{11}, w_{13}, w_{31} and w_{33} are retained. As an illustration, we present here the computer listing of $\mathcal{L}_{02}-\mathcal{G}_{02}$ which involves a_{11}, a_{31} and a_{33} only

$$
\begin{aligned}
\mathcal{L}_{02}-\mathcal{G}_{02} = \quad & 32 \; w(1,1)w(1,1)r(1,1)a(1,1)a(1,1)a(1,1) \\
& -48 \; w(1,1)w(1,3)a(1,1)a(1,1)a(1,1)a(3,3) \\
& +64 \; w(1,1)w(1,3)a(1,1)a(1,1)a(1,1)a(3,1) \\[4pt]
& +64 \; w(1,1)w(3,1)a(1,1)a(1,1)a(3,1)a(1,1) \\
& -64 \; w(1,1)w(3,1)a(1,1)a(1,1)a(3,3)a(1,1) \\[4pt]
& -112 \; w(1,1)w(3,3)a(1,1)a(1,1)a(3,1)a(3,3) \\
& +48 \; w(1,1)w(3,3)a(1,1)a(1,1)a(3,3)a(3,3) \\
& +64 \; w(1,1)w(3,3)a(1,1)a(1,1)a(3,1)a(3,1) \\[4pt]
& -48 \; w(1,3)w(1,3)a(1,1)a(3,3)a(1,1)a(3,1) \\
& +16 \; w(1,3)w(1,3)a(1,1)a(3,3)a(1,1)a(3,3) \\
& +32 \; w(1,3)w(1,3)a(1,1)a(3,1)a(1,1)a(3,1) \\[4pt]
& -112 \; w(1,3)w(3,1)a(1,1)a(3,3)a(3,1)a(1,1) \\
& +48 \; w(1,3)w(3,1)a(1,1)a(3,3)a(3,3)a(1,1) \\
& +64 \; w(1,3)w(3,1)a(1,1)a(3,1)a(3,1)a(1,1) \\[4pt]
& -160 \; w(1,3)w(3,3)a(1,1)a(3,3)a(3,1)a(3,1) \\
& +128 \; w(1,3)w(3,3)a(1,1)a(3,3)a(3,3)a(3,1) \\
& -32 \; w(1,3)w(3,3)a(1,1)a(3,3)a(3,3)a(3,3) \\
& +64 \; w(1,3)w(3,3)a(1,1)a(3,1)a(3,1)a(3,1) \\[4pt]
& +32 \; w(3,1)w(3,1)a(3,1)a(1,1)a(3,1)a(1,1) \\
& +160 \; w(3,1)w(3,1)a(3,3)a(1,1)a(3,3)a(1,1) \\
& -64 \; w(3,1)w(3,1)a(3,1)a(1,1)a(3,3)a(1,1) \\[4pt]
& -176 \; w(3,1)w(3,3)a(3,1)a(1,1)a(3,1)a(3,3) \\
& -240 \; w(3,1)w(3,3)a(3,3)a(1,1)a(3,3)a(3,3) \\
& +416 \; w(3,1)w(3,3)a(3,3)a(1,1)a(3,1)a(3,3) \\
& +64 \; w(3,1)w(3,3)a(3,1)a(1,1)a(3,1)a(3,1) \\[4pt]
& -112 \; w(3,3)w(3,3)a(3,1)a(3,3)a(3,1)a(3,1) \\
& -272 \; w(3,3)w(3,3)a(3,3)a(3,3)a(3,3)a(3,1) \\
& +272 \; w(3,3)w(3,3)a(3,1)a(3,3)a(3,3)a(3,1) \\
& +80 \; w(3,3)w(3,3)a(3,3)a(3,3)a(3,3)a(3,3) \\
& +32 \; w(3,3)w(3,3)a(3,1)a(3,1)a(3,1)a(3,1).
\end{aligned}
$$

(D1)

Appendix E: Evaluation of $\int_0^1\int_0^1 R_2\varphi_r(x)\varphi_s(y)dxdy$

Let us evaluate the three integrals in the order that they appear in R_2. First, we have

$$\int_0^1\int_0^1 w_{xxxx}\varphi_r(x)\varphi_s(y)dxdy=$$

$$= \pi^4\sum_{m=1}^{\infty}\sum_{i=1}^{m}\sum_{j=1}^{r} w_{ms}a_{mi}a_{rj}\int_0^1\{-4i(i^2+1)C_i(x)+((i^2+1)^2+4i^2)S_i(x)\}S_j(x)dx$$

$$= -\frac{\pi^4}{8}\sum_{m=1}^{\infty}\sum_{i=1}^{m} w_{ms}a_{mi}\left\{a_{ri}[(i+i)^4+(i-i)^4] - a_{r(i-2)}(i-1)^4 - a_{r(i+2)}(i+1)^4\right\}. \quad (E1)$$

The notation $C_i(x)=\cos(i\pi x)\cos\pi x$ is used for the first equality and the second equality follows from Eqs. (H3) and (H4) of Appendix H. Using the notation $\Sigma_I f(I)=f(1)+f(-1)$ of Maekawa [10], we have $\{..\}=-\Sigma_j\Sigma_I^{'}JIa_{r(i+I+J)}(i+I)^4$. Hence,

$$\int_0^1\int_0^1 w_{xxxx}\varphi_r(x)\varphi_s(y)dxdy=-\frac{\pi^4}{8}\sum_{m=1}^{\infty}\sum_{i=1}^{m} w_{ms}a_{mi}\Sigma_I^{'}\Sigma_j^{'}JIa_{r(i+I+J)}(i+I)^4. \quad (E2)$$

By symmetry, we can write at once

$$\int_0^1\int_0^1 w_{yyyy}\varphi_r(x)\varphi_s(y)dxdy=-\frac{\pi^4}{8}\sum_{n=1}^{\infty}\sum_{j=1}^{n} w_{rn}a_{nj}\Sigma_I^{'}\Sigma_j^{'}JIa_{s(j+I+J)}(j+I)^4. \quad (E3)$$

Similarly,

$$\int_0^1\int_0^1 w_{xxyy}\varphi_r(x)\varphi_s(y)dxdy$$

$$=\frac{\pi^4}{8^2}\sum_{m=1}^{\infty}\sum_{n=1}^{\infty} w_{mn}\left\{\sum_{i=1}^{m}a_{mi}\Sigma_I^{'}\Sigma_j^{'}JIa_{r(i+I+J)}(i+I)^2\right\}\left\{\sum_{j=1}^{n}a_{nj}\Sigma_I^{'}\Sigma_j^{'}JIa_{s(j+I+J)}(j+I)^2\right\}. \quad (E4)$$

Hence, combining Eqs. (E2)-(E4) yields the final expresion

$$\int_0^1\int_0^1 R_2\varphi_r(x)\varphi_s(y)dxdy=\frac{\pi^4 D}{b^4}\ell_i, \quad (E5)$$

where

$$\ell_i=-\frac{\beta^4}{8}\sum_{m=1}^{\infty} w_{ms}\sum_{i=1}^{m}\Sigma_I^{'}\Sigma_j^{'}JIa_{r(i+I+J)}(i+I)^4 - \frac{1}{8}\sum_{n=1}^{\infty} w_{rn}\sum_{j=1}^{n}a_{nj}\Sigma_I^{'}\Sigma_j^{'}JIa_{s(j+I+J)}(j+I)^4$$

$$+\frac{\beta^2}{32}\sum_{m=1}^{\infty}\sum_{n=1}^{\infty} w_{mn}\left\{\sum_{i=1}^{m}a_{mi}\Sigma_I^{'}\Sigma_j^{'}JIa_{r(i+I+J)}(i+I)^2\right\}\left\{\sum_{j=1}^{n}a_{nj}\Sigma_I^{'}\Sigma_j^{'}JIa_{s(j+I+J)}(j+I)^2\right\}.$$

Appendix F: Evaluation of $\int_0^1 \int_0^1 R_4 \varphi_r(x)\varphi_s(y)\,dx\,dy$

Let us evaluate the three terms in the order that they appear in N_4. For the first term we write

$$\int_0^1 \int_0^1 W_{xx} F_{yy} \varphi_r(x) \varphi_s(y)\,dx\,dy = \pi^2 b^2 P_x \ell_3 + \frac{\pi^4 Eh}{4}\ell_4. \tag{F1}$$

Here, ℓ_3 is evaluated as in Appendix E

$$\ell_3 = -(1/8)\sum_{m=1}^{\infty} W_{ms}\sum_{i=1}^{m} a_{mi}\Sigma_I'\Sigma_J' JI a_{r(i+I+J)}(i+I)^2. \tag{F2}$$

The evaluation of ℓ_4 is complicated due to the presence of F_{pq}

$$\ell_4 = -4\sum_{m=1}^{\infty}\sum_{n=1}^{\infty} W_{mn}\sum_{p=0}^{\infty}\sum_{q=0}^{\infty} F_{pq}q^2$$

$$\times\left\{\sum_{c=1}^{m}\sum_{i=1}^{r} a_{mc}a_{ri}\int_0^1 (2cC_c(x)-(c^2+1)S_c(x))S_i(x)\cos(p\pi x)\,dx\right\}$$

$$\times\left\{\sum_{d=1}^{n}\sum_{j=1}^{s} a_{nd}a_{sj}\int_0^1 S_d(y)S_j(y)\cos(q\pi y)\,dy\right\}, \tag{F3}$$

where $C_n(x)=\cos(n\pi x)\cos\pi x$. After the integration with the aid of Eqs. (H7-H8) of Appendix H, the result may be put in the form

$$\ell_4 = -(1/8^2)\sum_{m=1}^{\infty}\sum_{n=1}^{\infty} W_{mn}\sum_{p=0}^{\infty}\sum_{q=0}^{\infty} F_{pq}q^2\left\{\sum_{c=1}^{m} a_{mc}Q_{cpr}\right\}\left\{\sum_{d=1}^{n} a_{nd}R_{dqs}\right\},$$

where

$$Q_{cpr} = \Sigma_J'\Sigma_I' JI(c+I)^2\left[a_{r(c+I+J-p)} + a_{r(c+I+J+p)} - a_{r(-c-I-J+p)}\right],$$

$$R_{dqs} = -\delta_d^1\Sigma_I' I(2-I)\left[a_{s(2+I-q)} + a_{s(2+I+q)} - a_{s(-2-I+q)}\right]$$

$$-(1-\delta_d^1)\Sigma_J'\Sigma_I' JI\left[a_{s(d+I+J-q)} + a_{s(d+I+J+q)} - a_{s(-d-I-J+q)}\right].$$

Note that in R_{dqs} the factor δ_d^1 picks out the first term $d=1$, and only the second term is retained for $d>1$. Although it is possible to consolidate the three terms in Q_{cpr} and R_{dqs}, we prefer to leave them in their present form for readability.

For the second term we have by symmetry

$$\int_0^1 \int_0^1 W_{yy} F_{xx} \varphi_r(x)\varphi_s(y)\,dx\,dy = \pi^2 a^2 P_y \ell_5 + \frac{\pi^4 Eh}{4}\ell_6. \tag{F4}$$

where

$$\ell_5 = -(1/8)\sum_{n=1}^{\infty} W_{rn}\sum_{j=1}^{n} a_{nj}\Sigma_I'\Sigma_J' JI a_{s(j+I+J)}(j+I)^2.$$

$$Q_6 = -(1/8^2)\sum_{m=1}^{\infty}\sum_{n=1}^{\infty}W_{mn}\sum_{p=0}^{\infty}\sum_{q=0}^{\infty}F_{pq}p^2\left\{\sum_{c=1}^{m}a_{mc}R_{cpr}\right\}\left\{\sum_{d=1}^{n}a_{nd}Q_{dqs}\right\}.$$

And, for the last term we have

$$\int_0^1\int_0^1 w_{xy}F_{xy}\varphi_r(x)\varphi_s(y)dxdy = \frac{\pi^4 Eh}{4}Q_7. \tag{F5}$$

Here, we have

$$Q_7 = \sum_{m=1}^{\infty}\sum_{n=1}^{\infty}W_{mn}\sum_{p=0}^{\infty}\sum_{q=0}^{\infty}F_{pq}pq\left\{\sum_{i=1}^{m}\sum_{c=1}^{r}a_{mi}a_{rc}\int_0^1 A_i(x)\sin(p\pi x)S_c(x)dx\right\}$$

$$\times\left\{\sum_{j=1}^{n}\sum_{d=1}^{s}a_{nj}a_{sd}\int_0^1 A_j(y)\sin(q\pi y)S_d(y)dy\right\},$$

using $A_n(x) = n\cos(n\pi x)\sin\pi x + \sin(n\pi x)\cos\pi x$. Integrating with the aid of Eqs. (H9-H10) of Appendix H yields

$$Q_7 = (1/8^2)\sum_{m=1}^{\infty}\sum_{n=1}^{\infty}W_{mn}\sum_{p=0}^{\infty}\sum_{q=0}^{\infty}F_{pq}pq\left\{\sum_{i=1}^{m}a_{mi}S_{ipr}\right\}\left\{\sum_{j=1}^{n}a_{nj}S_{jqs}\right\},$$

where

$$S_{ipr} = \sum_J'\sum_I' JI(I+I)\left[a_{r(i+I+J-p)} - a_{r(i+I+J+p)} - a_{r(-i-I-J+p)}\right].$$

Therefore, by combining Eqs. (F1), (F4) and (F5), we obtain the final expression

$$\int_0^1\int_0^1 R_4\varphi_r(x)\varphi_s(y)dxdy = -\frac{\beta^2\pi^2}{b^4}(P_x b^2 Q_3 + P_y a^2 Q_5) - \frac{\beta^2\pi^4 Eh}{4b^4}\mathcal{J}_{rs}, \tag{F6}$$

where $\mathcal{J}_{rs} = Q_4 + Q_6 - 2Q_7$.

Again, as an illustration we enumerate $\mathcal{J}_{rs}$ for w_{11}, w_{13}, w_{31} and w_{33}:

$$\mathcal{J}_{11} = g_1 W_{11} + g_2 W_{13} + g_3 W_{31} + g_4 W_{33},$$

$$\mathcal{J}_{13} = g_2 W_{11} + g_5 W_{13} + g_6 W_{31} + g_7 W_{33},$$

$$\mathcal{J}_{31} = g_3 W_{11} + g_6 W_{13} + g_8 W_{31} + g_9 W_{33},$$

$$\mathcal{J}_{33} = g_4 W_{11} + g_7 W_{13} + g_9 W_{31} + g_{10} W_{33}, \tag{F7}$$

where

$$g_1 = -14.222(F_{02}+F_{20})+14.222(F_{04}+F_{40})+14.222F_{22}-7.111(F_{24}+F_{42}),$$

$$g_2 = 7.951F_{02}-50.883F_{04}+42.933F_{06}+12.721(F_{20}-F_{40})-27.032F_{22}+44.523F_{24}$$
$$-23.851F_{26}+23.056F_{42}-19.081F_{44}+2.385F_{46},$$

$$g_3 = 12.721(F_{02}-F_{04})+7.951F_{20}-27.032F_{22}+23.056F_{24}-50.883F_{40}+44.523F_{42}$$
$$-19.081F_{44}+42.933F_{60}-23.851F_{62}+2.385F_{64},$$

$$g_4 = -7.111(F_{02}+F_{20})+45.511(F_{04}+F_{40})-38.4(F_{06}+F_{60})-14.222F_{22}-29.156(F_{24}+F_{42})$$
$$+46.933(F_{26}+F_{62})+34.133F_{44}-27.733(F_{46}+F_{64}),$$

$$g_5 = -2.844F_{02}-22.756F_{04} \quad 76.8F_{06}+102.4F_{08}-113.78(F_{20}-F_{40})+36.978F_{22}$$
$$+28.444F_{24}+42.667F_{26}-51.2F_{28}-35.556F_{42}-17.067F_{44} \quad 4.267F_{46},$$

$$g_6 = -7.111(F_{02}+F_{20})+45.511(F_{04}+F_{40})-38.4(F_{06}+F_{60})+65.778F_{22}-157.16(F_{24}+F_{42})$$
$$+94.933(F_{26}+F_{62})+238.93F_{44}-104.53(F_{46}+F_{64})+28.8F_{66},$$

$$g_7 = 2.544F_{02}+20.353F_{04}+68.692F_{06}-91.589(F_{08}-F_{44})+63.604F_{20}-24.487F_{22}$$
$$-46.431F_{24}-126.89F_{26}+166.01F_{28}-407.06F_{40}+131.02F_{42}+118.3F_{46}$$
$$-137.38F_{48}+343.46F_{60}-107.81F_{62}-55.335F_{64}-25.760F_{66}+17.173F_{68},$$

$$g_8 = -2.844F_{02}-22.756F_{04}-76.8F_{06}+102.4F_{08}-113.78(F_{20}-F_{40})+36.978F_{22}$$
$$+28.444F_{24}+42.667F_{26}-51.2F_{28}-35.556F_{42}-17.067F_{44} \quad 4.267F_{46},$$

$$g_9 = 63.604F_{02}-407.06F_{04}+343.46F_{06}+2.544F_{20}-24.487F_{22}+131.02F_{24}-107.81F_{26}$$
$$+20.353F_{40}-46.431F_{42}-55.335F_{46}+68.692F_{60}-126.89F_{62}+118.30F_{64}$$
$$-25.760F_{66}-91.589(F_{80}-F_{44})+166.01F_{82}-137.38F_{84}+17.173F_{86},$$

$$g_{10} = -22.756(F_{02}+F_{20})-182.04(F_{04}+F_{40})-614.4(F_{06}+F_{60})+819.2(F_{08}+F_{80})$$
$$+14.222F_{22}+60.302(F_{24}+F_{42})+192.85(F_{26}+F_{62})-256(F_{28}+F_{82})+54.613F_{44}$$
$$+98.987(F_{46}+F_{64})-122.88(F_{48}+F_{84})+46.080F_{66}-30.720(F_{68}+F_{86}). \tag{F8}$$

Appendix G: Evaluation of $<<(\frac{\partial w}{\partial x})^2>>$ and $<<(\frac{\partial w}{\partial y})^2>>$ based on Eq. (3.15)

We first write in detail

$$<<(\frac{\partial w}{\partial x})^2>> = \int_0^1\int_0^1 (\frac{\partial w}{\partial x})^2 dxdy = \pi^2 \sum_{m=1}^{\infty} \sum_{n=1}^{\infty} \sum_{r=1}^{\infty} w_{mn}w_{rn}\sum_{i=1}^{m}\sum_{j=1}^{r} a_{mi}a_{rj}\int_0^1 A_i(x)A_j(x)dx,$$

where $A_i(x) = i\cos(i\pi x)\sin\pi x + \sin(i\pi x)\cos\pi x$.   Then, using Eqs. (H3), (H4) and (H5) of Appendix H, we obtain

$$<<(\frac{\partial w}{\partial x})^2>> = \frac{\pi^2}{8}\sum_{m=1}^{\infty}\sum_{n=1}^{\infty}$$

$$\sum_{r=1}^{\infty} w_{mn}w_{rn}\sum_{i=1}^{m} a_{mi}\left[2(i^2+1)a_{ri} - (i+1)^2 a_{r(i+2)} - (i-1)^2 a_{r(i-2)}\right]. \qquad (G1)$$

Let us consolidate the $\{..\}$ in Eq. (G1) by the notation $\sum_I^{\prime} f(I) = f(1) + f(-1)$ of Maekawa [10]

$$<<(\frac{\partial w}{\partial x})^2>> = \pi^2 \ell_3, \qquad (G2)$$

where

$$\ell_3 = -\frac{1}{8}\sum_{m=1}^{\infty}\sum_{n=1}^{\infty}\sum_{r=1}^{\infty} w_{mn}w_{rn}\sum_{i=1}^{m} a_{mi}\sum_J^{\prime}\sum_I^{\prime} JI a_{r(i+I+J)}(i+I)^2.$$

By symmetry we have

$$<<(\frac{\partial w}{\partial y})^2>> = \pi^2 \ell_9, \qquad (G3)$$

where

$$\ell_9 = -\frac{1}{8}\sum_{m=1}^{\infty}\sum_{n=1}^{\infty}\sum_{s=1}^{\infty} w_{mn}w_{ms}\sum_{j=1}^{n} a_{nj}\sum_J^{\prime}\sum_I^{\prime} JI a_{s(j+I+J)}(j+I)^2.$$

Appendix H: <u>Integrals used in Galerkin's procedure</u>

$$\int_0^1 \sin(a\pi x)\sin(b\pi x)\cos(p\pi x)dx = (1/4)[\delta^a_{b-p} - \delta^a_{p-b} + \delta^a_{p+b}], \tag{H1}$$

$$\int_0^1 \cos(a\pi x)\sin(b\pi x)\sin(p\pi x)dx = (1/4)[\delta^a_{b-p} - \delta^a_{p-b} - \delta^a_{p+b}], \tag{H2}$$

$$\int_0^1 \sin(a\pi x)\sin(b\pi x)\sin^2\pi x dx = (1/8)[(2+\delta^1_b)\delta^b_a - \delta^b_{a-2} - \delta^b_{a+2}], \tag{H3}$$

$$\int_0^1 \cos(a\pi x)\sin(b\pi x)\cos\pi x \sin\pi x dx = (1/8)[\delta^1_b \delta^b_a - \delta^b_{a-2} + \delta^b_{a+2}], \tag{H4}$$

$$\int_0^1 \cos(a\pi x)\cos(b\pi x)\sin^2\pi x dx = (1/8)[(2-\delta^1_b)\delta^b_a - \delta^b_{a-2} - \delta^b_{a+2}], \tag{H5}$$

$$\int_0^1 \sin(a\pi x)\sin(b\pi x)\cos^2\pi x dx = (1/8)[(2-\delta^1_b)\delta^b_a + \delta^b_{a-2} + \delta^b_{a+2}], \tag{H6}$$

$$\int_0^1 \sin(a\pi x)\sin(b\pi x)\cos(p\pi x)\sin^2\pi x dx = (1/16)[2\delta^b_{a-p} + 2\delta_{a+p} - 2\delta^b_{-a+p}$$
$$-\delta^b_{a+2-p} - \delta^b_{a+2+p} - \delta^b_{a-2-p} - \delta^b_{a-2+p} + \delta^b_{-a-2+p} + \delta^b_{-a+2+p} + \delta^b_{-a+2-p}], \tag{H7}$$

$$\int_0^1 \cos(a\pi x)\sin(b\pi x)\cos(p\pi x)\cos\pi x \sin\pi x dx = (1/16)[\delta^b_{a+2-p} + \delta^b_{a+2+p}$$
$$-\delta^b_{a-2-p} - \delta^b_{a-2+p} - \delta^b_{-a-2+p} + \delta^b_{-a+2+p} + \delta^b_{-a+2-p}], \tag{H8}$$

$$\int_0^1 \sin(a\pi x)\sin(b\pi x)\sin(p\pi x)\cos\pi x \sin\pi x dx = (1/16)[\delta^b_{a+2-p} - \delta^b_{a+2+p}$$
$$-\delta^b_{a-2-p} + \delta^b_{a-2+p} - \delta^b_{-a-2+p} + \delta^b_{-a+2+p} - \delta^b_{-a+2-p}], \tag{H9}$$

$$\int_0^1 \cos(a\pi x)\sin(b\pi x)\sin(p\pi x)\sin^2\pi x dx = (1/16)[-2\delta^b_{a-p} + 2\delta_{a+p} + 2\delta^b_{-a+p}$$
$$+\delta^b_{a+2-p} - \delta^b_{a+2+p} + \delta^b_{a-2-p} - \delta^b_{a-2+p} - \delta^b_{-a-2+p} - \delta^b_{-a+2+p} + \delta^b_{-a+2-p}]. \tag{H10}$$

Since the indices for a_{ij} and w_{mn} and F_{pq} are restricted to positive, the terms with negative indices are left out of the above formulas. For instance, $\delta^a_{-(p+b)}$ is excluded from Eqs. (H1-H2). Note also that Eqs. (P -H8) reduce to Eqs. (H3-H4), respectively, for p=0.

Appendix I: Comparison of Eq. (3.22) with Paul's results

By simply imposing $a_{ij} = \delta_j^i$, it is not possible to reduce Eq. (F1) of Appendix F, $\int_0^1 \int_0^1 W_{xx} F_{yy} \varphi_r(x) \varphi_s(y) dx dy$, to Paul's expression $\int_0^1 \int_0^1 W_{xx} F_{yy} f_r(x) g_s(y) dx dy$, where $f_r(x) = \cos[(r-1)\pi x/a] - \cos[(r+1)\pi x/a]$ and $g_s(y)$ is defined similarly for y. The reason is that φ_r are orthogonal but f_r are not. To begin with, let us reproduce Eq. (71) of Paul [6] in his notations

$$\int_0^1 \int_0^1 W_{xx} F_{yy} f_r(x) g_s(y) dx dy =$$

$$-\frac{\pi^2 h b P_x}{4a} \left\{ -[(r+1)^2 + (r-1)^2][(C_1 + 1)W_{rs} - W_{r(s+2)} - W_{r(s-2)}] + \right.$$

$$+ (r+1)^2[(C_1 + 1)W_{(r+2)s} - W_{(r+2)(s+2)} - W_{(r+2)(s-2)}]$$

$$\left. + (r-1)^2[(C_1 + 1)W_{(r-2)s} - W_{(r-2)(s+2)} - W_{(r-2)(s-2)}] \right\}$$

$$- \frac{\pi^4 E h^3}{16ab} \sum_{m,n=1}^{\infty} W_{mn} \left\{ (m+1)^2[2(n+s)^2 A_1(n+s) - (n+s-2)^2 A_1(n+s-2) - (n+s+2)^2 A_1(n+s+2) \right.$$

$$- 2(n-s)^2 A_1(n-s) + (n-s-2)^2 A_1(n-s-2) + (n-s+2)^2 A_1(n-s+2)]$$

$$+ (m-1)^2[2(n+s)^2 A_2(n+s) - (n+s-2)^2 A_2(n+s-2) - (n+s+2)^2 A_2(n+s+2)$$

$$\left. - 2(n-s)^2 A_2(n-s) + (n-s-2)^2 A_2(n-s-2) + (n-s+2)^2 A_2(n-s+2)] \right\}, \quad (I1)$$

where

$$A_1(k) = C(m+r+2)F_{(m+r+2)k} + C(m-r)F_{(m-r)k} - C(m+r)F_{(m+r)k} - C(m-r+2)F_{(m-r+2)k},$$

$$A_2(k) = C(m+r-2)F_{(m+r-2)k} + C(m-r)F_{(m-r)k} - C(m+r)F_{(m+r)k} - C(m-r-2)F_{(m-r-2)k},$$

$$C(k) = \begin{cases} 2 & \text{for } k = 0 \\ 1 & \text{for } k \neq 0 \end{cases}, \quad C_1 = \begin{cases} 2 & \text{for } s = 1 \\ 1 & \text{for } s \neq 1 \end{cases}.$$

We shall now attempt to compare Eq. (I1) with Eq. (F1) of Appendix F. First, note that Eq. (F1) consists of two terms ℓ_3 and ℓ_4, given Eqs. (F2-F3) respectively. Since the orthogonality has been used in Eq. (F2), We repeat the derivation of ℓ_3 with the replacement of $\int_0^1 \phi_n(y) \phi_s(y) dy$ by $\int_0^1 \sin(n\pi y) \sin(s\pi y) \sin^2 \pi y \, dy$ and obtain

$$\ell_3 = -\frac{1}{8^2} \sum_{\substack{m=1 \\ n=1}}^{\infty} W_{mn} \left\{ -[(m+1)^2 + (m-1)^2]\delta_m^r + (m+1)^2 \delta_{m+2}^r + (m-1)^2 \delta_{m-2}^r \right\}$$

$$\times \left\{ (2+\delta_s^1)\delta_s^n - \delta_{s+2}^n - \delta_{s-2}^n \right\}. \quad (I2)$$

It is easily checked that $\sum W_{mn}\{..\}\{..\}$ in Eq. (I2) is identical to the first $\{..\}$ term in Eq. (I1), multiplied by $\pi^2 h b P_x/4a$.

On the other hand, the orthogonality is not used in Eq. (F3), hence ℓ_4 becomes upon imposing $a_{ij} = \delta_j^i$

-73-

$$\mathcal{L}_4 = -4\sum_{m=1}^{\infty} \sum_{n=1}^{\infty} W_{mn} \sum_{p=0}^{\infty} \sum_{q=0}^{\infty} F_{pq} q^2$$

$$\times \left\{ \int_0^1 (2mC_m(x) - (m^2+1)S_m(x))S_r(x)\cos(p\pi x)dx \right\} \left\{ \int_0^1 S_n(y)S_s(y)\cos(q\pi y)dy \right\},$$

where $C_m(x) = \cos(m\pi x)\cos\pi x$. After integrating with the aid of Eqs. (H7-H8) of Appendix H, we put the resulting expression in the form

$$\mathcal{L}_4 = -(1/8^2)\sum_{m=1}^{\infty} \sum_{n=1}^{\infty} W_{mn} \sum_{p=0}^{\infty} \sum_{q=0}^{\infty} F_{pq} q^2$$

$$\times \left\{ -((m+1)^2+(m-1)^2)[\delta^p_{m-r} + \delta^p_{-(m-r)} - \delta^p_{m+r}] + (m+1)^2[\delta^p_{m+2-r} + \delta^p_{-(m+2-r)} - \delta^p_{m+2+r}] \right.$$

$$\left. + (m-1)^2[\delta^p_{m-2-r} + \delta^p_{-(m-2-r)} - \delta^p_{m-2+r} - \delta^p_{-(m-2+r)}] \right\}$$

$$\times \left\{ 2[\delta^q_{n-s} + \delta^q_{-(n-s)} - \delta^q_{n+s}] - [\delta^q_{n+2-s} + \delta^q_{-(n+2-s)} - \delta^q_{n+2+s}] \right.$$

$$\left. - [\delta^q_{n-2-s} + \delta^q_{-(n-2-s)} - \delta^q_{n-2+s} - \delta^q_{-(n-2+s)}] \right\}. \tag{13}$$

As pointed out in Appendix H, Eqs. (H7-H8) exclude terms with negative indices. Hence, the terms excluded from the first $\{..\}$ in Eq. (13) are

$$((m+1)^2+(m-1)^2)\delta^p_{-(m+r)} - (m+1)^2\delta^p_{-(m+2+r)}, \tag{14}$$

and

$$-2\delta^q_{-(n+s)} + \delta^q_{-(n+2+s)}, \tag{15}$$

are left out of the second $\{..\}$ in Eq. (13). Then, inserting Eqs. (14-15) back into Eq. (13) we have

$$\mathcal{L}_4 = -(1/8^2)\sum_{m=1}^{\infty} \sum_{n=1}^{\infty} W_{mn} \sum_{p=0}^{\infty} \sum_{q=0}^{\infty} F_{pq} q^2$$

$$\times \left\{ (m+1)^2[\delta^p_{m+2-r} + \delta^p_{-(m+2+r)} + \delta^p_{m-r} + \delta^p_{-(m-r)} - \delta^p_{m+r} - \delta^p_{-(m+r)} - \delta^p_{m+2-r} - \delta^p_{-(m+2-r)}] \right.$$

$$\left. + (m-1)^2[\delta^p_{m-2-r} + \delta^p_{-(m-2+r)} + \delta^p_{m-r} + \delta^p_{-(m-r)} - \delta^p_{m+r} - \delta^p_{-(m+r)} - \delta^p_{m-2-r} - \delta^p_{-(m+--r)}] \right\}$$

$$\times \left\{ 2\delta^q_{n-s} + 2\delta^q_{-(n-s)} - \delta^q_{n-2+s} - \delta^q_{-(n-2+s)} - \delta^q_{n+2+s} - \delta^q_{-(n+2+s)} - 2\delta^q_{n-s} - 2\delta^q_{-(n-s)} \right.$$

$$\left. + \delta^q_{n-2-s} + \delta^q_{-(n-2-s)} + \delta^q_{n+2-s} + \delta^q_{-(n+2-s)} \right\}. \tag{16}$$

Under the symmetry $F_{\pm p, \pm q} = F_{p,q}$ imposed by Paul [6], one finds that $\Sigma F_{pq} q^2 \{..\}\{..\}$ in Eq. (16) can be put in the form of the second $\{..\}$ in Eq. (11), multiplied by $(\pi^4 Eh^3/16ab)\Sigma W_{mn}$.

In a similar fashion, one can compare Eqs. (F4-F5) with the formulas given by Eqs. (70) and (72) in Ref. [6].

Appendix J: The coefficients $a_1 - a_{20}$

$$a_1 = (3/4)\left[(1-\mu^2)\{\beta^4+1\}+2(\beta^4+1+2\mu\beta^2)\right],$$

$$a_2 = (27/2)\left[9(1-\mu^2)\beta^2\{1/(\beta+4\beta^{-1})^2+1/(4\beta+\beta^{-1})^2\}+2(\beta^4+1+2\mu\beta^2)\right],$$

$$a_3 = -3(1-\mu^2)\beta^4,$$

$$a_4 = -3(1-\mu^2),$$

$$a_5 = (3/2)\left[(1-\mu^2)\beta^2\{9\beta^2+4\beta^{-2}+16/(\beta+\beta^{-1})^2+1/(4\beta+\beta^{-1})^2\}+2(9\beta^4+1+10\mu\beta^2)\right],$$

$$a_6 = (3/2)\left[(1-\mu^2)\beta^2\{9\beta^{-2}+4\beta^2+16/(\beta+\beta^{-1})^2+1/(\beta+4\beta^{-1})^2\}+2(\beta^4+9+10\mu\beta^2)\right],$$

$$a_7 = -27(1-\mu^2)\beta^2\{\beta^2+1/(4\beta+\beta^{-1})^2\},$$

$$a_q = -27(1-\mu^2)\beta^2\{\beta^{-2}+1/(\beta+4\beta^{-1})^2\},$$

$$a_8 = -3(1-\mu^2)\beta^2\{9\beta^2+64/(\beta+\beta^{-1})^2+25/(4\beta+\beta^{-1})^2\},$$

$$a_{10} = -3(1-\mu^2)\beta^2\{9\beta^{-2}+64/(\beta+\beta^{-1})^2+25/(\beta+4\beta^{-1})^2\},$$

$$a_{11} = 48(1-\mu^2)\beta^2/(\beta+\beta^{-1})^2,$$

$$a_{12} = 27(1-\mu^2)\beta^2\{4(\beta^2+\beta^{-2})+25/(\beta+4\beta^{-1})^2+25/(4\beta+\beta^{-1})^2\},$$

$$a_{13} = (3/4)\left[(1-\mu^2)\beta^2\{\beta^2+9\beta^{-2}\}+2(\beta^4+81+18\mu\beta^2)\right],$$

$$a_{14} = (27/2)\left[(1-\mu^2)\beta^2\{\beta^2+36\beta^{-2}+144/(\beta+9\beta^{-1})^2+9/(4\beta+9\beta^{-1})^2\}+2(\beta^4+9+10\mu\beta^2)\right],$$

$$a_{15} = -243(1-\mu^2),$$

$$a_{16} = (3/2)\left[(1-\mu^2)\beta^2\{272/(\beta^2+\beta^{-2})^2+625/(\beta+4\beta^{-1})^2+625/(4\beta+\beta^{-1})^2\}+2(9\beta^4+9+2\mu\beta^2)\right],$$

$$a_{17} = (3/4)\left[(1-\mu^2)\beta^2\{81\beta^2+\beta^{-2}\}+2(81\beta^4+1+18\mu\beta^2)\right],$$

$$a_{18} = -243(1-\mu^2)\beta^4,$$

$$a_{19} = (27/2)\left[(1-\mu^2)\beta^2\{36\beta^2+\beta^{-2}+144/(9\beta+\beta^{-1})^2+9/(9\beta+4\beta^{-1})^2\}+2(9\beta^4+1+10\mu\beta^2)\right],$$

$$a_{20} = (243/4)\left[(1-\mu^2)(\beta^4+1)+2(\beta^4+1+2\mu\beta^2)\right].$$

For $\beta=1$ we find that $a_1 - a_{20}$ reduce to the coefficients $C_1 - C_{13}$ previously defined by Lee [15]

$$C_1 = a_1/4, \quad C_2 = a_2/4, \quad C_3 = a_{20}/4, \quad C_4 = -a_3/4 = -a_4/4, \quad C_5 = a_5/4 = a_6/4,$$

$$C_6 = a_{13}/4 = a_{17}/4, \quad C_7 = a_{11}/4, \quad C_8 = -a_7/4 = -a_q/4, \quad C_9 = -a_8/4 = -a_{10}/4,$$

$$C_{10} = a_{12}/4, \quad C_{11} = a_{16}/4, \quad C_{12} = -a_{15}/4 = -a_{18}/4, \quad C_{13} = a_{14}/4 = a_{19}/4.$$

Note that the factor (1/4) is due to $\psi_m \sim \sqrt{2}\sin(m\pi x)$, in contrast to $\Phi_m \sim \sin(m\pi x)$ used in Ref. [15].

Appendix K: <u>Listing of SSP-5 under $\beta=1.2$ and $\mu^2=0.1$</u>

$(SSP-5)_{11} = 0.32205e+02xW(1,1)W(1,1)W(1,1)+0.22165e+03xW(1,1)W(3,1)W(3,1)$
$-0.16796e+02xW(1,1)W(1,1)W(1,3)-0.10298e+03xW(1,1)W(3,1)W(3,3)$
$+0.15569e+03xW(1,1)W(1,3)W(1,3)-0.81000e+01xW(1,1)W(1,1)W(3,1)$
$-0.52005e+02xW(1,1)W(1,3)W(3,3)-0.11364e+03xW(1,3)W(3,1)W(3,1)$
$+0.36889e+03xW(1,3)W(3,1)W(3,3)+0.30093e+02xW(1,1)W(1,3)W(3,1)$
$-0.89215e+02xW(1,3)W(1,3)W(3,1)+0.24040e+03xW(1,1)W(3,3)W(3,3),$

$(SSP-5)_{13} = -0.55987e+01xW(1,1)W(1,1)W(1,1)-0.11364e+03xW(1,1)W(3,1)W(3,1)$
$+0.15569e+03xW(1,1)W(1,1)W(1,3)+0.36889e+03xW(1,1)W(3,1)W(3,3)$
$-0.26003e+02xW(1,1)W(1,1)W(3,3)-0.17843e+03xW(1,1)W(1,3)W(3,1)$
$+0.15046e+02xW(1,1)W(1,1)W(3,1)+0.77192e+03xW(1,3)W(1,3)W(1,3)$
$+0.18377e+04xW(1,3)W(3,3)W(3,3)-0.65610e+03xW(1,3)W(1,3)W(3,3)$
$+0.84062e+03xW(1,3)W(3,1)W(3,1),$

$(SSP-5)_{21} = -0.27000e+01xW(1,1)W(1,1)W(1,1)-0.89215e+02xW(1,1)W(1,3)W(1,3)$
$+0.22165e+03xW(1,1)W(1,1)W(3,1)+0.36889e+03xW(1,1)W(1,3)W(3,3)$
$-0.51491e+02xW(1,1)W(1,1)W(3,3)-0.22727e+03xW(1,1)W(1,3)W(3,1)$
$+0.15046e+02xW(1,1)W(1,1)W(1,3)+0.84062e+03xW(1,3)W(1,3)W(3,1)$
$+0.15191e+04xW(3,1)W(3,1)W(3,1)-0.13605e+04xW(3,1)W(3,1)W(3,3)$
$+0.31848e+04xW(3,1)W(3,3)W(3,3),$

$(SSP-5)_{23} = -0.26003e+02xW(1,1)W(1,1)W(1,3)+0.24040e+03xW(1,1)W(1,1)W(3,3)$
$+0.36889e+03xW(1,1)W(1,3)W(3,1)-0.51491e+02xW(1,1)W(1,1)W(3,1)$
$-0.21870e+03xW(1,3)W(1,3)W(1,3)+0.18377e+04xW(1,3)W(1,3)W(3,3)$
$-0.45350e+03xW(3,1)W(3,1)W(3,1)+0.31848e+04xW(3,1)W(3,1)W(3,3)$
$+0.26086e+04xW(3,3)W(3,3)W(3,3).$

Appendix L: Summary of h's and g's under Eq. (6.8)

Under Eq. (6.8), Eq. (4.8) reduces to

$$h_1 = A(1+\beta^{-2}), \quad h_2 = -A[1+2/(\beta^2+1)], \quad h_3 = -A[\beta^{-2}+2/(\beta^2+1)],$$

$$h_4 = h_{10} = 0, \quad h_5 = -h_7 = 9A/\beta^2, \quad h_6 = 8A/(\beta^2+1), \quad h_8 = -h_9 = 9A, \tag{L1}$$

where $A = \delta_v T_c/2$.

On the other hand, Eq. (F8) of Appendix F reduces to

$$g_1 = 14.222B[1+\beta^{-2}+1/(\beta^2+1)],$$

$$g_2 = -7.951B - 12.721B/\beta^2 - 27.032B/(\beta^2+1),$$

$$g_3 = -12.721B - 7.951B/\beta^2 - 27.032B/(\beta^2+1),$$

$$g_4 = 7.111B(1+\beta^{-2}) - 14.222B/(\beta^2+1),$$

$$g_5 = 2.844B + 113.78B/\beta^2 + 36.978B/(\beta^2+1),$$

$$g_6 = 7.111B(1+\beta^{-2}) + 65.778B/(\beta^2+1),$$

$$g_7 = -2.544B - 63.604B/\beta^2 - 24.487B/(\beta^2+1),$$

$$g_8 = 2.844B + 113.78B/\beta^2 + 36.978B/(\beta^2+1),$$

$$g_9 = -63.604B - 2.544B/\beta^2 - 24.487B/(\beta^2+1),$$

$$g_{10} = 22.756B(1+\beta^{-2}) + 14.222B/(\beta^2+1), \tag{L2}$$

where $B = \delta_v T_0/16$.

Appendix M: Random response under stationary zero-mean Gaussian excitations

For completeness, we shall present here the Wiener-Khinchin theorem, the input-output relation for a damped linear oscillator under stationary zero-mean Gaussian excitations, and the equivalent linearization technique applied to a Duffing nonlinear oscillator under the same excitations.

Wiener-Khinchin theorem: For a stochastic process $x(t)$ we define the correlation $R_{XX}(t_1, t_2) = \langle x(t_1)x(t_2) \rangle$, where $\langle \rangle$ is the ensemble average. When the process is stationary, the correlation function depends only on the time difference $\tau = t_2 - t_1$, hence $R_{XX}(t_1, t_2) = R_{XX}(\tau)$. (Note that τ was the dimensionless time in Sec. VI.) Moreover, when the process is ergodic the ensemble average may be replaced by time average; however, we shall use $\langle \rangle$ to denote both the ensemble and time averages. The correlation $R_{XX}(\tau)$ is expressed by the power spectral density function $g_{XX}(f)$ and the inverse relation also exists through the Fourier transform

$$R_{XX}(\tau) = \int_{-\infty}^{\infty} g_{XX}(f)e^{i2\pi f\tau}df,$$

$$g_{XX}(f) = \int_{-\infty}^{\infty} R_{XX}(\tau)e^{-i2\pi f\tau}d\tau. \tag{M1}$$

Using the angular frequency $\omega = 2\pi f$ and $\phi_{XX}(\omega) = g_{XX}(f)/2\pi$, Eq. (M1) becomes

$$R_{XX}(\tau) = \int_{-\infty}^{\infty} \phi_{XX}(\omega)e^{i\omega\tau}d\omega,$$

$$\phi_{XX}(\omega) = \frac{1}{2\pi}\int_{-\infty}^{\infty} R_{XX}(\tau)e^{-i\omega\tau}d\tau, \tag{M2}$$

known as the Wiener-Khinchin theorem [8]. One often finds Eq. (M2) defined in terms of $G_{XX}(\omega) = 2\phi_{XX}(\omega)$, with the constant pair $(1, 1/2\pi)$ of Eq. (M2) being replaced by $(1/2, 1/\pi)$ [25]. Since $R_{XX}(\tau)$ and $\phi_{XX}(\omega)$ are even functions, Eq. (M2) may be reduced to the cosine Fourier transform relations

$$R_{XX}(\tau) = 2\int_{0}^{\infty} \phi_{XX}(\omega)\cos\omega\tau\,d\omega,$$

$$\phi_{XX}(\omega) = \frac{1}{\pi}\int_{0}^{\infty} R_{XX}(\tau)\cos\omega\tau\,d\tau. \tag{M3}$$

It is important to note that $R_{XX}(0) = \langle x^2 \rangle$ is the mean square amplitude (i.e., the energy), hence

$$\langle x^2 \rangle = \int_{-\infty}^{\infty} \phi_{XX}(\omega)d\omega, \tag{M4}$$

which states that the power spectral density $\phi_{XX}(\omega^*)$ represents energy contained in a small band of $\Delta\omega$ about $\omega = \pm\omega^*$.

Linear input-output relation: Consider a damped linear oscillator

$$\ddot{x} + \beta\dot{x} + kx = f(t), \tag{M5}$$

where β is the damping coefficient and k the stiffness (Note that β was the aspect ratio in Sec. II). Assume that $f(t)$ is a stationary Gaussian process with the power spectral density $\phi_{ff}(\omega)$. In terms of the frequency response function of Eq. (M5)

$$H(\omega) = \frac{1}{(k-\omega^2) + i\beta\omega}, \tag{M6}$$

the input-output relation is [8]

$$\phi_{xx}(\omega) = \phi_{ff}(\omega)|H(\omega)|^2. \tag{M7}$$

Now, it is simplest to let $\phi_{ff}(\omega)$ be a constant K over the range of ω in which $|H(\omega)|^2$ is significantly different from zero. We then have

$$\langle x^2 \rangle = K \int_{-\infty}^{\infty} |H(\omega)|^2 d\omega. \tag{M8}$$

To evaulate the integral $I = \int_{-\infty}^{\infty}|H(\omega)|^2 d\omega$ by the method of residues, we write it as $I = \int_{-\infty}^{\infty} f(z)dz$, where $f(z) = 1/[(k-z^2)^2 + (\beta z)^2]$. Since the poles of $f(z)$ are

$$z_1 = [\sqrt{4k-\beta^2}+i\beta]/2, \ z_2 = [-\sqrt{4k-\beta^2}+i\beta]/2, \ z_3 = [\sqrt{4k-\beta^2}-i\beta]/2, \ z_4 = [-\sqrt{4k-\beta^2}-i\beta]/2, \tag{M9}$$

the residues of the simple poles z_1 and z_2 give

$$I = 2\pi i[(z-z_1 f(z)|_{z=z_1} + (z-z_2)f(z)|_{z=z_2}] = \frac{\pi}{\beta k}. \tag{M10}$$

Hence,

$$\langle x^2 \rangle = \frac{\pi K}{\beta k}. \tag{M11}$$

In standard linear oscillator notations $\beta = 2\zeta\omega_0$ and $k = \omega_0^2$, we therefore recover $\langle x^2 \rangle = \pi K/2\zeta\omega_0^3$, given by Eq. (5-42) of Lin [8]. Since for small β, the I represents contributions from the sharp resonance peaks at $\omega \approx \pm\sqrt{k}$, one may approximate $\langle x^2 \rangle$ by

$$\langle x^2 \rangle \approx \frac{\pi\phi_{ff}(\sqrt{k})}{\beta k}, \tag{M12}$$

which is asymtotically correct as $\beta \to 0$ (see, Fig 5.3 in Ref [8]).

Equivalent linearization: We now consider a damped Duffing oscillator with the cubic stiffness term

$$\ddot{x} + \beta\dot{x} + kx + \gamma x^3 = f(t), \tag{M13}$$

where γ denoting the strength of hard spring. Rather than solving Eq. (M13) by perturbation, the aim is to replace it by a linear system of the form

$$\ddot{x} + \beta\dot{x} + k_e x + e = f(t). \tag{M14}$$

By a judicious choice of the *equivalent* stiffness k_e, one attempts to capture the effect of nonlinearity of Eq. (M13) in a statistical sense, and the degree of failure is quantified by the error term $e=(-k_e+k)x+\gamma x^3$, which is nothing but the difference of Eqs. (M13) and (M14). In the equivalent linearization technique, k_e is found by minimizing the mean square error, i.e., $d<e^2>/dk_e=0$. Under the assumption that x is Gaussian with zero mean, a simple expression is obtained

$$k_e = k + 3\gamma<x^2>. \tag{M15}$$

When the error term is suppressed we see that Eq. (M14) has the same form as Eq. (M5). In view of Eq. (M12), we therefore have

$$<x^2> \approx \frac{\pi\phi_{ff}(\sqrt{k_e})}{\beta k_e}. \tag{M16}$$

Now, suppose that $\phi_{ff}(\omega)$ is more or less flat, i.e., $\phi_{ff}(\sqrt{k_e})\approx\phi_{ff}(\sqrt{k})$. Then inserting Eq. (M15) into Eq. (M16) and identifying $<x^2_{1in}>=\pi\phi_{ff}(\sqrt{k})/\beta k$ as the mean square amplitude of the linear system, the mean square amplitude of Eq. (M13) is given by the quadratic equation

$$\frac{3\gamma}{k}(<x^2>)^2 + <x^2> - <x^2_{1in}> =0. \tag{M17}$$

The positive root of Eq. (M17)

$$<x^2> = \frac{k}{6\gamma}\left[\sqrt{1+\frac{12\gamma<x^2_{1in}>}{k}} - 1\right], \tag{M18}$$

is physically relevant [9]. (It is not necessary to solve Eqs (M15-M16) iteratively, as suggested in Ref [11].)

It is instructive to examine the two limits of Eq. (M18). First, when the cubic nonlinearity is weak we obtain by Taylor expansion

$$\sqrt{1+\frac{12\gamma<x^2_{1in}>}{k}} \approx 1 + \frac{6\gamma<x^2_{1in}>}{k}.$$

Then, Eq. (M18) becomes $<x^2>\approx<x^2_{1in}>$, as expected. Second, for a strong nonlinearity, by ignoring $+1$ under the radical and -1 in the square brackets, we obtain

$$<x^2> \approx \sqrt{\frac{k<x^2_{1in}>}{3\gamma}},$$

hence $<x^2>$ is proportional to $<x^2_{1in}>^{1/2}$ or $(\phi_{ff})^{1/2}$.

Appendix N: <u>Extension of the equivalent linearization technique</u>

Suppose a constant forcing f_0 is added to the otherwise zero-mean Gaussian excitations for a damped harmonic oscillator

$$\ddot{x} + \beta\dot{x} + kx = f_0 + f(t), \tag{N1}$$

where β is the damping coefficient and k the stiffness. The general solution of Eq. (N1) has the form

$$x(t) = e^{-\beta t/2}[C_1\cos\bar{\omega}t + C_2\sin\bar{\omega}t] + \int_0^t h(t-\tau)(f_0 + f(\tau))d\tau, \tag{N2}$$

where

$$h(t) = \begin{cases} e^{-\beta t/2}\sin\bar{\omega}t/\bar{\omega} & \text{for } t>0, \\ 0 & \text{for } t<0, \end{cases} \tag{N3}$$

and $\bar{\omega} = \frac{1}{2}(4k^2 - \beta^2)^{1/2}$. (In standard oscillator notations $\beta = 2\zeta\omega_0$ and $k = \omega_0^2$, Eq. (N3) reduces to $h(t) = e^{-\zeta\omega_0 t}\sin\bar{\omega}t/\bar{\omega}$, where $\bar{\omega} = \omega_0(1-\zeta^2)^{1/2}$ [26].) The first term of Eq. (N2) is a homogeneous solution reflecting the initial condition specified by constants C_1 and C_2, which eventually dies out as $t \to \infty$. The second integral term is the particular solution. Consider the contribution of f_0

$$\int_0^t h(t-\tau)f_0 d\tau = \frac{f_0}{k\bar{\omega}}[-e^{-\beta t/2}(\frac{\beta}{2}\sin\bar{\omega}t + \bar{\omega}\cos\bar{\omega}t) + \bar{\omega}]. \tag{N4}$$

After a long time, Eq. (N4) settles down to steady state

$$\int_0^\infty h(t-\tau)f_0 d\tau \to \frac{f_0}{k}, \tag{N5}$$

which we shall denote by $\bar{x}$; i.e.,

$$\bar{x} = \frac{f_0}{k}. \tag{N6}$$

With this preliminary, we are now in a position to formulate the input-output relation. By splitting x into the mean $\bar{x}$ and fluctuation y

$$x = \bar{x} + y, \tag{N7}$$

we rewrite Eq. (N1) as

$$\ddot{y} + \beta\dot{y} + ky + (k\bar{x} - f_0) = f(t). \tag{N8}$$

Because of Eq. (N6), we find that Eq. (N8) reduces to Eq. (M5) of Appendix M after a long time, hence

$$\langle y^2\rangle \approx \frac{\pi\Phi_{ff}(\sqrt{k})}{\beta k}, \tag{N9}$$

is the stationary response, as already given by Eq. (M12) of Appendix M. Since $\bar{x}$ is constant and $\langle y\rangle = 0$, we have

$$\langle x^2 \rangle = \bar{x}^2 + \langle y^2 \rangle. \tag{N10}$$

In other words, the total mean square amplitude is sum of the squared steady level and mean square amplitude due to the zero-mean Gaussian excitations.

Our goal here is to estimate the response of a damped Duffing oscillator under nonzero-mean Gaussian excitations, that is

$$\ddot{x} + \beta\dot{x} + kx + \gamma x^3 = f_0 + f(t). \tag{N11}$$

We again split x into the mean $\bar{x}$ and fluctuation y, and recast Eq. (N11) into the following form

$$\ddot{y} + \beta\dot{y} + (k+3\gamma\bar{x}^2)y + 3\gamma\bar{x}y^2 + \gamma y^3 + k\bar{x} + \gamma\bar{x}^3 - f_0 = f(t). \tag{N12}$$

We shall now replace Eq. (N12) by an equivalent linear system

$$\ddot{y} + \beta\dot{y} + k_e y + e = f(t), \tag{N13}$$

where the error term is

$$e = (-k_e + k + 3\gamma\bar{x}^2)y + 3\gamma\bar{x}y^2 + \gamma y^3 + k\bar{x} + \gamma\bar{x}^3 - f_0. \tag{N14}$$

Following the equivalent linearization procedure, the k_e is chosen to minimize the mean square error; i.e., $d\langle e^2 \rangle / dk_e = 0$. Under the usual zero-mean Gaussian assumption for y, we obtain

$$k_e = k + 3\gamma\bar{x}^2 + 3\gamma\langle y^2 \rangle. \tag{N15}$$

Again, dropping the error term in Eq. (N13), we can write down the mean square of amplitude y

$$\langle y^2 \rangle \approx \frac{\pi\phi_{ff}(\sqrt{k_e})}{\beta k_e}, \tag{N16}$$

in analogy to Eq. (N9). Inserting Eq. (N15) into Eq. (N16) and denoting by $\langle y_{lin}^2 \rangle \approx \pi\phi_{ff}(\sqrt{k_e})/\beta k$ the mean square amplitude of linear equation, the positive root of the quadratic equation is given by

$$\langle y^2 \rangle = \frac{k}{6\gamma}\left[\sqrt{(1+\frac{3\gamma\bar{x}^2}{k})^2 + \frac{12\gamma\langle y_{lin}^2 \rangle}{k}} - (1+\frac{3\gamma\bar{x}^2}{k}) \right], \tag{N17}$$

in analogy to Eq. (M18) of Appendix M. Note that the mean $\bar{x}$ in Eq. (N17) can be related to f_0 via Eq. (N6) which now has the form

$$\bar{x} = \frac{f_0}{k_e}. \tag{N18}$$

By inserting Eq. (N15) into Eq. (N18), we obtain

$$3\gamma\bar{x}^3 + (k+3\gamma\langle y^2\rangle)\bar{x} - f_0 = 0, \tag{N19}$$

the real root of which is given by

$$\bar{x} = A - B, \tag{N20}$$

where

$$A = \sqrt[3]{\frac{f_0}{6\gamma} + \sqrt{\left(\frac{f_0}{6\gamma}\right)^2 + \left(\frac{k+3\gamma\langle y^2\rangle}{9\gamma}\right)^3}} \quad \text{and} \quad B = \sqrt[3]{-\frac{f_0}{6\gamma} + \sqrt{\left(\frac{f_0}{6\gamma}\right)^2 + \left(\frac{k+3\gamma\langle y^2\rangle}{9\gamma}\right)^3}}.$$

The pair of Eqs. (N17) and (N20) can be solved for $\langle y^2\rangle$ and $\bar{x}$, afterwards the mean square of amplitude $\bar{x}$ is obtained by Eq. (N10).

In the limiting case of $f_0 = 0$, Eq. (N20) yields $\bar{x} = 0$ because $A = B$. Then, Eq. (N17) degenerates to Eq. (M18) of Appendix M, which was derived under the assumption of zero-mean Gaussian excitations.

Appendix O: <u>Normal stress and strain components</u>

We consider here only the normal components of stress and strain tensors. Let us begin by writing the three terms separately in the order that they appear in Eq. (2.24)

$$\sigma_x = \sigma_x^m + \sigma_x^b + \sigma_x^t,$$
$$\sigma_y = \sigma_y^m + \sigma_y^b + \sigma_y^t, \tag{O1}$$

where the superscript 'm' denotes the membrane stress, 'b' the bending stress, and 't' the thermal stress. By using the nondimensional variables of Eqs. (4.1-4.2), the three terms in Eq. (O1) can be put in a dimensionless form which we shall denote by an overhead karat

$$\hat{\sigma}_x = \hat{\sigma}_x^m + \hat{\sigma}_x^b + \hat{\sigma}_x^t,$$
$$\hat{\sigma}_y = \hat{\sigma}_y^m + \hat{\sigma}_y^b + \hat{\sigma}_y^t, \tag{O2}$$

so that the stress is now measured in units of $\pi^2 E h^2/b^2$; i.e.,

$$\sigma_x = \frac{\pi^2 E h^2}{b^2} \hat{\sigma}_x, \quad \sigma_y = \frac{\pi^2 E h^2}{b^2} \hat{\sigma}_y. \tag{O3}$$

Also, by inserting Eq. (O3) into Eq. (2.1), we obtain the expression for the strain tensor

$$\varepsilon_x = \frac{\pi^2 h^2}{b^2} \hat{\varepsilon}_x, \quad \varepsilon_y = \frac{\pi^2 h^2}{b^2} \hat{\varepsilon}_y. \tag{O4}$$

Here, the nondimensional $\hat{\varepsilon}_x$ and $\hat{\varepsilon}_y$ are given by

$$\hat{\varepsilon}_x = \hat{\sigma}_x - \mu\hat{\sigma}_y + \frac{\alpha b^2}{\pi^2 h^2}T^*\hat{T},$$
$$\hat{\varepsilon}_y = \hat{\sigma}_y - \mu\hat{\sigma}_x + \frac{\alpha b^2}{\pi^2 h^2}T^*\hat{T}, \tag{O5}$$

where $T^* = T_s^*$ for a simply-supported plate and $T^* = T_c^*$ for a clamped plate.

A. Expansion for the stress tensor

Let us now express the stress tensor in series expansions.

<u>Simply-supported plate:</u> Introduce Eqs. (3.1), (3.3), (3.5) and (3.12) into Eq. (O1). With the use of Eqs. (4.1-4.2), we obtain the dimensionless stress components when $T^* = \pi^2 h^2(\beta^2+1)/12\alpha b^2(1+\mu)$

$$\hat{\sigma}_x^m = -\frac{(\beta^2+1)T_0}{12(1-\mu^2)} + \frac{1}{2(1-\mu^2)}\sum_{m=1}^{\infty}\sum_{n=1}^{\infty}W_{mn}^2(m^2\beta^2+n^2\mu)$$

$$- \frac{(\beta^2+1)}{12(1+\mu)}\sum_{p=0}^{\infty}\sum_{q=0}^{\infty}(-\frac{T_{pq}}{p^2\beta^2+q^2})q^2\cos p\pi x \cos q\pi y$$

$$-\sum_{p=0}^{\infty}\sum_{q=0}^{\infty}\left\{\frac{\varepsilon_{pq}}{(p^2\beta+q^2/\beta)^2}\right\}q^2\cos p\pi x\,\cos q\pi y,$$

$$\hat{\sigma}_x^b = \frac{Z}{(1-\mu^2)}\sum_{m=1}^{\infty}\sum_{n=1}^{\infty}W_{mn}(m^2\beta^2+n^2\mu)\psi_m(x)\psi_n(y),$$

$$\hat{\sigma}_x^t = \hat{\sigma}_y^t = -\frac{(\beta^2+1)Z\theta}{12(1-\mu^2)},$$

$$\hat{\sigma}_y^m = -\frac{(\beta^2+1)T_0}{12(1-\mu^2)} + \frac{1}{2(1-\mu^2)}\sum_{m=1}^{\infty}\sum_{n=1}^{\infty}W_{mn}^2(m^2\beta^2\mu+n^2)$$

$$-\frac{\beta^2(\beta^2+1)}{12(1+\mu)}\sum_{p=0}^{\infty}\sum_{q=0}^{\infty}\left(\frac{T_{pq}}{p^2\beta^2+q^2}\right)p^2\cos p\pi x\,\cos q\pi y$$

$$-\beta^2\sum_{p=0}^{\infty}\sum_{q=0}^{\infty}\left\{\frac{\varepsilon_{pq}}{(p^2\beta+q^2/\beta)^2}\right\}p^2\cos p\pi x\,\cos q\pi y,$$

$$\hat{\sigma}_y^b = \frac{Z}{(1-\mu^2)}\sum_{m=1}^{\infty}\sum_{n=1}^{\infty}W_{mn}(m^2\beta^2\mu+n^2)\psi_m(x)\psi_n(y), \tag{06}$$

where $Z=z/h$ ranges over $(1/2,-1/2)$.

Clamped plate: Instead, introduce Eqs. (3.1), (3.12), (3.15) and (3.16) into Eq. (01). Then, with $T^*=\pi^2 h^2(\beta^4+2\beta^2/3+1)/3\alpha b^2(1+\mu)(\beta^2+1)$ we obtain the dimensionless stress components in a similar fashion

$$\hat{\sigma}_x^m = -\frac{(\beta^4+2\beta^2/3+1)T_0}{3(1-\mu^2)(\beta^2+1)} + \frac{1}{2(1-\mu^2)}[\beta^2\ell_3+\mu\ell_9]$$

$$-\frac{(\beta^4+2\beta^2/3+1)}{3(1+\mu)(\beta^2+1)}\sum_{p=0}^{\infty}\sum_{q=0}^{\infty}\left(\frac{T_{pq}}{p^2\beta^2+q^2}\right)q^2\cos p\pi x\,\cos q\pi y$$

$$-\sum_{p=0}^{\infty}\sum_{q=0}^{\infty}\left\{\frac{P_{pq}}{(p^2\beta+q^2/\beta)^2}\right\}q^2\cos p\pi x\,\cos q\pi y,$$

$$\hat{\sigma}_x^b = -\frac{Z}{(1-\mu^2)}\left\{\beta^2\sum_{m=1}^{\infty}\sum_{n=1}^{\infty}W_{mn}\varphi_m''(x)\varphi_n(y) + \mu\sum_{m=1}^{\infty}\sum_{n=1}^{\infty}W_{mn}\varphi_m(x)\varphi_n''(y)\right\},$$

$$\hat{\sigma}_x^t = \hat{\sigma}_y^t = -\frac{(\beta^4+2\beta^2/3+1)Z\theta}{3(1-\mu^2)(\beta^2+1)},$$

$$\hat{\sigma}_y^m = -\frac{(\beta^4+2\beta^2/3+1)T_0}{3(1-\mu^2)(\beta^2+1)} + \frac{1}{2(1-\mu^2)}[\beta^2\mu\ell_3+\ell_9]$$

$$-\frac{\beta^2(\beta^4+2\beta^2/3+1)}{3(1+\mu)(\beta^2+1)}\sum_{p=0}^{\infty}\sum_{q=0}^{\infty}\left(\frac{T_{pq}}{p^2\beta^2+q^2}\right)p^2\cos p\pi x\,\cos q\pi y$$

$$- \beta^2 \sum_{p=0}^{\infty} \sum_{q=0}^{\infty} \left\{ \frac{P_{pq}}{(p^2\beta + q^2/\beta)^2} \right\} p^2 \cos p\pi x \cos q\pi y,$$

$$\hat{\sigma}_y^b = -\frac{Z}{(1-\mu^2)} \left\{ \beta^2 \mu \sum_{m=1}^{\infty} \sum_{n=1}^{\infty} W_{mn} \varphi_m''(x)\varphi_n(y) + \sum_{m=1}^{\infty} \sum_{n=1}^{\infty} W_{mn}\varphi_m(x)\varphi_n''(y) \right\}. \tag{07}$$

Under the temperature variation discussed in Sec. VI for which T_{pq} obey
Eq. (6.8), the sum involving T_{pq} in $\hat{\sigma}_x^m$ has only two terms

$$\sum_{p=0}^{\infty} \sum_{q=0}^{\infty} \left(\frac{T_{pq}}{p^2\beta^2 + q^2} \right) q^2 \cos p\pi x \cos q\pi y = -\frac{\delta_v T_0}{4}\cos 2\pi y + \frac{\delta_v T_0}{4(\beta^2+1)}\cos 2\pi x \cos 2\pi y, \tag{08}$$

and the corresponding sum in $\hat{\sigma}_y^m$ reduces to

$$\sum_{p=0}^{\infty} \sum_{q=0}^{\infty} \left(\frac{T_{pq}}{p^2\beta^2 + q^2} \right) p^2 \cos p\pi x \cos q\pi y = -\frac{\delta_v T_0}{4\beta^2}\cos 2\pi x + \frac{\delta_v T_0}{4(\beta^2+1)}\cos 2\pi x \cos 2\pi y. \tag{09}$$

B. Stress tensor involving W_{11} only

For the simplest case involving only the W_{11}, Eqs. (06-09) simplify to give

Simply-supported plate:

$$\hat{\sigma}_x^m = -\frac{(\beta^2+1)T_0}{12(1-\mu^2)} + \frac{(\beta^2+\mu)}{2(1-\mu^2)}W_{11}^2$$
$$- \frac{(\beta^2+1)}{12(1+\mu)}(\frac{\delta_v T_0}{4})\left\{ -\cos 2\pi y + \frac{1}{(\beta^2+1)}\cos 2\pi x \cos 2\pi y \right\} - \frac{\beta^2}{2}W_{11}^2\cos 2\pi y,$$

$$\hat{\sigma}_x^b = \frac{Z(\beta^2+\mu)}{(1-\mu^2)}W_{11}\psi_1'(x)\psi_1(y),$$

$$\hat{\sigma}_x^t = \hat{\sigma}_y^t = -\frac{(\beta^2+1)Z\theta}{12(1-\mu^2)},$$

$$\hat{\sigma}_y^m = -\frac{(\beta^2+1)T_0}{12(1-\mu^2)} + \frac{(\beta^2\mu+1)}{2(1-\mu^2)}W_{11}^2$$
$$- \frac{\beta^2(\beta^2+1)}{12(1+\mu)}(\frac{\delta_v T_0}{4})\left\{ \frac{-1}{\beta^2}\cos 2\pi x + \frac{1}{(\beta^2+1)}\cos 2\pi x \cos 2\pi y \right\} - \frac{1}{2}W_{11}^2\cos 2\pi x,$$

$$\hat{\sigma}_y^b = \frac{Z(\beta^2\mu+1)}{(1-\mu^2)}W_{11}\psi_1(x)\psi_1'(y). \tag{010}$$

Clamped plate:

$$\hat{\sigma}_x^m = -\frac{(\beta^4 + 2\beta^2/3 + 1)T_0}{3(1-\mu^2)(\beta^2+1)} + \frac{2(\beta^2+\mu)}{3(1-\mu^2)}W_{11}^2$$

$$-\frac{(\beta^4 + 2\beta^2/3 + 1)}{3(1+\mu)(\beta^2+1)}\left(\frac{\delta_v T_0}{4}\right)\left\{-\cos 2\pi y + \frac{1}{(\beta^2+1)}\cos 2\pi x \cos 2\pi y\right\}$$

$$-\frac{32}{9}W_{11}^2\left\{\frac{\beta^2}{4}\cos 2\pi y - \frac{\beta^2}{16}\cos 4\pi y - \frac{\cos 2\pi x \cos 2\pi y}{2(\beta + \beta^{-1})^2} + \frac{\cos 2\pi x \cos 4\pi y}{(\beta + 4\beta^{-1})^2} + \frac{\cos 4\pi x \cos 2\pi y}{4(4\beta + \beta^{-1})^2}\right\},$$

$$\hat{\sigma}_x^b = -\frac{2Z}{(1-\mu^2)}W_{11}a_{11}[\beta^2 \cos 2\pi x \varphi_1(y) + \mu \varphi_1(x)\cos 2\pi y],$$

$$\hat{\sigma}_x^t = \hat{\sigma}_y^t = -\frac{(\beta^4 + 2\beta^2/3 + 1)Z\theta}{3(1-\mu^2)(\beta^2+1)},$$

$$\hat{\sigma}_y^m = -\frac{(\beta^4 + 2\beta^2/3 + 1)T_0}{3(1-\mu^2)(\beta^2+1)} + \frac{2(\beta^2\mu + 1)}{3(1-\mu^2)}W_{11}^2$$

$$-\frac{(\beta^4 + 2\beta^2/3 + 1)}{3(1+\mu)(\beta^2+1)}\left(\frac{\delta_v T_0}{4}\right)\left\{-\cos 2\pi x + \frac{\beta^2}{(\beta^2+1)}\cos 2\pi x \cos 2\pi y\right\}$$

$$-\frac{32}{9}W_{11}^2\left\{\frac{1}{4}\cos 2\pi x - \frac{1}{16}\cos 4\pi x - \frac{\beta^2 \cos 2\pi x \cos 2\pi y}{2(\beta + \beta^{-1})^2} + \frac{\beta^2 \cos 2\pi x \cos 4\pi y}{4(\beta + 4\beta^{-1})^2} + \frac{\beta^2 \cos 4\pi x \cos 2\pi y}{(4\beta + \beta^{-1})^2}\right\},$$

$$\hat{\sigma}_y^b = -\frac{2Z}{(1-\mu^2)}W_{11}a_{11}[\beta^2\mu\cos 2\pi x \varphi_1(y) + \varphi_1(x)\cos 2\pi y]. \tag{G11}$$

Note that for $\delta_v = 0$ the $\hat{\sigma}_x^m$ and $\hat{\sigma}_y^m$ given by Eq. (O10) agree with Eq. (34) of Wilcox & Clemmer [16] when $k_x = k_y = \infty$ is imposed in their equation.

For computation, however, it is more convenient to regroup Eqs. (O10) and (O11) in powers of W_{11}

Simply-supported plate:

$$\hat{\sigma}_x = -\frac{(\beta^2+1)T_0}{12(1-\mu^2)}\left\{1 + (1-\mu)\left(\frac{\delta_v}{4}\right)\left[-\cos 2\pi y + \frac{1}{(\beta^2+1)}\cos 2\pi x \cos 2\pi y\right] + Z\delta_g \sin \pi x \sin \pi y\right\}$$

$$+ \frac{2Z(\beta^2+\mu)}{(1-\mu^2)}\sin \pi x \sin \pi y W_{11} + \frac{1}{2}\left\{\frac{(\beta^2+\mu)}{(1-\mu^2)} - \beta^2 \cos 2\pi y\right\}W_{11}^2.$$

$$\hat{\sigma}_y = -\frac{(\beta^2+1)T_0}{12(1-\mu^2)}\left\{1 + (1-\mu)\left(\frac{\delta_v}{4}\right)\left[-\cos 2\pi x + \frac{\beta^2}{(\beta^2+1)}\cos 2\pi x \cos 2\pi y\right] + Z\delta_g \sin \pi x \sin \pi y\right\}$$

$$+ \frac{2Z(\beta^2\mu + 1)}{(1-\mu^2)}\sin \pi x \sin \pi y W_{11} + \frac{1}{2}\left\{\frac{(\beta^2\mu+1)}{(1-\mu^2)} - \cos 2\pi x\right\}W_{11}^2. \tag{O12}$$

Clamped plate:

$$\hat{\sigma}_x = -\frac{(\beta^4 + 2\beta^2/3 + 1)T_0}{3(1-\mu^2)(\beta^2+1)}$$

$$x\left\{1 + (1-\mu)(\frac{\delta_v}{4})\left[-\cos2\pi y + \frac{1}{(\beta^2+1)}\cos2\pi x\cos2\pi y\right] + Z\delta_z\sin^2\pi x\sin^2\pi y\right\}$$

$$- \frac{16Z}{3(1-\mu^2)}[\beta^2\cos2\pi x\sin^2\pi y + \mu\sin^2\pi x\cos2\pi y]W_{11} + \frac{2(\beta^2+\mu)}{3(1-\mu^2)}W_{11}^2$$

$$- \frac{32}{9}\left\{\frac{\beta^2}{4}\cos2\pi y - \frac{\beta^2}{16}\cos4\pi y - \frac{\cos2\pi x\cos2\pi y}{2(\beta+\beta^{-1})^2} + \frac{\cos2\pi x\cos4\pi y}{(\beta+4\beta^{-1})^2} + \frac{\cos4\pi x\cos2\pi y}{4(4\beta+\beta^{-1})^2}\right\}W_{11}^2 .$$

$$\hat{\sigma}_y = -\frac{(\beta^4+2\beta^2/3+1)T_0}{3(1-\mu^2)(\beta^2+1)}$$

$$x\left\{1 + (1-\mu)(\frac{\delta_v}{4})\left[-\cos2\pi x + \frac{\beta^2}{(\beta^2+1)}\cos2\pi x\cos2\pi y\right] + Z\delta_g\sin^2\pi x\sin^2\pi y\right\}$$

$$- \frac{16Z}{3(1-\mu^2)}[\beta^2\mu\cos2\pi x\sin^2\pi y + \sin^2\pi x\cos2\pi y]W_{11} + \frac{2(\beta^2\mu+1)}{3(1-\mu^2)}W_{11}^2$$

$$- \frac{32}{9}\left\{\frac{1}{4}\cos2\pi x - \frac{1}{16}\cos4\pi x - \frac{\beta^2\cos2\pi x\cos2\pi y}{2(\beta+\beta^{-1})^2} + \frac{\beta^2\cos2\pi x\cos4\pi y}{4(\beta+4\beta^{-1})^2} + \frac{\beta^2\cos4\pi x\cos2\pi y}{(4\beta+\beta^{-1})^2}\right\}W_{11}^2 .$$

(013)

C. Strain tensor involving W_{11} only

In view of Eqs. (6.4-6.5), the substitution of Eqs. (012-013) into Eq. (05) yields the dimensionless strain tensor

Simply-supported plate:

$$\hat{\varepsilon}_x = \frac{(\beta^2+1)}{12(1+\mu)}\delta_v T_0\left\{f_v - \frac{1}{4}\left[-(\cos2\pi y - \mu\cos2\pi x) + \frac{(1-\mu\beta^2)}{(\beta^2+1)}\cos2\pi x\cos2\pi y\right]\right\}$$

$$+ 2Z\beta^2\sin\pi x\sin\pi y W_{11} + \frac{1}{2}\left\{\beta^2 - (\beta^2\cos2\pi y - \mu\cos2\pi x)\right\}W_{11}^2 .$$

$$\hat{\varepsilon}_y = \frac{(\beta^2+1)}{12(1+\mu)}\delta_v T_0\left\{f_v - \frac{1}{4}\left[-(\cos2\pi y - \mu\cos2\pi x) + \frac{(\beta^2-\mu)}{(\beta^2+1)}\cos2\pi x\cos2\pi y\right]\right\}$$

$$+ 2Z\sin\pi x\sin\pi y W_{11} + \frac{1}{2}\left\{1 - (\cos2\pi y - \mu\beta^2\cos2\pi x)\right\}W_{11}^2 .$$

(014)

Clamped plate:

$$\hat{\varepsilon}_x = \frac{(\beta^4+2\beta^2/3+1)}{3(1+\mu)(\beta^2+1)}\delta_v T_0\left\{f_v - \frac{1}{4}\left[-(\cos2\pi y - \mu\cos2\pi x) + \frac{(1-\mu\beta^2)}{(\beta^2+1)}\cos2\pi x\cos2\pi y\right]\right\}$$

$$- \frac{16Z\beta^2}{3}\cos2\pi x\sin^2\pi y W_{11} + \frac{2\beta^2}{3}W_{11}^2$$

$$- \frac{32}{9}\left\{\frac{1}{4}(\beta^2\cos2\pi y - \mu\cos2\pi x) - \frac{1}{16}(\beta^2\cos4\pi y - \mu\cos4\pi x) - \frac{\cos2\pi x\cos2\pi y}{2(\beta+\beta^{-1})^2}(1-\mu\beta^2)\right.$$

$$\left. + \frac{\cos2\pi x\cos4\pi y}{(\beta+4\beta^{-1})^2}(1-\frac{\mu\beta^2}{4}) + \frac{\cos4\pi x\cos2\pi y}{(4\beta+\beta^{-1})^2}(\frac{1}{4}-\beta^2\mu)\right\}W_{11}^2 .$$

$$\hat{\varepsilon}_y = \frac{(\beta^4+2\beta^2/3+1)}{3(1+\mu)(\beta^2+1)}\delta_v T_0\left\{f_v - \frac{1}{4}\left[-(\cos2\pi x - \mu\cos2\pi y) + \frac{(\beta^2-\mu)}{(\beta^2+1)}\cos2\pi x\cos2\pi y\right]\right\}$$

$$- \frac{16Z}{3} \sin^2 \pi x \cos 2\pi y \dot{W}_{11} + \frac{2}{3} \dot{W}_{11}^2$$

$$- \frac{32}{9} \left\{ \frac{1}{4} (\cos 2\pi x - \mu \beta^2 \cos 2\pi y) - \frac{1}{16} (\cos 4\pi x - \mu \beta^2 \cos 4\pi y) - \frac{\cos 2\pi x \cos 2\pi y}{2(\beta + \beta^{-1})^2} (\beta^2 - \mu) \right.$$

$$\left. + \frac{\cos 2\pi x \cos 4\pi y}{(\beta + 4\beta^{-1})^2} \left(\frac{\beta^2}{4} - \mu \right) + \frac{\cos 4\pi x \cos 2\pi y}{(4\beta + \beta^{-1})^2} \left(\beta^2 - \frac{\mu}{4} \right) \right\} W_{11}^2 . \tag{C15}$$

Here, $f_v = \sin^2 \pi x \sin^2 \pi y$ should be inserted in Eqs. (O14-O15).